THE PROTEOMIC RESPONSE OF NORTHERN ELEPHANT SEAL (*MIROUNGA ANGUSTIROSTRIS*) PUPS TO PHYSIOLOGICAL STRESS DURING DEVELOPMENT

A Thesis
presented to
the faculty of California Polytechnic State University,
San Luis Obispo

In partial fulfillment
Of the requirements of the Degree
Master of Science in Biological Sciences

by
Melissa Patrice Voisinet
June 2019

COMMITTEE MEMBERSHIP

TITLE	The Proteomic Response of Northern Elephant Seal (*Mirounga angustirostris*) Pups to Physiological Stress during Development
AUTHOR	Melissa Patrice Voisinet
DATE SUBMITTED	June 2019
COMMITTEE CHAIR	Lars Tomanek, Ph.D. Professor of Biology
COMMITTEE MEMBER	Heather Liwanag, Ph.D. Assistant Professor of Biology
COMMITTEE MEMBER	Kristin Hardy, Ph.D. Associate Professor of Biology

ABSTRACT

The Proteomic Response of Northern Elephant Seal (*Mirounga angustirostris*) Pups to Physiological Stress during Development
Melissa Patrice Voisinet

Background: Northern elephant seals transition from terrestrial nursing pups to pelagic foraging juveniles in a short period of just 8-12 weeks. During the post-weaning period, pups rely solely on the energy reserves gained during nursing for their caloric demands and water supply. The prolonged absence of food after weaning is the first of many fasts for which the seals have evolved adaptations such as decreased urine production and increased blubber reserves. The stressors experienced from learning to dive for the first time are also stressors that they will experience frequently as an adult and for which they have evolved adaptations. The purpose of this study was to understand the tissue-specific molecular fasting- and diving- induced adaptive responses of pups during this critical transition.

Methods: To investigate these adaptive responses to fasting and diving, we collected skeletal muscle and (inner and outer) adipose tissue from early-fasting (< 1 week post-weaning) and late-fasting (8 weeks post-weaning) pups. We analyzed the samples with mass-spectrometry-based proteomics using two-dimensional gel electrophoresis. Proteomics is an invaluable tool for analyzing marine mammal physiology, as it provides a large, unbiased data set of proteins that offer a comprehensive set of mechanisms involved with the cellular processes being studied. Proteomics has only been used as analytical tool for marine mammal biology in two other studies, and it can be used as a tool leading to the discovery of novel, unanticipated results.

Results and Discussion: Because muscles are utilized during locomotion, we expected the proteome of skeletal muscle to highlight important physiological changes as the pups learn to dive. Inner adipose is more metabolically active than outer adipose, so we anticipated it would show important changes in metabolism throughout their fast. Outer adipose was useful to detect changes in the proteome due to thermoregulation, as it experiences the most drastic change in temperature and pressure while the pups learn to dive. In all tissues, we found significant shifts in energy metabolism proteins that show a decrease in lipid metabolism and urine production, and an increase in alternative metabolic pathways, such as the pentose phosphate pathway, which produces precursors for nucleic acid synthesis. We also found increases in cytoskeletal proteins, skeletal muscle proteins, and oxygen-binding proteins that facilitate the development of diving ability in late-fasting pups. Lastly, changes in the abundance of oxidative stress related proteins showed increased use of antioxidant proteins to control the production of reactive oxygen species in late-fasting pups. This study provides insight into cellular and physiological responses in marine mammals during ontogeny and their adaptive capacity during a key transition from a terrestrial to aquatic lifestyle.

Keywords: Marine Mammal, Pinnipedia, Post-weaning, Development, Energy Metabolism, Water Conservation, Diving

ACKNOWLEDGEMENTS

The completion of this thesis would not have been possible without the mentorship of Drs. Lars Tomanek, Heather Liwanag, Christina Vasquez, Melissa May, and Kristin Hardy.

The tissue collection, proteomic processing, and analysis of samples would not have been possible without the Crocker Lab (Drs. Dan Crocker, Cory Champagne, and Jane Khudyakov) and the Tomanek Lab (Drs. Lars Tomanek, Christina Vasquez, and Melissa May, as well as Cory Elowe, Shannon Kitchell, and Jaqueline Campbell).

The biology department was instrumental throughout the process of this project, including Ellen Calcagno, Melanie Gutierrez, Kristin Reeves, Rob Brewster, and Doug Brewster, as well as my fellow graduate students, including Emma Weitzner and Cameron Cooper.

Lastly, I would like to thank my parents, Sue and John Voisinet, and my sister, Danielle Voisinet, for their continual love and support.

This research was supported by generous funding from NSF (IOS 1146840) and William and Linda Frost and California Polytechnic State University, San Luis Obispo College of Science and Math.

TABLE OF CONTENTS

LIST OF TABLES

LIST OF FIGURES

CHAPTER 1: INTRODUCTION

1.1 NORTHERN ELEPHANT SEALS

Many animals have physiological adaptations which allow them to survive a wide range of environmental conditions. Despite the difficulties associated with these different environments, many animals have evolved to survive these non-ideal conditions. One group of particular interest, marine mammals, show clear physiological adaptations which allow them to survive in extreme environments. For instance, they are able to survive in cold water temperatures (e.g., Weddell seals, -2 to 10°C), high water pressures during deep dives (e.g., Northern elephant seals, 1530m), and prolonged periods of hypoxia during dives (e.g., Northern elephant seals, 20-60 minutes) (Berta et al., 2006; Hoelzel, 2002). While on land, many marine mammals experience periods of fasting (Lester and Costa, 2006; Worthy, 1991a). Northern elephant seals (NESs; *Mirounga angustirostris*), in particular, experience prolonged periods of fasting of up to three months, depending on age and sex (Le Boeuf and Peterson, 1969). The first of these occurs when NES pups undergo an eight- to twelve- week fast after weaning (Le Boeuf and Peterson, 1969; Somo et al., 2015). The ability to cope with these periods of fasting is crucial for survival, and is largely dictated by life history (Bartholomew, 1970).

1.1.1 Evolutionary History

NESs are part of the clade Pinnipedia within Carnivora (Bininda-Emonds et al., 1999). Pinnipedia, which are semi-aquatic mammals named after their feather-footed (*pinna* and *pedis*) flippers, includes Phocidae (seals), Otariidae (sea lions), and Odobenidae (walruses), which all share a common evolutionary origin within Arctoidea

(caniform carnivores) (Bininda-Emonds et al., 1999). Within the family Phocidae there are two main subfamilies, Phocinae (northern seals) and Monachinae (southern seals) (Davis et al., 2004), and within Monachinae there are three distinct groups, *Lobodontini*, *Monachus*, and *Mirounga* (elephant seals) (Fyler et al., 2005).There are two species of elephant seals that occur globally, NESs and southern elephant seals. The only species that lives in California; however, are NESs.

The evolutionary history of how the Pinniped clade came to be is currently in debate, with data supporting two main hypotheses (Berta and Wyss, 1994; Bininda-Emonds et al., 1999; Davis et al., 2004; de Muizon, 1982). Molecular data suggests that all three families form a sister clade with either Ursidae (Berta and Wyss, 1994) or Mustelidae (Bininda-Emonds et al., 1999); however, there is also evidence for Phocids evolving from Mustelidae, and Otariidae and Odobenidae evolving from Ursidae (de Muizon, 1982) or an Ursidae-Mustelid clade that is sister group to Pinnipedia (Davis et al., 2004). Despite the origin of the Pinnipedia clade, it is agreed Pinnipeds first split from terrestrial carnivores (whether Mustelidae or Ursidae) approximately 35.6 million years ago (mya) (Bininda-Emonds et al., 1999; Higdon et al., 2007). Within Pinnipedia, estimates suggest Phocidae split from Odobenidae and Otariidae about 23-27 mya, and Odobenidae and Otariidae split from each other around 14.2-18 mya (Bininda-Emonds et al., 1999; Higdon et al., 2007).

Marine mammals vary in the adaptation they have for an aquatic lifestyle, and the different lengths of time that each group of marine mammals has lived in the ocean is reflected in these adaptations (Reidman, 1990). The evolutionary relationships above suggest that Pinnipeds have had approximately 35.6 million years to adapt to an aquatic

lifestyle (Bininda-Emonds et al., 1999; Higdon et al., 2007). Like most mammalian evolution, the earliest adaptation that marine mammals evolved for an aquatic lifestyle is linked to foraging ecology (Uhen, 2007). For example, morphological data shows simplified dentation in pinnipeds to aid with feeding underwater (Mitchell and Tedford, 1973). These early adaptations are thought to be due to the high productivity of the oceans during the Oligocene (23.7-33.7 mya), driving pinnipeds towards resources in the water (Lipps and Mitchell, 1976). The idea that evolution is driven by feeding ecology is also supported by more recently-evolved marine mammals, such as polar bears and sea otters, spending the majority of their time in the water feeding (Uhen, 2007).

Pinnipeds have evolved many morphological synapomorphies that separate them from other marine mammals and terrestrial carnivores (Berta et al., 2006). The first is a larger infraorbital foramen than terrestrial mammals, which allows for the passage of blood vessels and nerves to the eyes, increasing the accuracy of sensory perception throughout the maxillary region (Berta et al., 2006; Gasser and Wise, 1972). Other synapomorphies, which are all related to the shape of the flippers to increase swimming efficiency, include and enlarged humeral tubercles (increases joint rotation), a shorter overall humorous, a large first digit on the fore flipper, and larger first and fifth digits on hind flippers compared to other marine mammals and terrestrial mammals (Berta et al., 2006).

Phocidae split from Odobenidae and Otariidae about 23-27 mya, and with this division evolved many more morphological synapomorphies that distinguish them from each other (Bininda-Emonds et al., 1999; Higdon et al., 2007). The first of the synapomorphies is that phocids are unable to rotate their hind flippers under their body,

due primarily to a large astrangular process and reduced calcaneal tuber (Berta et al., 2006). This most likely evolved to improve swimming by allowing for pelvic oscillation and propulsion in the water primarily using their hind limbs (Berta et al., 2006). Another adaptation seen in phocids is pachyostosis, which is an adaptation used for buoyancy control, and is characterized by increased compactness or volume of their bones (Houssaye, 2009). Pachyostosis is seen in the mastoid (ear) region of Phocids, but is absent in Otariids and Odobenidae (Berta et al., 2006). Lastly, Phocids have an everted ilia, which allows for increased muscle attachment of the iliocostalis lumborum muscle, which is the primary muscle utilized during lateral swimming (King, 1983).

Besides morphological differences, Phocids also differ from Otariids and Odobenidae in many behavioral and physiological adaptations (Berta et al., 2006). Earliest marine mammals were tied to freshwater; however, eventually the ability to retain water from food evolved. Otariids drink seawater in small amounts (mariposia) and freshwater marine mammals (e.g., Baikal Seals) commonly drink freshwater; however, this is not commonly seen within Phocids. Elephant seals are specifically unique from other pinnipeds because they have the largest spleen of any marine mammal (~4.5% of body weight), an adaptation that evolved to increase oxygen storage during dives (Berta et al., 2006), increasing diving capacity in Phocids (Mottishaw et al., 1999). Phocids also differ from Otariids and Odobenids in their breeding strategy; Phocids have a brief lactation period lasting day to several weeks, whereas Otariids and Odobenidae have a longer lactation period of several months to over 2 years (Reidman, 1990). With these different lactation strategies come differing levels of parental investment and physiological stress. The short lactation periods of Phocids are often accompanied by

complete fasting throughout nursing, whereas Otariids and Odobenidae leave their young for short periods to forage throughout nursing. Because of this lactation period, Phocid pups have extremely fast growth rates while nursing, primarily due to fattier milk produced by females.

1.1.2 Life History

Elephant Seals are found along the Western coast of North America during their breeding and molting seasons; however, during non-breeding or molting seasons, they spend the majority of their time out at sea and have a far wider distribution (Le Boeuf, 1974; Stewart and Delong, 2016). The males spend their time at sea along the coast of Alaska, feeding in the cold, nutrient-rich waters of the northern latitudes, whereas the females migrate Northeast to feed in the open ocean of the Central Pacific (Stewart and Delong, 2016). When elephant seals are on land, their distribution is clumped into breeding areas called rookeries. They exhibit philopatry, meaning they almost always return to the same rookery and same foraging locations every year (Reiter et al., 1978; Stewart and Delong, 2016).

NES follow an annual cycle of breeding and molting that is separated into four distinct phases: the breeding season, female and juvenile molt, male molt, and juvenile haul out (Thorson and Le Boeuf, 1994). The breeding season starts in early-December with the arrival of males claiming their harem territory (Le Boeuf, 1974; Le Boeuf et al., 1972). Elephant seals are polygamous, with one male controlling and mating with a harem of approximately 30-50 females, (Edwards, 2019; Le Boeuf, 1974; Le Boeuf et al., 1972), although multiple beta males may copulate simultaneously alongside alphas in

larger harems (40-300+ females) (Cox and Le Boeuf, 1977; Le Boeuf et al., 1972). The fight to become the alpha male is often a complex dominance hierarchy between alpha, beta, and gamma males (Cox and Le Boeuf, 1977), with the hierarchy of beta and gamma males changing approximately 15 times throughout a single breeding season (Reidman, 1990). Successful alpha males typically maintain their position throughout the entire season, and remain on the beach until the last female returns to sea in mid-March (Le Boeuf, 1974). The stress associated with being an alpha male is so intense that an alpha male usual dies within two years of their reproductive peak (Le Boeuf, 1974).

Pregnant females arrive at the rookery between mid-December and mid-February, and typically give birth within a week of arrival (Le Boeuf et al., 1972). After nursing their pup for 25-29 days depending on sex, the female abruptly weans her pup, is mated, and returns to sea, leaving her pup to learn how to swim and forage on its own (Le Boeuf et al., 1972). The now-weaners then experience an 8 to 12-week period called the post-weaning fast, in which they have no access to food or water as they learn to dive and forage (Reiter et al., 1978).

All NESs fast for their entire molting and breeding seasons, with a single season on land lasting up to four months depending on age and sex (Le Boeuf et al., 1972). This is because their food preferences live far from the rookery just off the continental shelf, with females preferring to feed on pelagic prey such as cephalopods and teleosts, and males preferring benthic prey such as elasmobranchs and cyclostomes (Condit and Le Boeuf, 1984; Le Boeuf et al., 2000; Thorson and Le Boeuf, 1994). However, NESs are well adapted for these fasts, as this is a regular part of their life history, with their first prolonged fasting period at just 4 weeks old (Reiter et al., 1978).

1.1.3 The Post-Weaning Fast

Following birth, NES pups nurse for approximately 25-29 days depending on sex, gaining over 100 kg (~4.5 kg per day) during the nursing period (Bryden, 1969; Le Boeuf et al., 1972; Reiter et al., 1978). Parental care is brief; pups are abruptly weaned after nursing and are left without having been taught how to forage or dive independently (Reiter et al., 1978). This is especially different from the typical transition to independence seen in other mammals, which often consists of many forms of parental investment and in the case of some otariids and ungulates, continued care after weaning (Altmann, 1958; Gosling, 1969; Lowther and Goldsworthy, 2016; Trillmich, 1979; Trites et al., 2006; Trivers, 1972). NES pups experience an 8 to 12-week post-weaning fast which coincides with when they begin to learn to feed and dive (Reiter et al., 1978). During this time, pups do not have a source of food or water, and lose approximately 25% of their body weight as they transition from a terrestrial to primarily aquatic lifestyle (Ortiz et al., 1978; Reiter et al., 1978).

After being weaned from their mothers, pups leave their harem and join a pod of other weaned pups, primarily due to hostility that arises from surrounding mothers and pups protective of their milk (Reiter et al., 1978). Within 1-2 days the newly weaned pup joins a weaner pod for protection from males, and they will spend most of their time during this period sleeping and interacting with other weaned pups These interactions (mainly space arguments and mock fighting) are novel, as the pups primarily interacted only with their mothers while nursing. As soon as their swimming becomes efficient, they begin to venture to areas of the rookery with fewer adults to avoid stressful negative interactions (Reiter et al., 1978), as the most immediate danger to the newly weaned pups

is being bitten, crushed, or mated by adult seals (Le Boeuf, 1974; Le Boeuf et al., 1972). It has been seen that nearing the end of the post-weaning fasting period, fewer than 10% of pups are still at the original area of the rookery where they were born (Reiter et al., 1978).

Approximately 2 to 3 weeks after weaning, the pups will begin to enter the water for the first time, typically following and learning from older weaners (Reiter et al., 1978). Pups born later in the season tend to enter the water more quickly than 2 to 3 weeks because the majority of other weaned pups have already began exploring the water. They are hesitant to enter the water for the first 2 to 3 days, going no deeper than their ventrum or occasionally placing their head blow the water. Approximately 3 to 5 weeks after weaning, the pups are more comfortable in the water and begin to venture deeper, beyond where they can touch the bottom. Here they will begin making their first dive attempts, although clumsy and uncoordinated, successfully lasting for several seconds at a time. Within a week of diving, their swimming is now effortless and coordinated, and can dive for up to 2 minutes. Within 2 to 3 weeks of entering the water, they can dive and sleep underwater for up to 7 minutes, and after 5 weeks of being in the water (7-8 weeks into their post-weaning fast) they can sleep for up to 15 minutes at a time underwater. After the pups have perfected their swimming and diving skills at approximately 8 to 12 weeks after weaning, they depart to sea for their first foraging season.

Weaned pups weigh approximately 128-144 kg when they are first weaned, and lose approximately 0.58 to 0.87 kg (0.5% to 1% of their body weight) per day while fasting, losing approximately a quarter of their total body weight over the entire fast

(Ortiz et al., 1978). Preliminary data from the Cal Poly Northern Elephant Seal Research Program has found similar average weights for weaned pups at the Piedras Blancas rookery (Peck-Burnett, 2019, unpublished).

Many stressors during the post-weaning fast could potentially affect NES pup physiology. The stressors experienced from learning to dive for the first time are stressors that they will experience frequently as an adult and have therefore evolved adaptations for. For instance, recently weaned pups experience novel social interactions (e.g., play fights and competition for space), morphological (e.g., molting). and behavioral changes (e.g., swimming, diving, and foraging), which all influence physiology (Reiter et al., 1978). The ontogeny of swimming and diving capabilities is particularly interesting because they are gradually introduced to the stressors of diving, such as temporary hypoxia, increased pressure with dive depth, and colder temperatures while learning to swim and forage for prey (Ponganis, 2011). The prolonged absence of food after weaning is the first of many fasts for which the seals have evolved adaptations, such as decreased urine production and increased blubber reserves.

1.1.4 Research Summary

The purpose of this study was to understand the fasting and diving-induced adaptive response of NES pups in two key tissues, skeletal muscle and adipose tissue, during the critical transition from a terrestrial to aquatic lifestyle. Proteomics, the analysis of the protein complements within a tissue, allowed us to identify shifts in cellular pathways involved with the physiological responses to these stressors. We hypothesized that the post-weaning fast would result in substantial changes in the pup's proteome due

to the stressors associated with prolonged fasting and learning to dive, and that these changes would provide evidence for known adaptations associated with fasting and diving. We also hypothesized to see differences in protein abundance between tissues based on the function of the tissue throughout the post-weaning fast.

In this study, we collected skeletal muscle, inner adipose, and outer adipose tissues to analyze physiological adaptations in NES pups throughout the post-weaning fast. Skeletal muscle is used for movements such as galumphing and swimming, which makes it an important tissue to study when analyzing physiological changes while learning to swim and dive. Because muscles are utilized during activity, the proteome of skeletal muscle highlights important physiological changes that occur as the pups learn to swim and dive (Kanatous et al., 1999). Adipose is used for both metabolism and thermoregulation. Inner adipose is more metabolically active than outer adipose, so we hypothesized that it will show more changes in metabolism throughout the fasting period (Debier et al., 2006; Hooker et al., 2001; Koopman et al., 1996). Outer adipose will be useful in detecting proteomic changes due to thermoregulation, as it experiences the most drastic change in temperature and pressure while the pups learn to dive (Hokkanen, 1990; Irving and Hart, 1957; Worthy, 1991b). We then processed the samples using a standard proteomic workflow (Tomanek and Zuzow, 2010), extracting the proteins through homogenization, precipitation, and quantification. Proteins were then separated with two-dimensional (2D) gel electrophoresis and identified with mass spectrometry (MS).

Many studies have been conducted on the physiology of NES during the post-weaning fast; however, our study is unique because it was the first to address this topic

using proteomics. Therefore, our results provide new insight into the adaptive capacity of marine mammals throughout this critical developmental stage.

1.2 NORTHERN ELEPHANT SEAL PHYSIOLOGY

Fasting and diving are natural components of NES life history, and the morphological and physiological adaptations to these stressors are well-studied (e.g., Adams and Costa, 1993; Bryden, 1969; Bryden, 1973; Crocker et al., 1998; Kanatous et al., 1999; Lester and Costa, 2006; Mottishaw et al., 1999; Ortiz, 2001; Ortiz et al., 1978; Ortiz et al., 1996; Ortiz et al., 2001; Ortiz et al., 2006; Rea and Costa, 2012; Schmidt-Nielsen et al., 1970; Vazquez-Medina et al., 2012; Vázquez-Medina et al., 2010). Despite the physiological stress associated with prolonged fasting, pups maintain electrolyte and fluid balance, as well as normal body temperatures and metabolic activity, with little to no long-term detrimental effects (e.g., Crocker et al., 1998; Ortiz et al., 1978; Ortiz et al., 2001; Ortiz et al., 2006; Vazquez-Medina et al., 2012; Vázquez-Medina et al., 2010).

During periods of prolonged fasting, seals must maintain water balance and fuel their energy needs, both with no incoming source of food or water. To help maintain water balance, seals have complex nasal turbinates, which decreases respiratory water loss by cooling air as it is exhaled, therefore causing the water to condense inside the nasal passageway (Lester and Costa, 2006; Schmidt-Nielsen et al., 1970). Complex nasal turbinates, in combination with apneic breathing, ultimately allow the seal to reduce their evaporative water loss well below the amount of water produced through metabolism (Lester and Costa, 2006). The seals also exhibit increased urine osmolality (Ortiz et al., 1996) and decreased urine production (Adams and Costa, 1993; Ortiz et al., 1996). They

also suppress their overall metabolism to conserve energy and water throughout the fast, therefore lengthening the time they can survive off their energy stores (Rea and Costa, 1992). Blubber stores, which compose up to 40% of total mass in pups, is also used for thermoregulation and maintaining metabolic activity while diving and fasting (Bryden, 1969).

NESs can dive up to 1530m, making them the second deepest diving marine mammal (other than sperm whales; 3000 m) (Berta et al., 2006). Known adaptations for diving in seals include increased myoglobin, hemoglobin, hematocrit, and total blood volume to increase oxygen stores (Kanatous et al., 1999; Mottishaw et al., 1999). Marine mammals also have an impressive mammalian dive response to reduce oxygen consumption during dives (Berta et al., 2006), including bradycardia (decreased heart rate), apnea (breath-holding), and vasoconstriction (shunting of blood to vital organs such as the brain, heart, and lungs) (Berta et al., 2006). Compared to other marine mammals, Phocids also have an increased buffering capacity of their blood in response to increased levels of carbon dioxide and acidic end-products of anaerobic metabolism (Berta et al., 2006; Boutilier et al., 1993), NES have adapted for diving through the evolution of a streamlined body shape, a reduced surface area to volume ratio and counter-current heat exchange system (to conserve heat), and the restructuring of muscles throughout the post-weaning fast (for efficient swimming) (Berta et al., 2006; Bryden, 1973).

Using proteomics, we were able to investigate the cellular and molecular processes underlying these known physiological adaptations. Our results revealed complex physiological changes in response to both prolonged fasting and diving, as well as tissue-specific trends in proteins abundance throughout the post-weaning fast. Our

results are discussed in terms of functional categories, which organize proteins by physiological processes. Therefore, the main physiological systems, and how these systems relate to fasting and diving physiology in NESs, will be discussed below.

1.2.1 Metabolism

1.2.1.1 Depression and Maintenance of Metabolism

In general, marine mammals have a higher resting metabolic rate (1.5-3x greater) than terrestrial mammals (Kooyman, 1981). However, during periods of diving and prolonged fasting, Phocids suppress their general metabolism (Berta et al., 2006; Rea and Costa, 1992). The decline in heart rate (i.e., bradycardia) that NESs experience as part of the mammalian dive response infers a reduction in metabolic activity to conserve oxygen during their dive (Berta et al., 2006). Our results support previous research that shows a balance between a general decline in metabolism while maintaining carbohydrate and lipid metabolism throughout diving and fasting throughout the post-weaning fast.

While fasting, NES pups continue to obtain energy through carbohydrates, lipids, and as a last resort, proteins (Champagne et al., 2005; Pernia et al., 1980). Carbohydrates are the preferred energy source because they are stored as glycogen in the liver and muscle (Champagne et al., 2005; Schutz, 2011), which can be quickly converted to glucose 1-phosphate for use in glycolysis (Chandel, 2015). When carbohydrates are limited, such as during the post-weaning fast, gluconeogenesis converts triglycerides to glycerol and fatty acids, and converts lactate to glucose to provide sufficient levels of blood glucose for glycolysis and to sustain brain function (Champagne et al., 2005). Our results suggest that during early-fasting periods, the pups are primarily relying of lipid

metabolism, but shift away from fatty acid metabolism near the end of their fast, utilizing instead pathways such as the pentose phosphate pathway (PPP), possibly to increase the production of DNA and RNA for cell growth or to provide more reducing equivalents, such as nicotinamide adenine dinucleotide phosphate hydrogen (NADPH), and nucleotide production, which are needed for biosynthesis (e.g., of fatty acids) and scavenging of reactive oxygen species (ROS).

1.2.1.1.1 Glycolysis and Related Pathways

In mammals, the main metabolic pathways of ATP production are glycolysis, fatty acid β-oxidation, the citric acid cycle (CAC), and the electron transport chain (ETC) to create adenosine triphosphate (ATP) (Chandel, 2015). There are two phases of glycolysis, the ATP-investment and the ATP-earning phases. The ATP-investment phase of glycolysis begins with a single glucose molecule, and uses 2 ATP molecules over the course of 4 reactions to convert that glucose to dihydroxyacetone phosphate and glyceraldehyde 3-phosphate, producing 2 adenosine diphosphate (ADP) as a byproduct. The glyceraldehyde 3-phosphate begins the ATP-earning phase, which over the course of 5 reactions uses 4 ADP, 2 NAD^+, and $2P_i$ to produce 1 pyruvate, 2 NADH, 4 ATP, and 1 molecule of metabolic water. When oxygen is present, NADH is transported to the ETC to be oxidized and transported back to the cytosol to fuel glycolysis, and pyruvate is transported to the mitochondria for us in the CAC. However, when oxygen is limited, NADH is oxidized to convert pyruvate to lactate.

The only pathway that can produce ATP in anaerobic conditions is glycolysis, and many of the byproducts produced by glycolysis can be utilized during anaerobic

glycolysis (Chandel, 2015). When no oxygen is present, NADH must still be converted to NAD^+ in order for glycolysis to continue, and this is achieved through the reduction of pyruvate to lactate (and protons) by the reaction of lactate dehydrogenase (Chandel, 2015). Marine mammals have been shown to have higher pH buffering capacities in their muscles than terrestrial mammals, allowing them to cope with the increased lactic acid from anaerobic metabolism (Castellini and Somero, 1981). Studies have also shown that NES utilize lactate as a precursor for gluconeogenesis during periods of fasting (Tavoni et al., 2013).

There are many smaller pathways that can feed into this core metabolism, and many pathways that can stem from it. The intermediates of glycolysis can be used for many different pathways, such as the PPP, glycogen production, the hexosamine pathway (glycoprotein and glycolipid production), triglyceride production through dihydroxyacetone phosphate, regulation of hemoglobin through 2,3-bisphosphoglycerate, and amino acid production (i.e., serine, glycine, cysteine, and alanine) (Chandel, 2015). One pathway we found in our results that stems from glycolysis is the PPP (Chandel, 2015). The PPP starts with glucose 6-phosphate, which is the first molecule produced from glucose during the ATP-investment phase of glycolysis. There are two branches of PPP, the oxidative and non-oxidative branches. The oxidative phase uses $NADP^+$ and water to produce ribulose 5-phosphate, and is the main producer of NADPH in the cytosol. The ribulose 5-phosphate is converted to ribose 5-phosphate during the non-oxidative phase, which is the base for nucleic acids. The non-oxidative phase can produce more NADPH than the oxidative phase depending on the mode that is occurring (Chandel, 2015; Neuhaus and Emes, 2000). The pentose sugars produced by the

oxidative branch of the PPP can be converted into metabolites of glycolysis and gluconeogenesis (Chandel, 2015). Depending on the metabolic demand (i.e., cellular glucose 6-phosphate, glucose 6-dehydrogenase, and 6-phosphogluconate dehydrogenase concentrations), the PPP has four "modes" that vary slightly. Mode 1 utilizes the conversion of glucose 6-phosphate to fructose 6-phosphate (via transaldolase) and glyceraldehyde 6-phosphate (via transketolase) to produce ribose 5-phosphate, producing no NADPH during the non-oxidative phase . Mode 2 is the traditional PPP mode, and produces a balance of NADPH and ribose 5-phosphate (Chandel, 2015). Mode 3 primarily produces NADPH, as the ribose 5-phosphate produced is recycled to fructose 6-phosphate (via transaldolase) and glyceraldehyde 6-phosphate (via transketolase) for use in glycolysis. The intermediates of glycolysis are then converted back to glucose 6-phosphate through gluconeogenesis for use in the oxidative phase of the PPP to produce more NADPH. Lastly, mode 4 is similar to mode 3, except the ribose 5-phosphate is converted into glycolytic intermediates for the production of ATP rather than more NADPH .

1.2.1.1.2 The Citric Acid Cycle and Related Pathways

The CAC follows glycolysis and begins after pyruvate is converted to acetyl-CoA, which combines with oxaloacetate and water to produce citrate (Chandel, 2015). The CAC is referred to as cyclic because the end-product, oxaloacetate, although commonly used in other pathways, is primarily recycled to start the cycle over again. The primary purpose of the CAC is the production of the hydroquinone form of flavin adenine dinucleotide ($FADH_2$) and NADH for the ETC. One cycle of the CAC produces 1

guanosine triphosphate (GTP) (converted to ATP), 1 $FADH_2$, 3 NADH, and 2 CO_2 molecules. NADH and $FADH_2$ feed into complex I and II of the ETC, respectively.

Intermediates of the CAC can also be utilized by many other pathways, such as fatty acid and sterol production from citrate, glutamate production from α-ketoglutarate, porphyrin and heme production from succinyl-CoA, NADPH production via isocitrate dehydrogenases and malic enzymes, and both glucose (via phosphoenol pyruvate) and nucleotide (via aspartate) production from oxaloacetate (Chandel, 2015). We found a decreased abundance of glutamate dehydrogenase in late-fasting seals, which combines α-ketoglutarate, NH_4^+, and NADPH to produce glutamate, which can be utilized for the production of many different amino acids (i.e., alanine, aspartate, ornithine and arginine). Glutamate dehydrogenase can also work in reverse as part of the urea cycle, in which it converts glutamate to α-ketoglutarate, releasing NADPH and NH_4^+ that will eventually need to be excreted as urea.

1.2.1.1.3 The Electron Transport Chain and Related Pathways

The ETC is the final energy metabolism pathway utilized for the production of ATP, and is composed of NADH dehydrogenase (complex I), succinate dehydrogenase (complex II), ubiquinone, ubiquinol-cytochrome c reductase (complex III), cytochrome c oxidase (complex IV), and ATP synthase (complex V) (Chandel, 2015). The ETC begins when the NADH and $FADH_2$ produced by the CAC enter complexes I and II, which pass their electrons to ubiquinone (Chandel, 2015). Complex III then transfer the electrons from ubiquinone to cytochrome c, and complex IV transfers that electron to oxygen. Complexes I, III, and IV function as proton pumps, releasing H^+ across the inner

mitochondrial membrane into the intermembrane space, generating the proton motive force. H^+ ions re-enter the mitochondrial matrix through complex V, generating ATP from ADP through oxidative phosphorylation. The ETC creates the majority of ATP, approximately 2.5 ATP per molecule of NADH and 1.5 ATP per molecule of $FADH_2$. Approximately <0.1% of electrons that enter the ETC leak from the process, reducing O_2 to O_2^-, a ROS (discussed further in 1.2.2.1).

1.2.1.1.4 Lipid Metabolism

When glucose is limited, such as during the post-weaning fast, fatty acid β-oxidation is the main source of ATP for NESs (Champagne et al., 2005; Chandel, 2015). The purpose of β-oxidation is to convert fatty acid molecules to acetyl-CoA, NADH, and $FADH_2$ for use in the CAC (Chandel, 2015). The fatty acids that feed into β-oxidation are produced through lipolysis, which is the hydrolyzation of lipids (e.g., triglycerides, such as those stored in adipose tissue in seals) into fatty acids. The process of hydrolyzing lipids to produce fatty acids also produces glycerol, which is converted to dihydroxyacetone phosphate for use in glycolysis. Fatty acid oxidation is also a significant source of metabolic water discussed further in 1.2.1.4.1) (Chandel, 2015; Ortiz, 2001).

Lipids can also be broken down for use in the modification of proteins (e.g., N-myristoylation, S- or N-palmitoylation, and S-prenylation) or as signaling molecules. Current estimates suggest there are approximately 1000 proteins that have some form of a lipophilic group (e.g., fatty acid, phospholipid, isoprenoids) attached to them, which provide crucial, yet reversible, modifications to the function of the protein (Chandel,

2015). The main functional modification that lipids provide is the ability for water-soluble proteins to attach to hydrophobic membranes. Lipids can also play a role in stabilizing the conformation of a protein at both the tertiary and quaternary levels.

There are also a number of lipid biosynthetic pathways that stem from the core metabolism discussed above, such as fatty acid, cholesterol, and lipid synthesis (Chandel, 2015). The majority of these synthesis pathways begin with the citrate intermediate from the CAC, which then breaks down into oxaloacetate and Acetyl-CoA. Acetyl-CoA can then either enter the mevalonate pathway to produce cholesterol, or be converted to palmitate to produce fatty acids and lipids. Fatty acid and lipid synthesis can also stem from glycolysis, beginning with the intermediate dihydroxyacetone phosphate being converted to glycerol 3-phosphate.

1.2.1.2 Osmoregulation

Water balance during prolonged fasting is dictated by the balance between metabolically generated water and obligatory water loss from urine and respiratory evaporation (Condit and Ortiz, 1987; Lester and Costa, 2006; Ortiz et al., 1978). Mammals produce more water per weight with fatty acid oxidation than any other metabolic process (Ortiz, 2001), which is the main metabolism occurring during the post-weaning fast (Champagne et al., 2005; Chandel, 2015). Previous studies have shown that although NES pups survive without any incoming source of water during prolonged fasting periods, they exhibit no signs of dehydration (e.g., increased plasma osmolarity, electrolytes, or total protein) or any decrease in total body water (Ortiz et al., 1978; Ortiz et al., 2000).

NES pups decrease the amount of urine they produce from ~430 ml day-1 in the early-fasting to ~70 ml day-1 by the end of the fast (Lester and Costa, 2006). Two well-studied mechanisms to decrease urine production include increased urine osmolarity and the reduction of nitrogen load on the kidneys (Adams and Costa, 1993; Ortiz et al., 1996; Pernia et al., 1980). Nitrogen load on the kidneys is primarily reduced through a decrease in protein catabolism (Adams and Costa, 1993). NESs have been shown to be able to concentrate their urine well above the osmolarity of sea water, primarily through hormonal regulation and decreasing the rate of urine formation (Ortiz, 2001). NESs, in particular, have been shown to have a water flux rate that is approximately 3x lower than other Phocids (Ortiz et al., 1978). Hormonal regulation primarily involves the following hormones: angiotensin (I, II, and III), atrial natriuretic peptide, aldosterone, and vasopressin (Ortiz, 2001). These hormones are particularly important for the reabsorption of Na^+ and K^+ through increasing the response of the renin-angiotensin-aldosterone system, which recycles Na^+ and K^+ without increasing vasopressin levels, inhibiting the reabsorption of H^+ ions. Inhibiting the reabsorption of H^+ ions is one way that the seals mitigate metabolic acidosis during fasting as well.

1.2.2 Proteostasis and Cell Signaling

Every protein must fold into a specific three-dimensional structure in order to have the correct functional activity (Hartl et al., 2011; Lovrić, 2011). However, there are both acute and chronic cellular conditions that may compromise the ability for a protein to function properly (Hartl et al., 2011). Proteostasis (i.e., protein homeostasis) is a biological concept describing the regulation of correct protein function through pathways

involved with protein synthesis, folding, trafficking, aggregation, and degradation (Hartl et al., 2011; Powers et al., 2009).

1.2.2.1 Epigenetic Regulation of Protein Expression

Epigenetic changes are modifications to gene expression due to something other than changes in the genetic code (Bird, 2007). This phenotypic plasticity can be important for organisms in adapting to physiological stressful situations (Bird, 2007). There are many mechanisms by which protein expression can be modified through epigenetics, such as histone modification (acetylation), DNA methylation, expression of repressor proteins, and RNA editing (Bird, 2007; Blanc and Davidson, 2003).

Mammalian genomes are commonly regulated via DNA methylation, which is the addition of a methyl group on 5′-CpG-3′ dinucleotides associated with regulatory portions of a gene (Blanc and Davidson, 2003). For example, in mammals, starvation is associated with an inactive form of triiodothyronine (T3), a metabolism-driving thyroid hormone, due to an increase in the activity of the deiodinase type 3 (DI3) gene (Martinez et al., 2016). However, in fasting NES pups, the inactive form of T3 remains low despite the pups remaining metabolically active with thyroid hormone-mediated components upregulated. It was discovered that these low levels are due to the methylation of the DI3 gene, which suppresses the transcription of the inactive form of T3, providing insight into epigenetically-regulated adaptations in marine mammals to periods of prolonged fasting.

1.2.2.2 Protein Folding and Degradation

Although there are hundreds of proteins involved with maintaining proteome homeostasis (Powers et al., 2009), it is primarily achieved through molecular chaperones, the ubiquitin−proteasome system (UPS), and autophagy system (Hartl et al., 2011).

1.2.2.2.1 Protein Folding

Although it has been shown *in vitro* that proteins contain the necessary information in their DNA to fold correctly on their own, many proteins require molecular chaperones to fold quickly and correctly (Hartl et al., 2011). A molecular chaperone is any protein that is not present in the final protein structure, but helps a protein reach its correct functional conformation. Chaperones participate in proteostasis processes through initial folding, refolding of incorrectly folded proteins, trafficking, and proteolytic degradation. It is thought that chaperones evolved for two main reasons, as a way to minimize protein aggregations in densely packed cells during folding and to provide a mechanism for folding to still occur in the presence of mutations, promoting the evolution of new protein phenotypes.

There are several classes of molecular chaperones, called heat shock proteins (HSPs), that are named based on their molecular weight: HSP40, HSP60, HSP70, HSP90, HSP100, and small HSPs (Hartl et al., 2011). HSP40s can directly interact with unfolded proteins, as well as recruit HSP70s to unfolded proteins. If a protein is unable to be folded by HSP70s, it is then passed to chaperonins (HSP60) for folding. Chaperonins completely enclose the protein they are folding in a cage that requires several other proteins, such as actin and tubulins. HSP90s are essential for suppressing the effects of

destabilizing mutations that could potentially arise during important signaling pathways, such as vesicle-mediated transport, cell-cycle progression, and protein degradation, by buffering the signaling noise, thereby stabilizing developmental pathways. HSP90s often work together with or downstream from other HSPs, particularly HSP70s, in multi-chaperone complexes.

1.2.2.2.2 Protein Degradation

When proteins are not folded correctly, it is crucial that the cell has a way to rid itself of those proteins. One such pathway is the UPS, which is the main cellular system responsible for most quality-control protein degradation in eukaryotes (Tomko and Hochstrasser, 2013). This pathway works by attaching a chain of ubiquitin proteins (forming polyubiquitin) to the target protein, flagging it for delivery to the proteasome. Once at the proteasome, the polyubiquitin tag is removed and the protein is unfolded and cleaved into smaller peptides. Another cellular process is autophagy, which is a pathway that removes intracellular protein aggregates and misfolded proteins by binging them to lysosomes for degradation (Powers et al., 2009).

1.2.2.3 Oxidative Stress

It has been shown that increased oxidative stress can be associated with both physiological (e.g., metabolism) and psychological (e.g., fear) stressors (Clinchy et al., 2013; Moller et al., 1996; Vazquez-Medina et al., 2012). The nursing period is associated with increased metabolism as the pup rapidly gains mass, while the late-fasting period is associated with a transition from a terrestrial to an aquatic lifestyle (Rea and Costa, 1992;

Reiter et al., 1978). The transition to an aquatic lifestyle includes increased lipid metabolism, exercise, ischemia/reperfusion, and hypoxia, which are all also known factors to produce ROS (Allen and Vazquez-Medina, 2019; Moller et al., 1996; Vazquez-Medina et al., 2012, in prep.; Wilhelm Filho et al., 2002). The increased vasoconstriction, bradycardia and organ reperfusion associated with the mammalian dive response during the post-weaning fast have also been shown to increase the production of ROS in seals (Irving et al., 1942; Murdaugh Jr. et al., 1961; White et al., 1973; Wilhelm Filho et al., 2002; Zapol et al., 1979).

Oxidative stress occurs when ROS, produced during the processes described above, are not converted to less damaging molecule, thus causing cellular damage, such as mutations in DNA, protein degradation, and fatty acid oxidation (Somero et al., 2017). To mitigate the damage from ROS (specifically superoxide anions), superoxide dismutase (SOD) converts the superoxide anion (O_2^-) to hydrogen peroxide (H_2O_2), a less damaging molecule. That hydrogen peroxide is then converted into H_2O by peroxidases (e.g., peroxiredoxins, glutathione peroxidase and catalases). If hydrogen peroxide is not broken down in a timely matter, it may react with ferrous iron (Fe^{2+}) and be converted to a hydroxyl radical via the Fenton reaction, which is even more reactive than a superoxide anion. However, cells produce molecules (e.g., ferritin and hemopexin) to bind to ferrous iron and prevent it from reacting with hydrogen peroxide.

Despite all of the potential factors contributing to oxidative stress during the post-weaning fast, it has been found that there is no significant cellular oxidative damage in NES pups during the post-weaning fast as a result of increased ROS (Vazquez-Medina et al., 2012; Vázquez-Medina et al., 2010). The most common explanation for the lack of

cellular oxidative damage in NESs is that NESs mitigate the negative impacts of oxidative stress through a 40-60% increase in antioxidant abundance throughout the post-weaning fast (e.g., SOD, catalase, glutathione peroxidase, glutathione S-transferase, and glutathione disulfide reductase) (Vázquez-Medina et al., 2010).

1.2.3 Cytoskeleton

1.2.3.1 Restructuring of the Muscle Tissue

During the post-weaning fast, pups experience a restructuring of skeletal muscle as they begin to swim for the first time (Reiter et al., 1978), such as changes in muscle fiber type, and changes in the isoforms of proteins involved with the structure and function of skeletal muscle. Previous studies have shown that swimming promotes changes in skeletal muscle function and structure, such as increased density of mitochondria, citrate synthase, and myoglobin in multiple species of pinnipeds, which function to increase oxygen stores and the amount of energy available to muscles (Kanatous et al., 1999). Also, studies have shown that the vasoconstriction occurring as a natural diving response has an effect on the structure of smooth skeletal muscle (Irving et al., 1942). Vasoconstriction is most commonly activated by epinephrine and norepinephrine that directly innervate the muscle and result in a signaling cascade increasing the amount of intracellular calcium. Calcium in turn complexes with calmodulin, which phosphorylates myosin light chains to stimulate cross-bridge cycling and muscle contraction (Wilson et al., 2005). Cross-bridge cycling that occurs during vasoconstriction incorporates many of the proteins that increased in abundance (tropomyosin) or shifted isoforms (myosin and troponin T) in the late-fasting pups.

Therefore, the shifts in the isoforms of skeletal proteins being utilized before and after the post-weaning fast indicates that there was a restructuring of skeletal muscle fibers during the fast most likely due to modulate actomyosin interactions and muscle function.

Previous studies have also shown that although there is an overall decrease in muscle mass throughout the post-weaning fast, there is also atrophy and hypertrophy of different muscle groups as the pups utilize new muscles and learn to swim and dive (Bryden, 1969). On land, NESs move primarily using the muscles of the abdominal wall, sub-lumbar muscles, and muscles supporting the forelimb. However, the mode of locomotion changes when the pups begin to swim, as they mainly start to utilize the muscles surrounding the spinal column, the proximal muscles of the hind limb, and the muscles that extend the tarsals and flex the digits. Our study obtained skeletal muscle samples from a single location on the pups, the latissimus dorsi, a muscle near the hind limb involved with aquatic locomotion.

This restructuring of skeletal muscle is supported by the increased PPP activity seen in the late-fasting pups. As discussed above (in 1.2.1.1.1) the PPP is useful for the production of amino acids. Ribose-5-phosphate is a precursor for nucleotide synthesis (Herrmann and Weaver, 1999), and erythrose-4-phosphate is used in the synthesis of aromatic amino acids, both of which are required for growth. Growth is important throughout the post-weaning fast as the pup develops the ability to swim and forage independently.

1.2.3.2 Restructuring of the Cytoskeleton

Many studies have shown that increased external and internal pressure affects cellular structure (Davies, 1995; Franke et al., 1984; Maniotis et al., 1997). External pressure increases with dive depth, and internal pressure increases from the general vasoconstriction that maintains normal levels of blood pressure as the heart rate slows with bradycardia (Irving et al., 1942). Previous studies have shown that transmembrane matrix receptors, cytoskeleton filaments, and nuclear scaffolds respond nearly immediately to external mechanical stress (Maniotis et al., 1997). Studies also show that internal pressure, such as stress from blood pressure, promotes stress fiber growth and increased cell adhesion to its substrate (Davies, 1995). Changes in actin are thought to protect the endothelium from potential injury and detachment related to increased pressure on the cells (Franke et al., 1984).

There is also evidence that temperature can affect the cytoskeletal structure of cells (Hokkanen, 1990; Irving and Hart, 1957; Lepock, 2003; Welch and Suhan, 1985; Worthy, 1991b). Although the blubber layers in marine mammals are extremely effective insulation, many studies have shown that the body temperature at the blubber-muscle border is significantly lower than the core body temperature when the animal is submerged in cold water (Hokkanen, 1990; Irving and Hart, 1957; Worthy, 1991b). NES are thought to decrease the temperature of the outermost muscle on purpose through vasoconstriction specific to the outermost muscle, keeping excess heat production there to a minimum (Hokkanen, 1990; Zapol et al., 1979). Vasoconstriction also occurs as part of the mammalian dive response, in which the seal restricts blood flow to essential organs (i.e., lungs, heart, brain) while diving to decrease the amount of oxygen being used by

non-essential body parts (Berta et al., 2006). Some studies have shown changes in cellular structure due to changes in temperature. For example, previous studies have seen a disassembly of cytoskeletal components such as microtubules and actin filaments at lower body temperatures (Stapulionis et al., 1997), whereas other studies have shown increased polymerization of actin filaments (Hoffmeister et al., 2001), a complex necessary for protein synthesis (Stapulionis et al., 1997). Previous studies also suggest that changes in the cytoskeleton due to decreased temperature may result in translational machinery being disrupted, which would inhibit protein synthesis altogether (Al-Fageeh and Smales, 2006).

1.2.4 Iron-Binding

Marine mammals can have up to 10-20x higher myoglobin concentrations than terrestrial mammals, like cotton rats, due to their diving demands (Kanatous et al., 1999). Previous studies have shown that total blood volume and hematocrit levels (although variable) generally increase in weaned pups (Ortiz, 2001; Somo et al., 2015). Hemoglobin is found inside erythrocytes, so both increased total blood volume and hematocrit are associated with increased oxygen storage ability. Total blood volume accounts for 68% of total oxygen storage ability (Ponganis, 2011) and is the main factor determining breath-holding ability in NES (Hassrick et al., 2010).

1.2.4.1 Hemoglobin

Mammals use hemoglobin to store oxygen in their blood and transport the oxygen to different areas of the body (Hsia, 1998). Hemoglobin concentrations increase

approximately 3.6g/dL over the first 8 weeks of the post-weaning fast (Thorson and Le Boeuf, 1994). We found both increases and decreases in the abundance of hemoglobin, suggesting a shift in the specific isoforms being utilized by the seals. Some studies suggest the different isoforms of hemoglobin subunit β have been evolutionarily selected for different functions (Gilman, 2017; Projecto-Garcia et al., 2013; Rashid and Weber, 1999). This may be because different isoforms of hemoglobin have different affinities for oxygen due to structural difference in the heme pocket (Rashid and Weber, 1999). Previous studies have shown that there is a correlation between hemoglobin's affinity for oxygen and the concentration of oxygen available to the organism (Projecto-Garcia et al., 2013). Therefore, the shift in hemoglobin isoforms may indicate an adaptive response of increasing oxygen transport abilities as the pups experience increased hypoxia during diving.

In order for an organism to produce hemoglobin and myoglobin, they must synthesize heme groups (Somo et al., 2015). Heme synthesis begins by combining glycine with succinyl-CoA, a CAC intermediate, to produce δ-aminolevulinic acid (Chandel, 2015). Through a series of reactions, δ-aminolevulinic acid is converted to a heme ring using ferrous iron (Chandel, 2015). Hemoglobin can also be broken down or recycled, primarily utilizing haptoglobin, which we found had a decreased abundance in late-fasting pups (Faulstick et al., 1962). Haptoglobin binds to hemoglobin, and the entire haptoglobin-hemoglobin complex is removed by the reticuloendothelial system (Faulstick et al., 1962).

1.2.4.2 Myoglobin

Mammals use myoglobin to store oxygen in muscles for use when the oxygen from hemoglobin is depleted (Ordway and Garry, 2004). The increase in myoglobin we found is consistent with previous studies, which state that the myoglobin concentrations of pinnipeds was significantly greater in swimming muscles than non-swimming muscles, and that neonatal pinnipeds are born with 31% of the myoglobin concentration as adults (Kanatous et al., 1999; Noren et al., 2001; Thorson and Le Boeuf, 1994). Myoglobin concentrations increase up to 1.5g/100g of muscle over the first 8 weeks of the post-weaning fast (Thorson and Le Boeuf, 1994).

This increase in myoglobin is necessary to store more oxygen so marine mammals can dive for longer periods of time (Kanatous et al., 1999).

1.2.4.3 Regulation of Iron

The regulation of iron is crucial for the proper function of oxygen-binding proteins; however, too low or too high of iron levels can be detrimental (Sigel et al., 2013). Iron deficiency can cause anemia, which results in insufficient oxygen delivery (Andrews, 1999; Sigel et al., 2013). Another important consideration when discussing iron regulation is oxygen storage, as hemoglobin and myoglobin both contain heme groups that require iron for synthesis (Somo et al., 2015). Therefore, low levels of iron (anemia) can results in a decreased ability to increase the abundance of hemoglobin and myoglobin necessary for storing enough oxygen for long foraging dives. However, previous studies have shown that serum iron levels increase early in the post-weaning fast, allowing seals to synthesize hemoglobin and myoglobin. Iron stores most likely

increased due to the mobilization of iron stores in the liver or from degraded hemoglobin and erythrocytes. We found that hemopexin is also increased in early-fasting pups, which binds to free heme groups and iron in the bloodstream to prevent iron loss (Tolosano and Altruda, 2002).

Excess iron can be detrimental as well because mammals have no mechanisms of iron excretion (Andrews, 1999; Sigel et al., 2013). Because iron is stored in the liver, the pancreas, and the heart, excess iron can result in liver cirrhosis, heart failure, and diabetes (Andrews, 1999). Excess iron can also react with hydrogen peroxide in the Fenton reaction to produce hydroxyl radicals, which damages macromolecules important for cell function (Poprac et al., 2017; Sies, 1991). Iron is stored until it is needed for the synthesis of myoglobin and hemoglobin (Tolosano and Altruda, 2002).

1.2.5 Immune System

During periods of prolonged fasting, NES pups have a depressed general metabolism and therefore limited resources available for various physiological processes (Berta et al., 2006; Rea and Costa, 1992). Cortisol has been shown to increase in both NES adults and pups during periods of prolonged fasting, presumably to aid in lipolysis, but also impacting their immune system (Ortiz et al., 2001; Peck et al., 2016). Previous studies have also found evidence that inflammation does not increase throughout the post-weaning fast (Vázquez-Medina et al., 2010). We found several components of an inflammatory response in our results, including but not limited to acute phase proteins (APPs), cytokine, and complement factors.

APPs are proteins whose concentrations in the blood increase or decrease in response to inflammation or starvation through the acute-phase reaction (Davidson, 2013;

Gabay and Kushner, 1999; Gruys et al., 2005). There are two classes of APPs: 1) those that decrease abundance in response to inflammation (negative APPs), and 2) those that increase abundance in response to inflammation (positive APPs) (Davidson, 2013; Gabay and Kushner, 1999). Positive APPs increase to inhibit the growth of microbes and simultaneously inhibit the inflammatory response through negative feedback (Gruys et al., 2005). Negative APPs decrease during inflammation to conserve amino acids for the production of positive APPs (Gruys et al., 2005). APPs are regulated by the secretion of cytokines by local inflammatory cells such as neutrophils, granulocytes, and macrophages (Gabay and Kushner, 1999; Janciauskiene et al., 2013). Cytokines then trigger the release of APPs by the liver as a response to inflammation (Davidson, 2013).

Complement factors are immune system proteins that clear damaged cells and microbes in the body by tagging them for phagocytosis, promote inflammation by attracting macrophages and neutrophils, and attack bacteria by rupturing their cell walls (Murphy and Weaver, 2017). Inactive complement factors are continually circulating in the bloodstream, but are activated by three different pathways: the classical complement pathway, the alternative complement pathway, and the lectin pathway.

1.3 PROTEOMICS

To analyze the molecular mechanisms underlying NES pup development during the post-weaning fast, we used a method called proteomics. Proteomics is a powerful tool used to identify which proteins are present in a given tissue and at what abundance (Lovrić, 2011). Proteomics targets what proteins are actually being utilized in a given environment, providing insight into the cellular into molecular phenotype (Tomanek,

2011). It is therefore a crucial component of studying physiology because it provides a large, unbiased data set of proteins which often provide a comprehensive set of mechanisms involved with the processes being studied. Proteomics has only been used to analyze marine mammal physiology a handful of times (e.g., Neely, Ellisor, & Davis, 2018; Sobolesky et al., 2016), and therefore leads to unanticipated and novel results (Görg et al., 2004). Due to the increasing number of genome sequences and well-annotated expressed sequence tag (EST) libraries, proteomic analyses of non-model organisms have recently become more feasible (Tomanek, 2011).

1.3.1 Overview of Proteomics

1.3.1.1 Analysis of the Proteome

The most broad definition of the proteome is that the proteome is all of the proteins expressed by a certain species (Lovrić, 2011). However, it must also be considered that no individual expresses every possible protein that a species has the potential to express. This is partly because a single protein might exist as one of many different isoforms in different individuals, but also because not all proteins are expressed throughout the entire lifetime of the individual, so a single individual will never express a complete proteome at any given point in time. Therefore, this more specific definition of a proteome is often used: the proteins expressed in a given organism, tissue, or culture under a certain defined condition. Different proteomes can then be compared to see how the complete proteome differs between conditions or species, allowing us to understand which proteins are involved with what specific physiological functions.

Proteomics can be used to analyze proteomes in many different ways. When deciding to use proteomics as a tool for any project, it must be considered if the results proteomics can provide will properly address the research question. Results from using proteomics fall into four main categories: detection and quantification of protein levels, protein modifications, protein locations, and protein interactions (Lovrić, 2011).

The level of protein expression can be measured either as the presence or lack of for a specific protein, or as the relative abundance of proteins. Relative abundance can be calculated using both MS based methods (e.g., isotope-coded protein labeling, area under the peak) or non-MS based methods (e.g., quantifying the intensity of protein spots on a 2D gel) (Lovrić, 2011). For our project, we used the relative intensity of protein spots on 2D gels as a proxy for the relative abundance of proteins from three different tissues (skeletal muscle, inner adipose, and outer adipose) and two time-points (early- and late-fasting).

Protein modifications, or post-translation modifications (PTMs), are modifications of proteins after biosynthesis that increase the functional diversity of a given protein (Tomanek, 2011). The most common PTMs include modifications through the formation of new disulfide bonds or by the addition or removal of low-molecular-weight group (e.g., phosphorylation, acetylation, methylation) (Somero et al., 2017). PTMs greatly impact the function of a protein, so are therefore crucial to understanding the functional physiology underlying the proteome in question. PTMs can be detected using 2D gel electrophoresis and a matrix-assisted laser desorption ionization tandem time-of-flight (MALDI-TOF-TOF) MS because they shift the molecular weight and isoelectric point of a protein, allowing each modified protein to be analyzed individually

(Mann et al., 2001). Therefore, we cannot say with certainty which PTMs occurred, but instead created hypotheses based on previous studies. New technology, such as the Orbitrap mass analysis or capillary electrophoresis mass spectrometer, can now predict with statistical significance which PTM occurred to a given protein (Faserl et al., 2017; Rose et al., 2012).

The locations of proteins within a cell can be analyzed by isolating a specific part of the cell, such as the mitotic spindle, during sample processing to elucidate specific cellular processes occurring at that sub-cellular location (e.g., Sauer et al., 2004). For our project, we did not specifically look for which proteins were located in which sub-cellular locations, but instead inferred location of the protein based on which isoform of the protein was identified, as some isoforms are known to be specific to certain locations, such as mitochondrial aldehyde dehydrogenase 2 (ALDH2) only occurring in the mitochondrial matrix (Ohta et al., 2004).

Analyzing protein interactions is often limited to focusing on the set of proteins interacting with one specific protein or within a single signaling module, although a more complete picture can be created with the combination of multiple projects (Lovrić, 2011). Protein interactions are very fragile, so these analyses are often incomplete; however, there are a few studies that have successfully creating genome and proteome maps, such as the multidimensional proteome map of a single yeast cell (Bader et al., 2003). For our project, we could not say with certainty which proteins were directly interacting with each other, but rather created hypotheses about which proteins were involved the same cellular networks based on previous research.

1.3.1.2 Common Uses of Proteomics

Most projects utilizing proteomics either aim to correlate the expression of specific proteins with certain function (functional proteomics), describe a complete proteome (profiling proteomics), or compare proteomes between various conditions, species, tissues, or cultures (differential proteomics) (Gupta and Kumar, 2016; Lovrić, 2011). The goal of our project was to describe the proteome of various NES pup tissues during different stages of their post-weaning fast, so therefore our strategy was primarily differential proteomics. However, the proteome of NES pups throughout the post-weaning fast had never previously been described, so our project also serves as a profiling project.

These different experimental approaches can be utilized in a variety of fields to address a variety of research questions. For example, proteomics is commonly used in the medical industry, primarily for drug development and biomarker discovery (e.g., de la Cuesta et al., 2009; Gao et al., 2009; Lau et al., 2010; Marko-Varga et al., 2007; Mini et al., 2006; Okano et al., 2007; Rix and Superti-Furga, 2009; Sodek et al., 2008). Biomarker studies have spanned a wide variety of diseases, such as atherosclerosis (de la Cuesta et al., 2009) and gastrointestinal infections (Mini et al., 2006), to help with understanding prevention, diagnosis, and treatment. Biomarkers are also commonly used in cancer research, such as understanding pathways that are associated with invasive cancer cells (Sodek et al., 2008) or prioritizing which biomarkers should be used in a clinical setting for diagnosis (Lau et al., 2010). Lastly, drug development studies have focused on a variety of topics, such as the toxicity of new drugs (e.g., Gao et al., 2009), finding targets within the body for drugs (e.g., Rix and Superti-Furga, 2009),

personalizing treatments for individuals (e.g., Marko-Varga et al., 2007), and understanding the body's response to new treatments (e.g., Okano et al., 2007).

Proteomics is also commonly used in industries, such as agriculture, for product development and analysis (e.g., Davoli and Braglia, 2007; Lücker et al., 2009; Mamone et al., 2009). For example, some agricultural studies include creating effective breeding strategies to improve meat quality (Davoli and Braglia, 2007), understanding ripening of grapes for wine (Lücker et al., 2009), and the impact of various food components on human health (Mamone et al., 2009).

Lastly, within the field of biology, proteomics is often used to understand fundamental biological processes, such as the discovery of new RNA splicing factors (Ambrósio et al., 2009) or finding evidence for insertional RNA editing in humans (Zougman et al., 2008). Proteomics can also dig deeper, attempting to understand the molecular mechanisms underlying these cellular processes, such as understanding how hyperphosphorylation potentially impacts the reorganization of microtubule networks (Lovrić et al., 1998). Lastly, biologists often utilize proteomics to determine the structure (Ho et al., 2002) and functions (Chen et al., 2009) of proteins. Our project is primarily concerned with understanding the underlying fundamental biological processes employed during diving and fasting and elucidating the molecular mechanisms behind those physiological adaptations.

1.3.2 Advantages and Disadvantages of Proteomics

Proteomics is just one of the many methods within the umbrella field of "-omics", which includes other methods such as transcriptomics and metabolomics (Lovrić, 2011).

Each “-omics” category attempts to analyze all components within its biological system to better understand physiological processes (Lovrić, 2011). Each “-omics” subcategory also has their pros and cons, and can be useful or fall short depending on the biological questions being addressed. Therefore, many recent research projects are combining these “-omics” methods to create a more comprehensive understanding of the physiological processes in question. For example, one recent metabolomics study on oxidative stress in NES found increased glutathione biosynthesis during the post-weaning fast, which they were able to further support by finding upregulated genes known to be involved with oxidative stress mediation (Crocker et al., 2016),

1.3.2.1 Advantages of Proteomics

Proteins are crucial biological molecules, as they are structurally and/or functionally involved in every physiological process (Chandel, 2015). There are many changes that can occur throughout the process of protein synthesis, and studies have shown that there are often many discrepancies between studies that combine transcriptomics and proteomics (Lovrić, 2011). This is primarily because proteomics targets what is actually being utilized in a given environment (Tomanek, 2011).

Proteomics is a comprehensive method in which scientists receive large datasets with hundreds to thousands of protein identifications and abundances (Beranova-Giorgianni, 2003). Large datasets are extremely useful for answering research questions, because it provides the tools to answer questions with a more complete explanation of an organism’s physiology. These large datasets also provide unbiased, often unanticipated results, which allows scientists to develop novel hypotheses (Görg et al., 2004). For

example, proteomics has only been used to analyze marine mammal physiology a handful of times (e.g., Neely, Ellisor, & Davis, 2018; Sobolesky et al., 2016), so current proteomic analyses allow for the discovery of patterns in protein expression that are previously undescribed.

1.3.2.2 Disadvantages of Proteomics

Proteins are made up of a series of amino acids averaging about 450 units in length, and can be made of any combination of the 20 amino acids that exist (Lovrić, 2011). Proteins have far more variety and complexity than other cellular components, such as DNA or RNA, which are fairly uniform in structure and are only composed of five different nucleotides. Therefore, when processing protein samples, there is no single protocol that will effectively extract and identify all proteins in a sample. For example, some buffers that work well for some proteins may degrade or add artificial PTMs to other proteins, thus changing their abundance and structure. Also, some proteins are more optimal for identification by MS due to their high quantities and distributions of arginine and lysine, where trypsin digest breaks peptide bonds (Olsen et al., 2004). The wide range of properties of various proteins makes absolute analyses and comparisons impossible (Lovrić, 2011).

Besides the variability in protein structure, there is also a wide range in the location of proteins. For example, transcription factors are only in an active conformation once they are transported to the nucleus (Kawamori et al., 2006), which although is only a difference of nanometers, makes a large difference in the interpretation of the proteome (Lovrić, 2011). Most organelles and sub-cellular structures can easily be isolated during

processing; however, this normally involves a longer and more complicated isolation procedure, often resulting in an increase of artificial artefacts (Lovrić, 2011).

Lastly, some calculations have suggested that there can be up to 2 million different proteins expressed in animals if including all potential PTMs, isoforms, and alternative splicing (Lovrić, 2011). However, it is estimated that an organism may only be expressing less than half of their proteome at any given moment, and since proteomics is typically not run on entire organisms, the number is further decreased by assuming not all proteins are expressed in every tissue (Lovrić, 2011). There is also an issue with the relative abundance in which these proteins are expressed. Although there could be one to two genes per cell controlling the expression of a protein, the expression can range from 1 to 10 million copies per cell (Futcher et al., 2015). For protein identification, a certain amount of protein (400ug for our project) is run through 2D gel electrophoresis (Tomanek and Zuzow, 2010). Therefore, the lower-abundant proteins may not show up in a high enough concentration to be detected on the 2D gel and analyzed with MS.

Technology is constantly improving to aid scientists in the mitigation these challenges, and although there are limitations to proteomics, careful use of the method leads to studies with exceptional results and implications. In addition, the strategic combination of different "-omics" fields can create a more comprehensive answer to a research question because of the limitations found within each "-omics" field.

1.3.3 The Proteomic Workflow

The general proteomic workflow involves the following steps: protein solubilization from the tissue, separation of proteins, and protein identification

(Beranova-Giorgianni, 2003; Lovrić, 2011; Tomanek, 2011). For our project, proteins were separated using 2D gel electrophoresis and identified through MALD-TOF/TOF MS. We followed the specific proteomic protocol described in Tomanek and Zuzow, 2010.

1.3.3.1 Protein Extraction

Tissue samples were diluted 1:5 (sample:buffer) in buffer containing 7 M urea, 2 M thiourea, 1% amidosulfobetaine-14 (ASB-14), 40 mmol tris-base, 0.001% Bromophenol Blue, 0.5% immobilized pH 3-10 gradient (IPG) buffer, and 0.6% dithiothreitol (DTT). The purpose of the homogenization buffer is to disrupt the cell and release proteins from inside without compromising the integrity of the proteins in interest (Simpson, 2010). Urea is used because of its effective unfolding of proteins at concentration over 2.8 M by rupturing non-covalent bonds between amino acid residues (Rajalingam et al., 2009; Shaw and Riederer, 2003). ASB-14 is a nonionic detergent, which form micelles around hydrophobic proteins to allow for extraction from cellular structures such as cellular membranes (Shaw and Riederer, 2003). Bromophenol Blue has a slight negative charge and migrates at a similar rate to proteins, and can therefore be used to visualize the movement of proteins through the gel during the first dimension (Rai et al., 2005). Thiourea improves the solubilization of hydrophobic membranes; however, thiourea has a reactive sulphur atom that bonds to iodoacetamide during equilibration, which hinders the alkylation of proteins after first dimension (Shaw and Riederer, 2003). Therefore, DTT and tris-base are added as a reducing agent to prevent this from occurring. DTT and tris-base are also useful for the reduction of disulfide

bonds, which aids in the solubilization of proteins within a mixture. The IPG buffer (ampholyte) is added to eliminate background staining, improve resolution and spot intensity, and ensure optimal conditions for uniform separation within our pH range by inhibiting interactions between hydrophobic proteins and immobilines (GE Healthcare).

Proteins were then precipitated from the supernatant with 10% trichloroacetic acid (TCA) in cold acetone. TCA binds well to unfolded proteins, which allows the protein to precipitate out of solution, forming a pellet that can then be washed of the TCA with cold acetone (Rajalingam et al., 2009). It is crucial to keep everything cold during these steps to reduce the activity of proteases and avoid proteins resuspending from the pellet before desired.

The pellet containing the precipitated proteins was immediately resuspended in rehydration buffer containing 7 M Urea, 2 M Thiourea, 2% CHAPS, 2% NP-40, 0.002% Bromophenol Blue, 0.5% IPG buffer, and 100mM dithioerythritol (DTE). The purpose of the rehydration buffer is to resuspend the precipitated protein pellets and prepare them for the first dimension. CHAPS and NP-40 are nonionic detergents (function described above) and CHAPS is currently the most commonly used for 2D gels (Shaw and Riederer, 2003). DTE is an alternative reducing agent to DTT and tris-base, and is used during the first dimension because it migrates towards the anode, resulting in re-oxidation of disulfide bonds on the basic end the gel, preventing some proteins (e.g., keratin) from being precipitated (Shaw and Riederer, 2003).

Protein concentrations were measured using a 2D Quantification Kit (GE Healthcare, Piscataway, NJ, USA). The 2D quantification kit resuspends precipitated proteins in a copper solution, and binds any unbound copper to a calorimetric agent,

allowing protein concentration to be estimated via spectrophotometry (GE Healthcare). The purpose of finding the concentration of our protein solutions is to standardize how much protein being put into each gel, therefore allowing us to estimate relative abundances.

1.3.3.2 Two-Dimensional Gel Electrophoresis

Samples were then added to IPG strips (11 cm, pH range 3–10 non-linear; Bio-Rad, Hercules, CA, USA) based on protein concentration. We chose to use the 3-10 pH range because it encompassed a larger range of proteins than the 5-8 pH gels, without losing too much resolution in the most concentrated areas of the gel. Proteins were then separated by isoelectric point and frozen at −80°C until further use. The isoelectric point of a protein is the pH at which the protein is neutral (i.e., pK_a) (Lovrić, 2011). The purpose of separating proteins by isoelectric point are so we can have a linear separation of proteins along x-axis of the 2D gel for further separation by molecular mass. This allows us to separate each individual protein because most proteins have a unique combination of isoelectric point and molecular mass.

To separate proteins according to the molecular mass, we first incubated IPG strips in equilibration buffer with DTT. Then the strips were soaked in iodoacetamide to prevent disulfide bonds from reforming and again quenched with DTT (Lovrić, 2011). Strips were placed on top of 11.8% polyacrylamide gels in SDS running buffer. Polyacrylamide is used for gels because it is stable in a wide range of temperatures and voltages, can be stained in a variety of ways, and is convenient for further digestion and extraction protocols (Rüchel et al., 1978). SDS is a strong detergent that surrounds the

polypeptide backbone of a protein, thus adding a consistent 1.4 g SDS/g of polypeptide (Deber et al., 2009). This additional mass eliminates any impact the original charge of protein may have on how the protein travels through the gel. The purpose of the second dimension is to separate the protein by molecular mass, and SDS allows proteins with similar molecular weights to migrate consistently, irrespective of their mass to charge ratio. Gels were immediately stained with colloidal Coomassie Blue (G-250). Coomassie Blue (G-250) binds to the proteins in the gel to allow us to visually quantify their relative abundances. Images of the gels were then scanned into a computer for analysis.

1.3.3.3 Spot Identification

Delta 2D gel analysis software (Version 4.3, Decodon, Greifswald, Germany) was used for image analysis and spot identification. For time-point comparison, protein spots on all 2D gels were detected and warped to a reference gel from each tissue and time-point combination. Subsequently, the reference gel from the early-fasting time-point was warped to the reference gel from the late-fasting time-point for each tissue. A master fused-image gel for each tissue was then created by fusing all the gel images for the given tissue to the fused reference gel image for each tissue (Fig. 1A-C). For tissue comparison, the fused image from each time-point was warped to a reference gel to create a master fused image for separate analysis (Fig. 1D). Fused gel images contain all spots detected in any gel and at their maximal intensity (Fig. 1A-D). Using a spot detection algorithm, spots on the master gel were detected and possible artifacts were removed after visual inspection. We then generated a proteome map, which represents mean volumes for each spot. Spot boundaries from the master gel were then exported to all individual gels,

thereby eliminating variability in spot detection and ensuring close spot matching. After background subtraction, protein spot volumes were normalized against the total spot volume of all proteins in a gel image.

1.3.3.4 Mass Spectrometry

Proteins that exhibited significant changes in abundance between both time-points were identified using MS. Protein spots were excised and de-stained twice, then subsequently digested with trypsin (Promega, Madison, WI, USA). Trypsin digest cleaves proteins at the c-terminal of arginine and lysine amino acids, this breaking the protein into smaller fragments that are more easily analyzed by MS (Olsen et al., 2004).

Trifluoroacetic acid (TFA) and acetonitrile were then used to extract digested proteins from the gel. TFA was used to stop the trypsin digestion (Hellman et al., 1995), and acetonitrile was used for the dehydration of the gel pieces (Lovrić, 2011). Individual digested protein samples were mixed with matrix solution (0.7mg/mL α-cyano-4-hydroxycinnamic acid (HCCA) in 85% Acetonitrile, 15% H_2O, 0.1% TFA, and 1mM $NH_4H_2PO_4$) and spotted twice on a target plate (Bruker Daltonics Inc., Billerica, MA, USA). The HCCA creates a crystallized matrix that covers our protein sample on the target plate. The purpose of this crystallized matrix is to act as a buffer between our sample and the laser, facilitate ionization, and carry the ionized samples through the flight tube. One set of the spotted proteins were then washed with 0.1% TFA and recrystallized using a mixture of acetone/ethanol/0.1% TFA.

A MALDI-TOF-TOF mass spectrometer (Ultraflex II; Bruker Daltonics Inc) was used to obtain peptide mass fingerprints (PMF or MS). This mass spectrometer works by

ionizing the isolated protein sample with a laser (MALDI), then measuring the time that the resulting ions are in flight through the flight tube (TOF) (Lovrić, 2011). TOF-TOF means that there are two time of flight stages, which increases the resolution of results.

Using Mascot (Version 3.1; Matrix Science Inc., Boston, MA, USA), a combination of PMF and tandem mass spectra (MS/MS) data were searched against four metazoan databases: 1) a National Center for Biotechnology Information (NCBI) -EST library limited to *Mirounga* that contained approximately 5,000 entries (August 2016), 2) a NCBI-EST library, limited to *Leptonychotes weddellii,* that contained approximately 26,000 entries (August 2016), 3) a NCBI-EST library limited to Rodentia that contained approximately 7,792,000 entries (August 2016), and 4) a NCBI dataset of non-redundant metazoan sequences that contained approximately 7,379,000 entries (August 2016) to identify proteins. A molecular weight search (MOWSE) score above the indicated value and a p-value < 0.05 confirmed that the probability of a match was not a random event.

1.3.3.5 Statistical Analysis

Normalized spot volumes for each time-point were analyzed individually for each tissue in Delta 2D using a t-test ($P < 0.05$) to determine which proteins significantly changed abundance between the early- and late-fasting time-points. Each tissue was analyzed independently. We used 1000 permutations to generate our own F-distribution and thereby account for unequal variance and non-normal distribution. A P-value of 0.05 was chosen to limit type I error. We then ran a 2-way analysis of variance (ANOVA) ($P < 0.05$) with 1000 permutations to investigate how protein expression differed between tissues across time-points.

We used hierarchical clustering with average linking (Delta 2D) and a Pearson correlation coefficient to group proteins with similar abundance patterns between early- and late-fasting time-points for the creation of heat maps. Hierarchical clustering is a type of cluster analysis that results in a set of clusters, with data in each cluster being distinct from other clusters and data within a cluster being broadly similar (Maimon and Rokach, 2005). We used hierarchical clustering to organize the proteins in a way that helped us identify trends. A Pearson correlation is an analysis that measures the linear correlation between two variables, and was used to determine which proteins would be included in which cluster (Benesty et al., 2009). These clusters are specific to each heat map and are used to characterize changes in protein abundances.

A principle component analysis (PCA) was then performed on significant spots to further analyze the variation between early- and late-fasting time-points for each tissue. A PCA is a statistical method used to account for variation between time-points and tissues. The x-axis is a linear combination of variables that have maximum variance, accounting for most the variation in the data (Wold, 1987). The y-axis is a combination of variables that accounts for the remaining variation between groups. PCAs provided a visual display of what time-points and tissues differ the most in their pattern of protein expression. The PCA is scaled by the protein's loading values, which is the difference in abundance between time-points and tissues.

Expression profiles, which are a graphical representation of a single protein's abundance between time-points and tissues, were created for each protein to effectively showcase differences in protein abundance. The x-axis represents the time-points or

tissue categories, and the y-axis represents the relative abundance of the protein with the normalized spot volume.

1.4 CONCLUSIONS

Marine mammals first began evolving approximately 35.6 mya, with Phocids splitting from other marine mammals approximately 23-27 mya (Bininda-Emonds et al., 1999; Higdon et al., 2007). Phocids in particular have evolved many unique life history traits, such as the 8 to 12-week post-weaning fast that NES pups experience after weaning (Reiter et al., 1978). During this post-weaning fast, NES pup experience a complete absence of food and water as they learn to dive and forage independently (Reiter et al., 1978).

Copious research has been conducted on these fasting and diving adaptations (i.e., Crocker et al., 2016); however, our project aimed to look deeper into elucidating the molecular mechanisms behind these known adaptations and the physiological stress associated with them. We looked at a wide range of physiological processes to answer our question in the most complete manner, including energy metabolism, cytoskeletal structure, proteostasis, oxygen storage, and the immune system. We also compared how different tissues vary in their patterns of protein expression across the post-weaning fast.

To accomplish these research goals we utilized proteomics, a technique which aims to quantify all proteins present in a given organism (i.e., the proteome) (Lovrić, 2011). Although there are many challenges associated with proteomics, it is an invaluable physiological tool, as it provides a large, unbiased data set of proteins which provide a

comprehensive set of mechanisms involved with the cellular processes being studied (Beranova-Giorgianni, 2003; Görg et al., 2004).

CHAPTER 2: THE POST-WEANING FAST

2.1 ABSTRACT

Northern elephant seals (*Mirounga angustirostris*) transition from terrestrial nursing pups to pelagic foraging juveniles in a short period of just 8-12 weeks. During this post-weaning period, pups rely solely on the energy reserves gained during nursing for their caloric demands and water supply. The prolonged absence of food after weaning is the first of many fasts for which the seals have evolved adaptations such as decreased urine production and increased blubber reserves. The purpose of this study was to understand the tissue-specific molecular fasting- and diving-induced adaptive responses of pups during this critical transition. To investigate this, we collected skeletal muscle and (inner and outer) adipose tissue from early-fasting (<1 week post-weaning) and late-fasting (8 weeks post-weaning) pups. We analyzed the samples with mass-spectrometry-based proteomics using two-dimensional gel electrophoresis. In all three tissues, we found significant shifts in energy metabolism proteins, including a decrease in lipolysis and urine production, and an increase in alternative metabolic pathways, such as the pentose phosphate pathway, which produces precursors for nucleic acid synthesis. We also found increases in cytoskeletal proteins, skeletal muscle proteins, and oxygen-binding proteins, which would facilitate the development of diving ability in late-fasting pups. Lastly, changes in the abundance of oxidative stress related proteins showed increased use of antioxidant proteins to control the production of reactive oxygen species in late-fasting pups. This study provides insight into cellular and physiological responses in marine mammals during ontogeny and their adaptive capacity during a key transition from a terrestrial to aquatic lifestyle.

2.2 INTRODUCTION

2.2.1 Elephant Seal Pups and The Post-Weaning Fast

Many animals have physiological adaptations that allow them to survive a wide range of environmental conditions (Somero et al., 2017). Marine mammals are characterized by physiological adaptations which allow them to survive in extreme environments. For instance, they are able to survive cold water temperatures (e.g., Weddell seals: -2 to 10°C), high water pressures during deep dives (e.g., northern elephant seals: 1530m), and prolonged periods of hypoxia during dives (e.g., northern elephant seals: 20-60 minutes) (Berta et al., 2006; Hoelzel, 2002). While on land, many marine mammals experience periods of prolonged fasting (Lester and Costa, 2006; Worthy, 1991a). Northern elephant seals (NESs; *Mirounga angustirostris*), in particular, experience periods of fasting for up to three months, depending on age and sex (Le Boeuf and Peterson, 1969). The first of these occurs when NES pups undergo an 8 to 12 week fast after weaning (Le Boeuf and Peterson, 1969; Somo et al., 2015). The ability to cope with these periods of fasting is crucial for survival, and is largely dictated by their life history (Bartholomew, 1970).

Following birth, NES pups nurse for 28 d, gaining approximately 100 kg during the nursing period (Bryden, 1969). Parental care is brief; pups are abruptly weaned after 28 days of nursing and are left without having been taught how to forage or dive independently (Reiter et al., 1978). This is especially common for phocid ("true") seals, but different from the typical transition to independence seen in other mammals, which often consists of many forms of parental investment and in the case of some otariids (eared seals) and ungulates, instances of limited continued care after weaning (Altmann, 1958; Gosling, 1969; Lowther and Goldsworthy, 2016; Trillmich, 1979; Trites et al.,

2006; Trivers, 1972). NES pups experience an 8-12-week post-weaning fast that coincides with when they begin to learn dive (Reiter et al., 1978). During this time, pups do not have a source of food or water, and they lose approximately 25% of their body weight as they transition from a terrestrial to primarily aquatic lifestyle (Ortiz et al., 1978; Reiter et al., 1978).

Many stressors during the post-weaning fast could potentially affect NES pup physiology. For instance, recently weaned pups experience novel social interactions (e.g., play fights and competition for space), morphological changes (e.g., molting) and behavioral changes (e.g., swimming and diving), which all influence physiology (Reiter et al., 1978). The ontogeny of swimming and diving capabilities is particularly interesting because it gradually introduces pups to the stressors of swimming in open water, such as temporary hypoxia, increased pressure with dive depth, and colder temperatures while learning to swim and search for prey (Ponganis, 2011). After the pups have perfected their swimming and diving skills, they begin swimming to nearby beaches, eventually departing to sea for their first foraging migration (Reiter et al., 1978).

Fasting is a natural component of NES life history. Thus, it is not surprising that despite the physiological stress associated with diving and prolonged fasting, pups maintain electrolyte and fluid balance, as well as normal body temperatures and metabolic activity, with no known long-term detrimental effects (Crocker et al., 1998; Ortiz et al., 1978; Ortiz et al., 2001; Ortiz et al., 2006; Vazquez-Medina et al., 2012; Vázquez-Medina et al., 2010). To maintain water balance while fasting, seals have complex nasal turbinates, which decrease respiratory water loss by cooling air as it is exhaled, therefore causing the water to condense inside the nasal passageway (Schmidt-

Nielsen et al., 1970). The seals also exhibit increased urine osmolality (Ortiz et al., 1996) and decreased urine production (Adams and Costa, 1993; Ortiz et al., 1996). Adaptations for swimming and diving in seals include high myoglobin and hemoglobin concentration to increase oxygen stores (Kanatous et al., 1999), a reduced surface area to volume ratio for thermoregulation, and large blubber stores (up to 40% of total mass in pups) for both thermoregulation and maintaining metabolic activity while diving and fasting (Bryden, 1969).

2.2.2 Proteomics

We used proteomics to analyze the molecular mechanisms underlying NES pup development during the post-weaning fast. Proteomics is a powerful tool used to identify which proteins are present in a given tissue and at what abundance. Proteomics is a crucial component when studying physiology because it provides a large, unbiased data set of proteins, which often provide a comprehensive set of biochemical mechanisms involved with the cellular processes being studied. This method has only been used to analyze marine mammal physiology a handful of times (e.g., Neely, Ellisor, & Davis, 2018; Sobolesky e al., 2016), and has often led to unanticipated and novel results (Görg et al., 2004). Due to the increasing number of genome sequences and well-annotated expressed sequence tag (EST) libraries, proteomic analyses of non-model organisms have become more feasible (Tomanek, 2011). Proteomics is a method of analysis in which the entire suite of proteins expressed in a cell are analyzed, and allows for a unique perspective on post-translational modifications (Tomanek, 2011). Post-translational modifications shift the molecular weight and isoelectric point of a protein, allowing each

modified protein to be analyzed individually (Mann et al., 2001). Therefore, proteomics targets what proteins are actually being utilized in a given environment, providing insight into the molecular phenotype (Tomanek, 2011).

In this study, we collected skeletal muscle, inner adipose, and outer adipose tissues to analyze physiological adaptations in NES pups throughout the post-weaning fast. Skeletal muscle is used for both terrestrial and aquatic movement, so the proteome of skeletal muscle will highlight important physiological changes that occur as the pups transition from a terrestrial to an aquatic lifestyle (Kanatous et al., 1999). Skeletal muscle is also highly metabolically active, which will provide important physiological insight into the impacts of prolonged fasting. Inner adipose is the first site fats are stored while nursing, and the first location fats are utilized during periods of fasting, thus highlighting proteomic changes due to fasting (Debier et al., 2006; Hooker et al., 2001; Koopman et al., 1996). The fats stored in the inner adipose layer also have thermoregulatory, so the inner adipose would potentially provide insight into physiological changes associated with diving. Outer adipose should be useful to detect changes in the proteome having to do with thermoregulation as well, as it is primarily used for thermoregulation and would experience drastic changes in temperature while the pups learn to dive (Hokkanen, 1990; Irving and Hart, 1957; Worthy, 1991b).

2.2.3 Objectives and Hypotheses

The purpose of this study was to understand the fasting and diving-induced adaptive responses of NES pups during the critical transition from a terrestrial to an aquatic lifestyle. I hypothesized that the post-weaning fast would result in substantial

changes in the pup's proteome due to the stressors associated with prolonged fasting and learning to dive, and that these changes would provide evidence for specific molecular mechanisms associated with fasting and diving. I also expected to see differences in protein expression among tissue types, based on the function of the tissues throughout the post-weaning fast.

2.4 MATERIALS AND METHODS

2.4.1 Experimental Design and Tissue Collection

Tissue samples were collected from NES pups at a rookery in Año Nuevo, CA, USA (37°07'14.7"N 122°20'17.2"W) on February 14th (early-fasting) and March 27th (late-fasting), 2015. The early-fasting pups had been weaned for less than one week, and the late-fasting pups had been weaned for 8 weeks. Animals were sedated and a local anesthetic was administered to the biopsy location. Tissue samples were taken from skeletal muscle and adipose tissue using a 6 mm disposable biopsy punch (Miltex, Plainsboro, NJ), and the inner and outer layers of adipose were separated at the point at which vascularization of the innermost adipose began to noticeably decrease. The samples were immediately flash frozen in liquid nitrogen, transported to California Polytechnic State University (Cal Poly) on dry ice, and kept at -80°C until homogenization. All protocols were performed under NMFS permit #19108 and IACUC protocols.

2.4.2 Sample Preparation and Proteomic Analysis

2.4.2.1 Protein Extraction

Tissue samples were diluted 1:5 (sample:buffer) in buffer containing 7 M urea, 2 M thiourea, 1% amidosulfobetaine-14 (ASB-14), 40 mmol tris-base, 0.001% Bromophenol Blue, 0.5% immobilized pH 3-10 gradient (IPG) buffer, and 0.6% dithiothreitol (DTT) (Tomanek and Zuzow, 2010) while kept on ice. Supernatant was collected after centrifugation at room temperature, and 400µl of protein from each sample was precipitated by adding 4 volumes of ice-cold acetone with 10% trichloroacetic acid and incubating at −20°C overnight. Precipitated proteins were collected by centrifugation at 4°C. The pellets were then washed with ice-cold acetone, centrifuged at 4°C, and air-dried for 5 minutes. The pellet containing the precipitated proteins was immediately resuspended in 400µl rehydration buffer containing 7 M Urea, 2 M Thiourea, 2% CHAPS, 2% NP-40, 0.002% Bromophenol Blue, 0.5% IPG buffer, and 100mM dithioerythritol (DTE) (Tomanek and Zuzow, 2010), and aliquots of the supernatant were stored in 2ml siliconized microcentrifuge tubes at −80°C. Protein concentrations were measured using a 2D Quantification Kit (GE Healthcare, Piscataway, NJ, USA) and the Specramax 384 Plus microplate reader (Molecular Devices, San Jose, CA, USA) at an absorbance of 480nm.

2.4.2.2 Two-Dimensional Gel Electrophoresis

Rehydrated proteins were added to IPG strips (11 cm, pH range 3–10 non-linear; Bio-Rad, Hercules, CA, USA) based on concentration, separated by isoelectric point, and frozen at −80°C until further use. To separate proteins according to the molecular mass,

we first incubated IPG strips in equilibration buffer with dithiothreitol (DTT), then in iodoacetamide to reduce any disulfide bonds, and finally quenched with DTT (Tomanek and Zuzow, 2010). Strips were placed on top of 11.8% polyacrylamide gels in SDS running buffer and proteins were separated at 200V for approximately 55 minutes at 10°C (Criterion Dodeca; Bio-Rad). Gels were immediately stained with colloidal Coomassie Blue (G-250) stain for 24h and subsequently de-stained by washing repeatedly with Milli-Q water for 48h. Images of the gels were digitized using an Epson 1680 transparency scanner.

2.4.2.3 Spot Identification

Delta 2D gel analysis software (Version 4.3, Decodon, Greifswald, Germany) was used for image analysis and spot identification. Protein spots on all 2D gels were detected and warped to a reference gel from each tissue and time-point combination. Subsequently, the reference gel from the early-fasting time-point was warped to the reference gel from the late-fasting time-point for each tissue. A master fused-image gel for each tissue was then created by fusing all the gel images for the given tissue to the fused reference gel image for each tissue (Fig. 1A-C). For tissue comparison, the fused image from each time-point was warped to a reference gel to create a master fused image for separate analysis (Fig. 1D). Fused gel images contain all spots detected in any gel and at their maximal intensity (Fig. 1A-D). Using a spot detection algorithm, spots on the master gel were detected and possible artifacts were removed after visual inspection. We then generated a proteome map, which represents mean volumes for each spot. Spot boundaries from the master gel were then exported to all individual gels, thereby

eliminating variability in spot detection and ensuring close spot matching. After background subtraction, protein spot volumes were normalized against the total spot volume of all proteins in a gel image.

2.4.2.4 Mass Spectrometry

Proteins that exhibited significant changes in abundance between both time-points were identified using mass spectrometry (MS). The following sample preparation for the mass spectrometer was used, following Tomanek and Zuzow (2010). Protein spots were excised and de-stained twice. Proteins were subsequently digested with trypsin (Promega, Madison, WI, USA) overnight at 37°C. Trifluoroacetic acid (TFA) and acetonitrile were then used to extract digested proteins from the gel. Individual digested protein samples were mixed with matrix solution (0.7mg/mL α-cyano-4-hydroxycinnamic acid (HCCA) in 85% acetonitrile, 15% H_2O, 0.1% TFA, and 1mM $NH_4H_2PO_4$) and spotted on a target plate (Bruker Daltonics Inc., Billerica, MA, USA). The spotted proteins were washed with 0.1% TFA and recrystallized using a mixture of acetone/ethanol/0.1% TFA. A matrix-assisted laser desorption ionization tandem time-of-flight (MALDI-TOF-TOF) mass spectrometer (Ultraflex II; Bruker Daltonics Inc) was used to obtain peptide mass fingerprints. Using Mascot (Version 3.1; Matrix Science Inc., Boston, MA, USA), a combination of peptide mass fingerprint (PMF or MS) and tandem mass spectra (MS/MS) data were searched against four metazoan databases: 1) an NCBI-EST library limited to *Mirounga* that contained approximately 5,000 entries (August 2016), 2) an NCBI-EST library limited to *Leptonychotes weddellii* that contained approximately 26,000 entries (August 2016), 3) an NCBI-EST library limited to Rodentia that contained

approximately 7,792,000 entries (August 2016), and 4) an NCBI dataset of non-redundant metazoan sequences that contained approximately 7,379,000 entries (August 2016) to identify proteins (Tables S1A, B). A molecular weight search (MOWSE) score above the indicated value and a p-value < 0.05 confirmed that the probability of a match was not a random event.

2.4.2.5 Statistical Analysis

Normalized spot volumes for each time-point were analyzed individually for each tissue in Delta 2D using a permutation t-test ($P < 0.05$) to determine which proteins significantly changed abundance between the early- and late-fasting time-points. Each tissue was analyzed independently. We used 1000 permutations to generate our own F-distribution and thereby account for unequal variance and non-normal distribution. A *P*-value of 0.05 was chosen to limit type I error. We then ran a 2-way ANOVA ($P < 0.05$) with 1000 permutations to investigate how protein expression differed between tissues across time-points.

We used hierarchical clustering with average linking (Delta 2D) and a Pearson correlation coefficient to group proteins with similar abundance patterns between early- and late-fasting time-points to create heat maps. These clusters are specific to each tissue heat map and are used to characterize changes in protein abundances.

A principal component analysis (PCA) was then performed on the identified spots to further analyze the variation between early- and late- fasting time-points for each tissue. The x-axis (principal component 1, PC1) is a linear combination of variables that explain the highest percentage of variation in the data, accounting for most the variation

in the data (Wold, 1987). The y-axis (principal component 2, PC2) is a combination of variables that accounts for the second highest orthogonal axis explaining the variation between groups (Wold, 1987). The PCAs provide a visual display of what time-points differ the most in protein abundance for each tissue. The PCA is scaled by the protein's loading values, which is the difference in abundance between time-points.

Expression profiles, which are a graphical representation of one specific protein's abundance between time-points and among tissues, were created for each protein to effectively showcase differences.

2.5 RESULTS

2.5.1 Protein Identification

The fused gel image analysis of skeletal muscle, inner adipose, and outer adipose tissue resulted in a total of 273, 272, and 315 distinct proteins spots for each tissue, respectively. Table 1 describes the subset of these total distinct protein spots that were identified and significantly changed abundance between the time-points, and the functional category to which each protein belongs.

2.5.2 Principal Component Analysis

For all PCAs, PC1 primarily describes the proteins that contribute the highest variation between time-points, and PC2 primarily describes the proteins that contribute to variation within tissues (Fig. 2A-D).

2.5.2.1 Muscle Tissue

PC1, which separated the early- and late-fasting time-points, accounted for 47.23% of the protein abundance variation (Fig. 2A). Cytoskeletal proteins (chain A structures of actin-bound protein, troponin T, myosin), proteostasis proteins (glutathione-S-transferase P, C→U-editing enzyme APOBEC-2, elongation factor 1 α), and a blood protein (myoglobin) showed the most positive loadings (i.e., higher abundance in late-fasting relative to early-fasting pups) for PC1 (Table 2). Proteins that contributed negative loadings (i.e., lower abundance in late-fasting relative to early-fasting pups) were energy metabolism proteins (mitochondrial aconitase, fructose-bisphosphate aldolase A), a cytoskeletal protein (myosin), proteostasis proteins (heat shock cognate 71kDa, heat shock protein β-1, peroxiredoxin-6, α-crystallin B chain, heat shock protein β-6, ES1 protein homolog mitochondrial 1), and one blood protein (serum albumin) (Table 2).

PC2 accounted for 16.20% of the protein abundance variation, and both time-points were found along the same plane on the y-axis (Fig. 2A). Energy metabolism proteins (glyceraldehyde-3-phosphate dehydrogenase, fructose-bisphosphate aldolase A), cytoskeletal proteins (slow skeletal muscle troponin T), and proteostasis proteins (α-crystallin B chain, heat shock protein β-6, heat shock protein β-1, peroxiredoxin-6, glutathione-S-transferase P) showed the most positive loadings for PC2 (Table 2). Proteins that contributed negative loadings were energy metabolism proteins (triosephosphate isomerase), cytoskeletal proteins (myosin, slow skeletal muscle troponin T), proteostasis proteins (C→U-editing enzyme APOBEC-2, heat shock protein, heat shock cognate 71kDa, Cu-Zn superoxide dismutase, ES1 protein homolog mitochondrial 1), and blood proteins (serotransferrin, serum albumin) (Table 2).

2.5.2.2 Inner Adipose Tissue

PC1, which separated the early- and late-fasting time-points, accounted for 52.96% of the protein abundance variation (Fig. 2B). Energy metabolism proteins (6-phosphogluconate dehydrogenase, pyruvate kinase PKM), and cytoskeletal proteins (fibulin-5, collagen α-2(VI) chain, collagen α-1(VI) chain, prolargin, galectin-3). showed the most positive loadings for PC1 (Table 3). Proteins that contributed negative loadings included an energy metabolism protein (monoglyceride lipase), proteostasis proteins (calreticulin, peroxiredoxin-2, heterogeneous nuclear ribonucleoprotein H1, cathepsin D), and blood proteins (haptoglobin, fibrinogen δ chain) (Table 3).

PC2 accounted for 9.55% of the protein abundance variation, and the treatment groups were found along the same plane on the y-axis (Fig. 2B). Energy metabolism proteins (mitochondrial glutamate dehydrogenase), cytoskeletal proteins (keratin type II cuticular Hb5, α-2-HS-glycoprotein isoform, prolargin, collagen α-1(VI) chain), and blood proteins (serotransferrin, α-1-antitrypsin, plasminogen isoform) showed the most positive loadings (Table 3). Proteins that contributed negative loadings were energy metabolism proteins (3-ketoacyl-CoA thiolase, apolipoprotein A-1), cytoskeletal proteins (actin-related protein 3), proteostasis proteins (Cu-Zn superoxide dismutase, calreticulin, cathepsin D) and blood proteins (complement C4-A, haptoglobin) (Table 3).

2.5.2.3 Outer Adipose Tissue

PC1, which separated the early- and late-fasting time-points, accounted for 43.77% of the protein abundance variation (Fig. 2C). Cytoskeletal proteins (collagen α-2(Vl) chain, collagen α-2(V) chain, four and a half LIM domains 1, collagen α-3(VI)

chain, keratin type I cuticular HA1) showed the most positive loadings (Table 4). Proteins that contributed negative loadings were energy metabolism proteins (apolipoprotein A-1, fatty acid-binding protein, triosephosphate isomerase), proteostasis proteins (calreticulin, Peroxiredoxin-1, cathepsin D), and blood proteins (serum albumin, haptoglobin) (Table 4).

PC2 accounted for 7.39% of the protein abundance variation and we found no separation along the y-axis (Fig. 2C). Energy metabolism proteins (transketolase, NADP isocitrate dehydrogenase, triosephosphate isomerase), cytoskeletal proteins (prolargin), proteostasis proteins (selenium-binding protein), and blood proteins (serotransferrin, complement factor B, fibrinogen β chain) showed the most positive loadings (Table 4). Proteins that contributed negative loadings were energy metabolism proteins (cytochrome oxidase subunit 1), cytoskeletal proteins (type II cuticular Hb3 keratin, cytoplasmic actin, keratin 81, mimecan, type I cytoskeletal 14 keratin), proteostasis proteins (BTB/POZ domain-containing KCTD12), and blood proteins (fibrinogen δ chain) (Table 4).

2.5.2.4 All Tissues and Time-points Combined

PC1, which primarily separated the early- and late-fasting time-points, accounted for 32.72% of the protein abundance variation (Fig. 2D). PC2, which primarily separated the different tissues accounted for 25.14% of the protein abundance variation (Fig. 2D). Proteins that contributed most to PC! And PC2 can be found in table 5.

2.6 DISCUSSION

Using proteomics, we were able to investigate the cellular and molecular changes that occur in NES pups during the ontogenetic shift after weaning and before migration out to sea. The early- and late-fasting time-points revealed complex physiological changes to prolonged fasting but also to the early ventures into swimming and diving. We also uncovered novel tissue-specific trends in proteins expression. These results will be discussed in terms of functional categories, which will organize proteins by function and tissue.

2.6.1 Comparison Between Time-points

2.6.1.1 Energy Metabolism

2.6.1.1.1 Decreased Lipid Metabolism while Fasting

When glucose is limited, such as during the post-weaning fast, fatty acid β-oxidation is the main fuel source for ATP in NESs (Champagne et al., 2005; Chandel, 2015). However, we found evidence of decreased abundance for proteins involved with lipolysis in the inner and outer adipose tissue of late-fasting pups, indicating a decrease in lipolysis as the pup nears the end of the post-weaning fast (Fig. 3B,C); this is consistent with studies that suggest an overall suppression of general metabolism during periods of prolonged fasting (Berta et al., 2006; Rea and Costa, 1992). There was a decreased abundance of two lipolysis proteins (apolipoprotein A-1, monoglyceride lipase) and an increased abundance of adipocyte fatty acid-binding protein in the inner adipose of late-fasting pups (Fig. 3B). We also found a decrease in all lipolysis and fatty acid β-oxidation proteins (apolipoprotein A-1, mitochondrial electron transfer flavoprotein α,

adipocyte fatty acid-binding protein, monoglyceride lipase) found in outer adipose tissue in late-fasting pups (Fig. 3C).

The abundance of lipolysis proteins were most likely increased in the early-fasting time-point due to the high fat content of the mother's milk (up to 55% fat) (Riedman and Ortiz, 1979). We saw evidence of this with a greater abundance of two lipolysis protein (apolipoprotein A-1, monoglyceride lipase) in early-fasting pups (Fig. 3B,C). Once a pup weans, however, it relies on fat stored during nursing for energy (Bryden, 1969). Following 8 to 12 weeks of fasting, the seals become visually emaciated from their depleted fat stores (30% mass decrease throughout the fast, 35% of which from lipids) (Bryden, 1969; Costa and Le Boeuf, 1986; Noren et al., 2003), which may act as a potential trigger to decrease lipid metabolism in preparation for independent foraging in the ocean. Previous studies in penguins have shown that reaching a certain minimum body fat mass corresponds to a metabolic shift from lipid metabolism to an increase in protein metabolism, due to a decreased effectiveness of protein-sparing (Robin et al., 1998). In elephant seal pups, the nitrogen in urea is recycled to decrease the need for protein metabolism during the post-weaning fast (Pernia et al., 1980). This change in metabolism near the end of the post-weaning fast is important, as pups need to prepare to transition from a lipid-based diet (i.e.,, mother's milk and blubber stores) to a protein-based diet comprised of mainly deep-sea organisms (e.g., cephalopods, teleost, elasmobranchs, and crustaceans) (Le Boeuf and Richard, 1994). Therefore, lipolysis of fat stores is a necessary process for growth and survival during initial fasting, but potentially decreases as the fast progresses and is replaced with increased protein

metabolism. The pups cannot deplete all lipid stores, as these stores are crucial to thermoregulatory success at the beginning of their first foraging migration.

We also found an increased abundance of adipocyte fatty acid-binding protein (AFABP), which acts as an intracellular lipid chaperone for fatty acids, in late-fasting pups (Haunerland and Spener, 2004; Smith et al., 2007). Fatty acids play an important role not only as an energy source, but also as a signal for regulating metabolism, modulating gene expression, and initiating both pro- and anti- inflammatory responses (Hotamisligil, 2006). Most notably, AFABP can form a protein complex with the rate-limiting lipolysis protein, hormone-sensitive lipase (HSL), which binds and inhibits HSL (Shen et al., 1999). As HSL functions in mobilization of stored fats and hydrolysis of triglycerides to free fatty acids, the concomitant increase in AFABP in late-fasting pups inhibits HSL function and provides another mechanism for decreasing lipolysis in late-fasting pups (Smith et al., 2007).

2.6.1.1.2 Increased Pentose Phosphate Pathway Activity

Proteins involved with the pentose phosphate pathway (PPP) increased in late-fasting pups, indicating an increase in biosynthesis (lipid, nucleotide, and amino acids) and synthesis of nicotinamide adenine dinucleotide phosphate hydrogen (NADPH) (Fig. 3B,C). In the PPP, glucose-6-P is shunted away from glycolysis to produce ribose 5-phosphate, erythrose-4-phosphate, NADPH, and pentose sugars, which serve as precursors for nucleotides such as RNA and DNA (Neuhaus and Emes, 2000). We found two proteins involved in the PPP (transketolase and decarboxylating-6-phosphogluconate dehydrogenase), both of which increased in the late-fasting time-point (Fig. 3B,C).

Decarboxylating 6-phosphogluconate dehydrogenase was found in the inner adipose tissue (Fig. 3B), and is involved in the oxidative phase of PPP, which primarily produces pentose sugars that can be converted into metabolites of glycolysis and gluconeogenesis (Kruger and von Schaewen, 2003). The multiple isoforms of transketolase found in both inner and outer adipose (Fig. 3B,C) are involved in the non-oxidative phase of PPP, which is the main pathway by which NADPH is produced in mammals (Kruger and von Schaewen, 2003; Neuhaus and Emes, 2000). NADPH is primarily used for biosynthesis and the scavenging of ROS (Chandel, 2015). We also found an increased abundance of cytoplasmic isocitrate dehydrogenase (NADP) in outer adipose tissue of late-fasting pups (Fig. 3C). The reaction of the NADP-ICD provides another mechanism for NADPH

Lastly, ribose-5-phosphate is a precursor for nucleotide synthesis (Herrmann and Weaver, 1999), and erythrose-4-phosphate is used in the synthesis of aromatic amino acids, both of which are required for growth. Growth is important throughout the post-weaning fast as the pup develops the ability to swim and forage independently. We found support for skeletal muscle restructuring that occurs as the pups utilize their muscles while learning how to swim, discussed in further detail in section 2.6.1.3 (Cytoskeletal Proteins).

2.6.1.1.3 Decreased Energy State after Fasting

During periods of diving and prolonged fasting, phocids have been shown to suppress their general metabolism (Berta et al., 2006; Rea and Costa, 1992). We found a decrease in two proteins (creatine kinase and carbonic anhydrase 3) involved with the overall energy state of late-fasting pups, supporting this decrease in the overall energy

state of the organism. There was a decreased abundance of M-type creatine kinase in the inner adipose (Fig. 3B), and a decreased abundance of carbonic anhydrase 3 in the outer adipose (Fig. 3C) of late-fasting pups.

Creatine kinase is important for a high rate of ATP production and regeneration, as it phosphorylates creatine to creatine phosphate and vice versa (Tryland et al., 2006), providing ATP for tissues that require energy (e.g., skeletal muscle) during periods of high ATP turnover (Kaneko et al., 2008). We suggest that the decrease in creatine kinase indicates a decrease in the necessity to provide high levels of ATP production, as the overall energy state of the pup is low despite the need to produce ATP anaerobically for diving (Tryland et al., 2006). Carbonic anhydrase is a catalyst that converts CO_2 and water, both byproducts of cellular respiration, to bicarbonate in order to maintain acid-base balance in the blood (Mookerjee et al., 2015). A decrease in metabolism would result in a decreased amount of CO_2 being produced, and ultimately result in the organism requiring less carbonic anhydrase. The decreased abundance of both creatine kinase and carbonic anhydrase suggest an overall decreased energy state in the adipose of late-fasting pups.

Other functions of carbonic anhydrase include buffering carbonic acid accumulating from increased CO_2 while diving, increasing diuresis, and promoting the release of oxygen from hemoglobin (Margaria and Green, 1933; Supuran, 2008). Therefore, a decrease in the abundance of carbonic anhydrase could also play a role in many other physiological processes and is used only as evidence to support trends seen in with many other metabolic proteins.

2.6.1.1.4 Osmoregulation

Water balance during prolonged fasting is dictated by the balance between metabolically generated water and obligatory water loss from urine and respiratory evaporation (Condit and Ortiz, 1987; Lester and Costa, 2006; Ortiz et al., 1978). Animals can produce more metabolic water proportionally with lipid oxidation than the oxidation of other substrates(Ortiz, 2001), so we would expect to see lipolysis proteins increase abundance throughout the fast to provide more water. However, we found a decreased abundance of most lipolysis proteins in late-fasting pups (e.g., apolipoprotein A-1, monoglyceride lipase), which suggests that the pups are relying more on metabolic water from carbohydrate metabolism instead. This idea is supported by the large number of metabolic proteins (77 in muscle, 49 in inner adipose, and 56 in outer adipose) that did not change abundance between the time-points, only a handful of which were involved with lipid metabolism (5 in muscle, 1 in inner adipose, and 5 in outer adipose). The suggestion that maintenance is occurring through glycolysis and related pathways is also supported by an increased abundance of three proteins involved with glycolysis and gluconeogenesis (fructose-bisphosphate aldolase A, glycerol-3-phosphate dehydrogenase, triosephosphate isomerase), and the decrease of only one protein (phosphoglycerate kinase 1) in the outer adipose of late-fasting pups; this indicates an increase in the use of glycolysis for the oxidation of glycerol, a key component of triglycerides, a storage fat (Fig. 3C).

Two well-studied mechanisms to decrease urine production include increased urine osmolarity and the reduction of nitrogen load on the kidneys (Adams and Costa, 1993; Ortiz et al., 1996; Pernia et al., 1980), which together help decrease the amount of

urine produced from ~430 ml day^{-1} in the early stages to ~70 ml day^{-1} by the end of the fast (Lester and Costa, 2006). We did not find evidence for increasing urine osmolarity or the recycling of nitrogen through the urea cycle at the protein level that we know is occurring. However, we did find a decreased abundance of two ammonia-related proteins, glutamate dehydrogenase in inner adipose (Fig. 3B) and glutamine synthetase in outer adipose tissue, in late-fasting pups (Fig. 3C). Glutamine synthetase uses ammonia to produce glutamine, which is used to synthesize nonessential amino acids and urea (Liaw et al., 1995). Glutamate dehydrogenase converts glutamate to α-ketoglutarate, an intermediate of Krebs cycle and an intermediate in the production on nonessential amino acids, producing ammonia as a byproduct (Chandel, 2015). Decreases in both glutamate dehydrogenase and glutamine synthetase would result in a decreased production of nonessential amino acids via these pathways, and therefore a decrease in ammonia production and degradation of ammonia to urea. This provides a potential mechanism for the decreased urine production that occurs during the post-weaning fast (Adams and Costa, 1993; Ortiz et al., 1996).

2.6.1.1.5 Maintenance of Carbohydrate and Lipid Metabolism

While fasting, NES pups continue to obtain energy through carbohydrates, lipids, and as a last resort, proteins (Champagne et al., 2005; Pernia et al., 1980). Carbohydrates are the preferred energy source because they are stored as glycogen in the liver and muscle (Champagne et al., 2005; Schutz, 2011). We identified proteins involved in carbohydrate metabolism in muscle of both early- and late-fasting pups. Specifically, proteins involved in glycolysis and gluconeogenesis (fructose-bisphosphate aldolase A,

triosephosphate isomerase, glyceraldehyde-3-phosphate dehydrogenase) and the Krebs cycle (mitochondrial aconitase) all decreased abundance in muscle of late-fasting pups, supporting the known suppression of metabolism occurring during the post-weaning fast (Berta et al., 2006; Rea and Costa, 1992) (Fig. 3A).

In inner adipose, two isoforms of proteins representing aerobic and anaerobic glycolysis (β-enolase, L-lactate dehydrogenase A chain) increased in abundance, and three protein isoforms (glyceraldehyde-3-phosphate dehydrogenase, pyruvate kinase muscle isozyme (PKM), L-lactate dehydrogenase B chain) decreased abundance in late-fasting pups (Fig. 3B). One inner adipose protein involved with ATP synthesis increased (ATP synthase α) in late-fasting pups, which forms the catalytic core of the F1 complex, possibly changing the catalytic properties of this key enzyme of energy metabolism (Fig. 3B) (Velours et al., 2002).

When carbohydrates are limited, such as during a post-weaning fast, gluconeogenesis converts triglycerides to glycerol and amino acids, and converts lactate to glucose to provide sufficient levels of blood glucose (Champagne et al., 2005). Supporting this interpretation, an increase of proteins involved in gluconeogenesis (Fig. 3A-C) and the conversion of lactate to pyruvate for gluconeogenesis (L-lactate dehydrogenase A chain) (Fig. 3B) were found in both early- and late-fasting pups. Most gluconeogenesis that occurs during fasting in marine mammals is from lipids that are stored as a blubber layer (Castellini et al., 1987; Ortiz et al., 2001). Our results are consistent with previous studies that show protein metabolism only accounts for approximately 2.2% of total metabolism during the post-weaning fast, indicating the continuation of lipid and carbohydrate metabolism throughout the post-weaning fast

(Pernia et al., 1980). Therefore, the pattern of protein abundance we found in early- and late-fasting pups suggests maintenance of carbohydrate and lipid metabolism throughout the post-weaning fast (Schutz, 2011).

2.6.1.2 Proteostasis and Cell Signaling

2.6.1.2.1 Regulation of Oxidative Stress Pathways

We found a shift in the antioxidant proteins used to control the concentration and proliferation of reactive oxygen species (ROS) in the early- and late-fasting time-points (Fig. 4A-C). It has been shown that increased oxidative stress can be associated with both physiological (e.g., metabolism) and psychological stressors (e.g., fear) (Clinchy et al., 2013; Moller et al., 1996; Vazquez-Medina et al., 2012). The early-fasting period is associated with a rapid gain in mass, whereas the late-fasting period is associated with a transition from a terrestrial to an aquatic lifestyle (Rea and Costa, 1992; Reiter et al., 1978). Stressors associated with both periods (e.g., vasoconstriction, reperfusion, bradycardia, fatty acid β-oxidation) are all known factors to produce ROS in marine mammals (Irving et al., 1942; Moller et al., 1996; Murdaugh Jr. et al., 1961; Vazquez-Medina et al., 2012; White et al., 1973; Wilhelm Filho et al., 2002; Zapol et al., 1979). However, despite all the potential factors contributing to oxidative stress, it has been shown that there is no significant cellular oxidative damage in NES pups during the post-weaning fast as a result of increased ROS (Vazquez-Medina et al., 2012; Vázquez-Medina et al., 2010), presumably due to an increase in enzymatic and non-enzymatic antioxidants.

Studies have shown that different isoforms of antioxidants are structurally and functionally different, therefore acting as antioxidants through different pathways depending on the nature of the ROS (Apel and Heribert, 2014; McIlwain et al., 2006). We identified both an increase and a decrease in two different isoforms of glutathione-S-transferase (GST), and an increase in peroxiredoxin-6 (PRX6; lysosome and cytoplasm) in the muscle tissue of late-fasting pups (Fig. 4A). We also found an increased abundance of selenium-binding protein 1 in the outer adipose of late-fasting pups, which is a protein involved in the synthesis of an amino acids required for the production of glutathione, an essential non-enzymatic antioxidant (Dilly et al., 2012). In inner adipose tissue, we found a decrease in PRX2 (cytoplasm and secretions) and an increase in *Cu-Zn* superoxide dismutase (Cu-Zn SOD) in late-fasting pups (Fig. 4B). We also found a decrease in PRX1 (cytoplasm, nucleus, and secretions) in the outer adipose of late-fasting pups (Fig. 4C).

The antioxidant *Cu-Zn* SOD functions as the first line of defense to scavenge ROS and converts superoxide anion to hydrogen peroxide within the mitochondrial intermembrane space or cytosol (Tomanek, 2015). Hydrogen peroxide is dismutated to water by the antioxidants PRX and thioredoxin using NADPH as a reducing equivalent to transfer between oxidized and reduced forms (Tomanek, 2015). Glutathionylation of proteins by GST is used to protect cysteine residues from oxidation and protect proteins from oxidative damage (Murphy et al., 2008). Thus, the NADPH produced by the increased PPP discussed earlier is useful to ameliorate the effects of ROS produced due to increased hypoxia and reoxygenation during diving and resurfacing (Juhnke et al., 1996; Tomanek, 2015). Late-fasting pups showed evidence of increased protein

abundance of GST and *Cu-Zn* SOD (Fig. **), whereas early-fasting pups showed increased abundance of GST and PRX1/2/6; together, these changes include three major ROS scavenging systems (Tomanek, 2015). Our results therefore support the idea that both the early- and late-fasting time-points are associated with different physiological stressors, thus resulting in oxidative stress ameliorated through slightly different ROS scavenging systems.

Lastly, we found a decreased abundance of mitochondrial aldehyde dehydrogenase (ALDH2) and flavin reductase (NADPH) in the outer adipose of late-fasting pups. ALDH2 functions as a protector against oxidative stress from lipid peroxidation (Ohsawa et al., 2003; Ohta et al., 2004), while flavin reductase (NADPH) may regulate ROS by providing NADPH. The decreased abundance of ALDH and flavin reductase in late-fasting pups suggests that NADPH production for enzymatic antioxidants (GST and PRX) primarily occurs through the PPP, as discussed in section 2.6.1.1.2 (Increased Pentose Phosphate Pathway Activity), rather than NADPH-producing reactions such as those by flavin reductase and ALDH2 (Fig. 4A-C). We predicted adipose tissue to be the most susceptible to oxidative damage due to lipid oxidation, but our results suggest there is limited ROS production in the outer adipose due to several antioxidant proteins increasing in abundance. It may be possible that ROS generation in adipose tissue is minimized by using flavin to shuttle electrons by FADH to complex II of the ETC, which bypasses complex I, thereby producing fewer ROS (Tomanek, 2015); however, this is a hypothesis requiring further investigation.

2.6.1.2.2 Epigenetic Regulation

We found a shift in isoforms of a gene regulatory protein, C→U-editing enzyme apolipoprotein B mRNA editing enzyme, catalytic polypeptide-like-2 (APOBEC2) (Fig. 4A), which provides evidence for the regulation of epigenetic changes in late-fasting pups. Epigenetic changes are modifications to gene expression due to something other than changes to the genetic code (e.g., development) (Bird, 2007), and this phenotypic plasticity is important for organisms in adapting to physiological stressful situations (Bird, 2007). There are many mechanisms by which gene expression can be modified through epigenetics, such as histone modification (including acetylation), deoxyribonucleic acid (DNA) methylation, expression of repressor proteins, post-translational modifications, ribonucleic acid (RNA) editing, and cell differentiation (Bird, 2007; Blanc and Davidson, 2003).

The increase in one isoform and decrease in two isoforms of APOBEC2 in muscle tissue of late-fasting pups (Fig. 4A) is potentially due to post-translational modifications (pI 5.2 to 7.75; MW 36 to 85 kDa). APOBEC2 is specifically involved with the changing of cytosine to uracil in RNA (Blanc and Davidson, 2003), and plays a role in the RNA editing of high affinity antibodies through deamination of single-stranded DNA and mRNA (Prochnow et al., 2007), both of which could substantially influence the protein being translated from a single gene. The latter suggests that the protein modifications are potentially specific to the immune response, which is discussed further in section 2.6.1.4.3 (Immune Response).

APOBEC2 is also instrumental in maintaining ratios of muscle fiber types in skeletal muscle, which all have different metabolic features for energy production (Sato

et al., 2010). APOBEC2 deficiency is associated with an increase in slow-twitch fibers, which primarily utilized aerobic metabolism, as opposed to fast-twitch fibers associated with anaerobic metabolism (Sato et al., 2010). We did not see a complete decrease in APOBEC2, but rather a shift in the isoforms being utilized. This shift in isoforms could potentially cause a shift in the ratio of muscle fiber types being utilized, which is supported by a shift in the isoforms of troponin T that are specific to slow skeletal muscle seen in the muscle tissue of late-fasting pups. The restructuring and atrophy/hypertrophy of skeletal muscle in late-fasting pups is discussed further in section 2.6.1.3 (Cytoskeletal Proteins).

2.6.1.2.3 Regulation of Signaling Pathways

We found changes in the abundance of cell signaling proteins that suggest cell signaling pathways underwent modifications during development. Signaling pathways are ubiquitous throughout the cell, and are involved in any number of cellular functions (Hamm, 1998).

We identified a decreased abundance of guanine nucleotide-binding protein (G-protein) and broad complex/tram-track/bric-a-brac/poxvirus and zinc finger (BTB/POZ) domain-containing protein potassium channel tetramerization domain (KCTD) 12 in the outer adipose of late-fasting pups (Fig. 4C), which is a protein involved with accelerating the onset and eventually promoting desensitization of cell signaling pathways (Schwenk et al., 2010). We found increases in a precursor for cell division control protein 42 (cdc42) homolog, a protein involved with regulating cytoskeletal networks during cell division (Oceguera-Yanez et al., 2005) in the inner adipose of late-fasting pups (Fig. 4B).

We also found an increased abundance of phosphatidylethanolamine binding protein 1 in the inner adipose of late-fasting pups (Fig. 4B). This protein interacts with mitogen-activated protein (MAP) kinase, a critical component of the MAP kinase signal transduction pathway involved with many different cellular functions, such as cell proliferation, differentiations, and development (Chambard et al., 2007; McCubrey et al., 2007). There was an increase in one protein involved with protein synthesis, elongation factor 1 α (EF1), suggesting an increase in the production of certain proteins (Fig. 6A). EF1, which increased in the muscle tissue of late-fasting pups (Fig. 6A), is responsible for bringing tRNAs to the ribosome for the synthesis of ubiquitously expressed proteins (Ban et al., 2015). Lastly, ES1 protein homolog mitochondrial 1, a protein believed to function as a small ribosomal protein and/or in basic mitochondrial function, showed a decrease in muscle tissue of late-fasting pups (Ban et al., 2015). Our results therefore provide evidence of regulation of cellular signaling pathways (primarily those involved with cell proliferation and cytoskeletal reorganization) through both increases (cell division protein 42, phosphatidylethanolamine, EF1) and decreases (G-protein, KCTD12, ES1) in protein abundances during the late-fasting time-points.

2.6.1.2.4 Regulation of Protein Degradation, Biosynthesis, and Folding

There was a decreased abundance of most molecular chaperones involved with the assembly and restructuring of proteins (Fig. 4A-C), including heat shock protein (HSP) 70 kDa, heat shock cognate 71kD, HSP β-1 33 kDa, and HSP β-6 22 kDa in the muscle tissue of late-fasting pups. In addition, we detected a decrease in the endoplasmic reticulum (ER) chaperone, calreticulin, in the inner adipose tissue of late-fasting pups.

The outer adipose tissue showed a decrease in two ER chaperones, 78kDa glucose-regulated protein and two isoforms of calreticulin, in late-fasting pups (Fig. 4A-C). Of the proteins that increased in abundance, HSP 70 and two isoforms of calreticulin were identified in outer and inner adipose tissue of late-fasting pups, respectively (Fig. 4A-C).

We suggest that the decrease in protein abundance of molecular chaperones we observed in late-fasting pups is most likely due to metabolic depression during the prolonged fast. Protein synthesis is energetically expensive, and limiting chaperone protein synthesis would conserve energy. One of the two chaperones that increased in late-fasting pups was HSP70, which hydrolyzes ATP with each chaperoning attempt (Somero et al., 2017). Moreover, a decreased abundance of proteolysis proteins in late-fasting pups (see paragraph below) suggests that proteins that are not degraded through proteolysis may be rescued by chaperones, such as HSP70. Therefore, our results suggest that the decreased abundance of most chaperone proteins in late-fasting pups is most likely due to metabolic depression while fasting, in turn affecting protein synthesis.

We found four proteins involved with protein degradation, three of which decreased in abundance in the late-fasting time-point (Fig. 4B,C), indicating reduced proteolysis. Cathepsin D, which decreased in both inner and outer adipose tissue of late-fasting pups (Fig. 4B,C), is a lysosomal protein that mainly functions in the activation of pre-lysosomal enzymatic precursors, activation and degradation of hormones and growth factors, and degradation of intracellular proteins. Proteasome subunit β type-1, which decreased in the outer adipose of late-fasting pups (Fig. 4C), is a subunit of the 20S proteasome complex that recognizes proteins to be removed because of damage or for regulation of biological pathways (Tomko and Hochstrasser, 2013). The decrease in

proteins involved with degradation is consistent with a decrease in overall metabolism, as this would lead to a decrease in available ATP needed for proteolysis in late-fasting pups.

2.6.1.3 Cytoskeletal Proteins

2.6.1.3.1 Restructuring of Muscle Tissue

We found an increase and decrease in the abundance of several different isoforms of muscle proteins (Fig. 5A-C), indicating a restructuring of skeletal muscle occurring throughout the post-weaning fast. We hypothesize that the restructuring of skeletal muscle is most likely a result of the NES pup's transition from a terrestrial to aquatic lifestyle as they use new muscles while learning to swim. There was an increased and decreased abundance of myosin, slow skeletal muscle troponin T, and a protein involved with the nucleation of actin in the muscle tissue of late-fasting pups (Fig. 5A). There was also a decrease in α-actinin and an increase in LIM domain-binding protein 3 in the muscle tissue of late-fasting pups (Fig. 5A). In the inner adipose tissue, there was increased abundance of actin (Fig. 5B), and in the outer adipose, there was an increased abundance of desmin, tropomyosin α-3 chain, and four and a half LIM domain protein 1 (FHL1) in the late-fasting pups (Fig. 5C).

During the post-weaning fast, pups experience a restructuring of skeletal muscle as they begin to swim for the first time (Reiter et al., 1978). Previous studies have shown for multiple species of pinnipeds that swimming promotes changes in skeletal muscle structure such as increased density of mitochondria, citrate synthase, and myoglobin, which function to increase oxygen stores and the amount of energy available to muscles (Kanatous et al., 1999). Also, studies have shown that the vasoconstriction occurring as a

natural diving response has an effect on the structure of smooth skeletal muscle (Irving et al., 1942). Vasoconstriction is most commonly activated by epinephrine and norepinephrine, which directly activate the muscle and result in a signaling cascade increasing the amount of intracellular calcium. Calcium in turn complexes with calmodulin, which phosphorylates myosin light chains to stimulate cross-bridge cycling and muscle contraction (Wilson et al., 2005). The cross-bridge cycling that occurs during vasoconstriction involves many of the proteins that increased in abundance (tropomyosin) or shifted isoforms (myosin and troponin T) in the late-fasting pups (Fig. 5A-C). Therefore, the shifts in the isoforms of skeletal proteins being utilized before and after the post-weaning fast indicate that there was a restructuring of skeletal muscle fibers during the fast most likely to modulate actomyosin interactions and muscle function.

Previous studies have also shown that although there is an overall decrease in muscle mass throughout the post-weaning fast, there is also Atrophy and hypertrophy of different muscle as the pups utilize new muscles and learn to swim and dive (Bryden, 1969). On land, NESs move primarily using the muscles of the abdominal wall, sub-lumbar muscles, and muscles supporting the forelimb (Bryden, 1973). However, the mode of locomotion changes when the pups begin to swim, as they mainly start to utilize the muscles surrounding the spinal column, the proximal muscles of the hind limb, and the muscles that extend the tarsals and flex the digits (Bryden, 1973). Our study obtained skeletal muscle samples from a single location on the pups, the latissimus dorsi, a muscle near the hind limb involved with aquatic locomotion. Although there is an overall decrease in the total muscle mass of the pups, the area we sampled may be an area experiencing growth or restructuring from increased use of the latissimus dorsi with

swimming, requiring more proteins and different isoforms (Fig. **). Therefore, our results are consistent with the notion of atrophy and hypertrophy of different muscles as the NES pups transition from a terrestrial to aquatic lifestyle.

2.6.1.3.2 Restructuring of the Cytoskeleton

We observed an increase and decrease of many cytoskeletal protein isoforms, suggesting a restructuring of the cytoskeleton occurring throughout the post-weaning fast (Fig. 5B,C). We hypothesize that the restructuring of cytoskeletal proteins is most likely a result of the pups learning to swim, which exposes them to cold temperatures (mean of 14.5°C surface sea water for March 2015) and increased pressure (1atm per ~10 meters of water depth) as they learn to dive (Station 46028 (LLNR 275) - Cape San Martin - 55NM West NW of Morro Bay, CA, 2015). We found both an increase and decrease in the abundance of multiple isoforms of keratin, a decrease in the abundance of α-2-HS-glycoprotein, and an increase in the abundance of cytoplasmic actin, different collagen chains, vimentin, mimecan, fibulin-5, and prolargin in the inner adipose of late-fasting pups (Fig. 5B). In outer adipose, we found both an increase and decrease in nidogen-2 and multiple isoforms of keratin. There were also increases in prolargin, desmin, cytoplasmic actin, mimecan, lumican, transgelin, gelsolin, multiple isoforms of collagen, prelamin-A/C, and dihydropyrimidinase-related protein 2, and a decreased abundance of galectin-1 in the outer adipose of late-fasting pups (Fig. 5C).

Many studies have shown that increased external and internal pressure affects cellular structure (Davies, 1995; Franke et al., 1984; Maniotis et al., 1997). During diving, external pressure increases with dive depth, and internal pressure increases from

the general vasoconstriction that maintains normal levels of blood pressure as the heart rate slows with bradycardia (Irving et al., 1942). Previous studies have shown that transmembrane matrix receptors, cytoskeleton filaments, and nuclear scaffolds respond nearly immediately to external mechanical stress (Maniotis et al., 1997). Studies have also shown that internal pressure, such as stress from blood pressure, promotes stress fiber growth and increased cell adhesion to its substrate (Davies, 1995). Changes in actin are thought to protect the endothelium from potential injury and detachment related to increased pressure on the cells (Franke et al., 1984). Therefore, the restructuring of cytoskeletal proteins in our results (e.g., actin, vimentin, desmin, keratin) are most likely related to the increased pressure the pups are experiencing when learning to dive.

There is also evidence that temperature can affect the cytoskeletal structure of cells (Hokkanen, 1990; Irving and Hart, 1957; Lepock, 2003; Welch and Suhan, 1985; Worthy, 1991b). Although the blubber layers in marine mammals are extremely effective insulation, several studies have shown that the body temperature at the blubber-muscle border is significantly lower than the core body temperature when the animal is submerged in cold water (e.g., Hokkanen, 1990; Irving and Hart, 1957; Worthy, 1991a). It is thought that the seal intentionally decreases the temperature of the outermost muscle through vasoconstriction specific to that muscle, keeping excess heat loss to a minimum (Hokkanen, 1990; Zapol et al., 1979). Previous studies have seen a disassembly of cytoskeletal components such as microtubules and actin filaments at lower body temperatures (Stapulionis et al., 1997), whereas other studies have shown increased polymerization of F-actin (Hoffmeister et al., 2001). Previous studies also suggest that changes in the cytoskeleton due to decreased temperature may result in translational

machinery being modified (Al-Fageeh and Smales, 2006). Therefore, exposure to cold temperatures, such as those experienced during diving, is likely an additional factor contributing to the protein abundance shifts seen in the cytoskeletal structure of muscle and adipose tissue of early- and late- fasting pups.

2.6.1.4 Blood Proteins (Iron Binding and Immunity)

2.6.1.4.1 Shifts in Myoglobin and Hemoglobin

We found a decrease in the abundance of some hemoglobin isoforms, but an increase in the abundance of myoglobin in the late-fasting time-point (Fig. 6A,C), which suggests modification to the oxygen-storage processes of late-fasting pups. We found a decrease in the abundance of hemoglobin subunit α in muscle (Fig. 6A), and a decrease in both hemoglobin subunits α and β in the outer adipose tissue of late-fasting pups (Fig. 6C). We found an increase in two isoforms of myoglobin, both of which increased in the muscle tissue of late-fasting pups (Fig. 6A). We also found an increased abundance of a protein involved with hemoglobin production, and a decreased abundance of a protein involved with hemoglobin degradation (Fig. 6B,C), providing evidence of a potential mechanism for the increased concentration of hemoglobin that is known to occur during the post-weaning fast (Thorson and Le Boeuf, 1994).

Mammals use hemoglobin and myoglobin to facilitate oxygen transport (Hsia, 1998), and studies have confirmed that concentrations of both proteins increase throughout the post-weaning fast (Noren et al., 2001; Thorson and Le Boeuf, 1994). Hemoglobin concentrations increase up to approximately 3.6g/dL and myoglobin concentrations increase to 1.5g/100g over the first 8 weeks of the post-weaning fast

(Thorson and Le Boeuf, 1994). Some studies suggest the different isoforms of hemoglobin subunit β have been evolutionarily selected for potentially different functions (Gilman, 2017; Projecto-Garcia et al., 2013; Rashid and Weber, 1999). For example, different isoforms of hemoglobin have different affinities for oxygen due to structural difference in the heme pocket (Rashid and Weber, 1999). Other studies have shown that there is a correlation between hemoglobin's affinity for oxygen and the concentration of oxygen available to the organism (Projecto-Garcia et al., 2013). Therefore, the shift in hemoglobin isoforms may indicate an adaptive response of increasing oxygen transport abilities as the pups experience decreased oxygen availability while they begin to dive for longer periods throughout the post-weaning fast.

One hemoglobin-producing pathway that was upregulated in late-fasting pups was the conversion of methemoglobin to hemoglobin via NADH- cytochrome b5 reductase (methemoglobin reductase) (Hultquist and Passon, 1971). We found that methemoglobin reductase increased in the inner adipose tissue of late-fasting pups (Fig. 6B). Methemoglobin occurs in mammalian blood when an iron in the heme group of hemoglobin is oxidized to a ferric state (Fe^{3+}) instead of a ferrous state (Fe^{2+}), making it unable to bind to oxygen (Percy et al., 2005). Trace amounts of methemoglobin naturally occur in mammalian blood, but studies have shown that the amount of methemoglobin can increase as a result of oxidant exposure (Hultquist and Passon, 1971; Percy et al., 2005). Therefore, an increased abundance of methemoglobin reductase indicates the increased presence of methemoglobin, potentially due to oxidative stress and the demand for oxygen-binding hemoglobin.

Another indicator of hemoglobin regulation is the decreased abundance of haptoglobin, which is part of a hemoglobin degradation pathway (Faulstick et al., 1962). We found decreases in four isoforms of haptoglobin in the inner adipose (Fig. 6B), and a decrease in two isoforms of haptoglobin in the outer adipose of late-fasting pups (Fig. 6C). Haptoglobin binds to hemoglobin, and the entire haptoglobin-hemoglobin complex is then removed by the reticuloendothelial system (Faulstick et al., 1962). The decrease in the abundance of haptoglobin indicates a decrease in the degradation of hemoglobin, aiding the organism in increasing the concentration of hemoglobin present. Therefore, both the increase in the abundance of methemoglobin reductase and the decrease in haptoglobin both provide evidence of a potential mechanism for the increased concentration of hemoglobin that is known to occur during the post-weaning fast (Thorson and Le Boeuf, 1994).

Mammals use myoglobin to store oxygen in muscles for use when the oxygen from hemoglobin is depleted (Ordway and Garry, 2004), and marine mammals are known to have 10-20x more myoglobin than terrestrial mammals due to their diving demands (Kanatous et al., 1999). The increase in myoglobin we found is consistent with previous studies, which have shown that the myoglobin concentrations of pinnipeds is significantly greater in swimming muscles than non-swimming muscles, and that neonatal pinnipeds are born with 31% of the myoglobin concentration as adults (Kanatous et al., 1999; Noren et al., 2001; Thorson and Le Boeuf, 1994). This increase in myoglobin is necessary to store more oxygen in muscles so marine mammals can dive for longer periods of time (Kanatous et al., 1999). Therefore, the increased abundance of myoglobin

is due to the increased need for oxygen storage as the NES pups begin diving for longer periods of time throughout the post-weaning fast.

2.6.1.4.2 Regulation of Iron

There was both an increase and decrease in the abundance of iron-binding proteins in late-fasting pups, which suggests that iron concentrations in the body are tightly regulated during development (Fig. 6A-C). The regulation of iron is crucial for the proper function of oxygen-binding proteins; however, iron levels that are too high or too low can be detrimental (Sigel et al., 2013). Iron deficiency can cause anemia, which results in insufficient oxygen delivery to organs (Andrews, 1999; Sigel et al., 2013). Excess iron can be detrimental as well, primarily because mammals have no mechanisms of iron excretion (Andrews, 1999; Sigel et al., 2013), and high levels of iron can facilitate bacterial growth (Janciauskiene et al., 2013). Because iron is stored in the liver, pancreas, and heart, excess iron can result in liver cirrhosis, heart failure, and diabetes (Andrews, 1999). Excess ferrous iron (Fe^{2+}) can also react with hydrogen peroxide in the Fenton reaction to produce hydroxyl radicals, which damage macromolecules important for cell function (Poprac et al., 2017; Sies, 1991).

We found a decreased abundance of hemopexin in the outer adipose (Fig. 6C), a decreased abundance of six isoforms of serotransferrin in all three tissues (Fig. 6A-C), and a decreased abundance of six isoforms of haptoglobin in the adipose of late-fasting pups (Fig. 6B, C). We also found three isoforms of serotransferrin that increased in abundance in the outer adipose tissue of late-fasting pups (Fig. 6C). Hemopexin, haptoglobin, and serotransferrin all bind to free iron in the blood stream, thus decreasing

the probability of the Fenton reaction occurring, as well as the occurrence of heme-mediated oxidative stress (Tolosano and Altruda, 2002). The decrease we observed in most isoforms of these proteins suggests a decrease in the amount of total iron available in the body. Previous studies suggest that phocid seals may be iron-limited during the post-weaning fast, although pups are extremely efficient at recycling iron (Burns et al., 2004). The majority of iron in pups is stored in erythrocytes, which are recycled as the pup loses mass throughout the fast, increasing total blood volume and maintaining iron levels in the blood. Erythrocytes that are destroyed can release iron for use in muscle myoglobin. Therefore, these proteins suggest the proper regulation of iron in the body and potential decrease in iron levels in the late-fasting time-period as free-iron is used for the synthesis of hemoglobin and myoglobin.

2.6.1.4.3 Immune Response

The patterns of acute phase protein (APP) abundances suggest increased inflammation in the late-fasting time-point (Fig. 6A-C). APPs are proteins whose concentrations in the blood increase or decrease in response to inflammation or starvation through the acute-phase reaction (Davidson, 2013; Gabay and Kushner, 1999; Gruys et al., 2005). There are two classes of APPs: 1) those that decrease abundance in response to inflammation (negative APPs), and 2) those that increase abundance in response to inflammation (positive APPs) (Davidson, 2013; Gabay and Kushner, 1999). These proteins are regulated through the secretion of cytokines by local inflammatory cells such as neutrophils, granulocytes, and macrophages (Gabay and Kushner, 1999; Janciauskiene

et al., 2013). Cytokines then trigger the response of APPs (secreted by the liver) as a response to inflammation (Davidson, 2013).

We found increases in many positive APPs in the late-fasting time-point (Fig. 6B,C), which included five different isoforms of complement factors. Positive APPs increase to inhibit the growth of microbes and simultaneously inhibit the inflammatory response through negative feedback (Gruys et al., 2005). Complement factors are immune system proteins that clear damaged cells and microbes in the body by tagging them for phagocytosis, promoting inflammation by attracting macrophages and neutrophils, and attacking bacteria by rupturing their cell walls (Murphy and Weaver, 2017). Inactive complement factors are continually circulating in the bloodstream, but are activated by three different pathways: the classical complement pathway, the alternative complement pathway, and the lectin pathway (Murphy and Weaver, 2017). One isoform of complement factor B increased in both inner and outer adipose tissue of late-fasting pups (Fig. 6B,C). The increased abundance in complement factor B, an alternative complement pathway protein, suggests a trigger of either complement factor 3 (C3) hydrolysis, foreign material, pathogens, or damaged cells (Murphy and Weaver, 2017). The increase in two isoforms of complement C4-A in the inner adipose of late-fasting pups (Fig. 6B), a part of both the classical complement pathway and the lectin pathway, indicates that the potential activation triggers may include the presence of antigens with or without antibody complexes or C3 hydrolysis (Murphy and Weaver, 2017). C3, which increased in the outer adipose of late-fasting pups (Fig. 6C), is potentially involved in all three pathways. Galectin-3 also increased in the inner adipose of late-fasting pups (Fig. 3B); although this protein is not an APP, its increase provides evidence of potential

inflammation based on its antimicrobial benefits and role in acute and chronic inflammation (Henderson and Sethi, 2009). The upregulation of these specific APPs and related proteins indicate inflammation in late-fasting pups.

We found decreases in negative APPs in late-fasting pups (Fig. A-C). Negative APPs decrease during inflammation to conserve amino acids for the production of positive APPs (Gruys et al., 2005). There was a decrease of serotransferrin and serum albumin in the muscle tissue of late-fasting pups (Fig. 6A). We found a decrease in the abundance of all isoforms of serotransferrin and antithrombin-III in the inner adipose of late-fasting pups (Fig. 6B). Lastly, there was both an increase and decrease in multiple isoforms of serotransferrin and serum albumin in the outer adipose of late-fasting pups (Fig. 6C). Antithrombin-III is of particular interest because it acts as serpin, inhibiting serine proteases such as thrombin that contribute to blood clotting by converting fibrinogen to fibrin (Gettins, 2002; Yin et al., 1971). The decreased abundance of antithrombin-III in the late-fasting pups is consistent with the decreases found in fibrinogen, adding support that the late-fasting period has increased inflammation. Serum albumin is important in maintaining blood homeostasis, such as maintaining oncotic pressure between blood and tissues by lowering blood pressure and allowing less fluid to enter the tissues (Emerson, 1989; Roche et al., 2008). Studies have shown that serum albumin also plays an important role in trapping the majority of free radicals in mammals as well (Bourdon and Blache, 2004). The decrease and increase in different isoforms of serum albumin suggests that blood homeostasis is tightly regulated during development.

Lastly, we also found decreases in the abundance of several positive APPs in late-fasting pups (Fig. 6B,C). Because positive APPs typically increase in abundance in the

presence of microbes (Gruys et al., 2005), this evidence adds a layer of complexity to our hypothesis that these pups are experiencing inflammation due to microbial infection. There were decreases in six isoforms of fibrinogen and α-1-antitrypsin in the adipose of late-fasting pups (Fig. 6B,C). Fibrinogen is a coagulation factor that traps invading microbes in blood clots (Esmon et al., 2012). However, studies have also shown that decreased abundance of fibrinogens decreases the virulence of certain bacteria (Rothfork et al., 2003). For example, wildtype *Staphylococcus aureus* with a quorum-sensing operon, *agr*, inhibits activation of the promotor for the *agr* effector, thus targeting the downstream production of hemolysin and capsule production (Rothfork et al., 2003). Moreover, expression of virulence genes is often density-dependent, and therefore is shown to increase with fibrinogen-mediated bacterial clumping in certain bacteria (Rothfork et al., 2003). This is also supported by an increased abundance of plasminogen in the inner adipose of late-fasting pups (Fig. 6B), which is not an APP, but is the precursor for plasmin, an important enzyme for the degradation of fibrin blood clots (Rossignol et al., 2004). Antitrypsin is a serpin that downregulates inflammation through binding and inhibiting proteases (Gettins, 2002). Although we would expect antitrypsin levels to increase in response to inflammation, studies have shown that reduced antitrypsin levels can result from changes in collagen metabolism (Hauck et al., 2004), such as the increase in collagen chain abundance found in the late-fasting time-point. Interestingly, six isoforms of haptoglobin and two isoforms of hemopexin, which decreased in protein abundance in the adipose of late-fasting pups, both play a role in the inhibition of microbial growth due to its high affinity for binding free iron microbes could otherwise use for proliferation (Martins et al., 2017; Tolosano and Altruda, 2002).

Therefore, the decreased abundance of these positive APPs would typically indicate a low level of microbial activity, but previous studies have provided evidence that a decrease in positive APPs can occur in the presence of certain microbes or due to other circumstances in the cell.

Our interpretation of increased inflammation in the late-fasting pups based on proteomic changes is contradictory to previous studies that have found inflammation decreases with fasting (Longo and Mattson, 2014), especially in NES pups (Vázquez-Medina et al., 2010). There are many reasons that inflammation may be increased in the pups, such as environmental factors specific to the 2015 breeding season (e.g., El Niño) (Jacox et al., 2016). The 2015 El Niño resulted in significant increases in water temperatures (Jacox et al., 2016), potentially yielding different physiological responses in the 2015 cohort of weaned pups. Factors associated with El Niño events, such as warmer surface water temperatures, have been shown to increase the frequency of microbial infections in marine mammals (Harvell et al., 1999), potentially causing the inflammation seen in late-fasting pups.

2.6.2 Comparison Among Tissues

2.6.2.1 Skeletal Muscle

We found evidence for two main protein abundance trends in muscle tissue: 1) only a few proteins significantly changed abundance in muscle tissue between the early- and late-fasting time-points (Fig. 2D), and 2) a large number of proteins expressed in muscle tissue across the fast were not expressed in any other tissue during either time-point (Fig. 7A). These trends are also both supported by a PCA for our two-way ANOVA

(Fig. 2D), which shows little change across both PC1 and PC2 between time-points in muscle tissue.

Although there is known to be restructuring and atrophy/hypertrophy of skeletal muscle throughout the post-weaning fast (Bryden, 1969; Reiter et al., 1978), we saw evidence for very little change in protein abundance between our two time-points (Fig. 2D), which we hypothesize is due to the hypertrophy of different skeletal muscle groups utilizing the same type of proteins as atrophying muscle groups. Skeletal muscle is not impacted by the cold stressors associated with diving as much as inner and outer adipose (Worthy, 1991a), although exposure to low oxygen conditions from diving has been shown to increase anaerobic and antioxidant pathways (Le Boeuf et al., 1987; Tavoni et al., 2013; Vázquez-Medina et al., 2010).

In our tissue-specific analysis, we did find a restructuring of proteins related to oxidative stress pathways (Fig. 3A) and 31 proteostasis proteins that did not significantly change abundance. This pattern is potentially due to the increase in ROS from hypoxia being offset by the decrease in general metabolism known to occur during the fast decreasing the number of ROS produced. We did not find evidence to support an increase in anaerobic metabolism, but rather found a large number of proteins involved with anaerobic metabolism that did not significantly change abundance throughout the fast. Previous studies have shown that lactate is crucial the recycling of glucose throughout the fast, which could explain why we did not see increases or decreases in anaerobic metabolism proteins (Tavoni et al., 2013). Although pups are known to decrease their overall energy state throughout the fast, a certain level of metabolic activity must be maintained in order for the muscle to function properly. This is also supported by our

tissue-specific analysis, which showed a decrease in 6 metabolism proteins and no significant change in the abundance of 77 metabolism proteins in skeletal muscle. All skeletal muscle proteins that significantly changed abundance (32 proteins) are discussed in more detail previously in section 2.6.1 (Comparison Between Early- and Late-Fasting Pups).

Many proteins (21 metabolism, 16 cytoskeletal, 6 proteostasis, and 2 blood proteins) were found constitutively in muscle tissue, but were not found in adipose tissue during either time-point (Fig. 7A). Given the higher metabolic demand of muscle tissue than adipose tissue, it is reasonable to infer that muscle tissue expresses more proteins and different proteins than adipose tissue (Hokkanen, 1990). Skeletal muscle also has a very different cytoskeletal structure than adipose tissue, and many of 16 cytoskeletal proteins that were only expressed in skeletal muscle are involved with skeletal muscle structure (e.g. myosin and troponin T). As discussed before, studies have shown that different isoforms of antioxidants are structurally and functionally different (Apel and Heribert, 2014; McIlwain et al., 2006), and several were unique to muscle, suggesting different cellular conditions or functional needs of the cell against oxidative stress in skeletal muscle.

2.6.2.2 Inner Adipose

We found evidence for limited changes in protein abundance between the two time-points in inner adipose (Fig. 2D). However, there was one cluster of proteins that significantly increased abundance in the inner adipose of late-fasting pups, and these proteins are of particular interest because they also had a significantly increased

abundance in the outer adipose of early-fasting pups (Fig. 7B). There were no proteins exclusively upregulated in inner adipose..

Inner adipose showed very little change in protein expression between the two time-points, and there were no proteins that were expressed solely in inner adipose tissue. However, this is a logical finding, as inner adipose has important characteristics of both skeletal muscle (e.g., metabolically active) and outer adipose (e.g., thermoregulation) (Best et al., 2003). We would therefore not expect a dramatic change in protein abundance between the two time-points in inner adipose because it is carrying out both of these functions during both time-points of the fast. Inner adipose proteins that did significantly change abundance (72 proteins) in our tissue-specific analysis are discussed in more detail previously in section 2.6.1 (Comparison Between Early- and Late-Fasting Pups).

There was one cluster of proteins, however, that had increased abundance in the inner adipose of late-fasting pups as well as the outer adipose of early-fasting pups (Fig. 7B). These proteins were primarily cytoskeletal (19 proteins), with only a few involved with proteostasis (4 proteins), and none involved with blood or energy metabolism. Fatty acids created through metabolism are deposited initially in the inner adipose (Best et al., 2003). These fatty acids are deposited as polyunsaturated fatty acids (PUFAs), which are also the primary fatty acids to mobilize during periods of fasting. The outer adipose is considered more stable in its composition of fatty acids, and has been found to have higher levels of monounsaturated fatty acids (MUFAs) than PUFAs. PUFAs have been shown to have a better ability to conserve heat (Dunstan et al., 1999), and inner adipose has been found to have higher ratios of PUFA to MUFA compared to outer adipose

tissue, potentially to keep heat from leaving the animal's core (Best et al., 2003). The outer adipose of nursing pups is newly developed, like the inner adipose, during early fasting and has not yet become the stable tissue that is primarily used for thermoregulation, but by the end of the fast this tissue has become more like a stable, distinct tissue (Best et al., 2003). Studies have shown that fatty acids ratios, particularly PUFAs, influence cytoskeletal structure when in the form of phospholipids (Schmidt et al., 2015). We therefore hypothesize that the observed patterns of cytoskeletal protein abundance in inner and outer adipose is potentially due to differences in fatty acid composition.

2.6.2.3 Outer Adipose

The outer adipose had the most variable pattern of protein abundance of all the tissues collected, with three main trends being identified: 1) there was a large number of proteins unique to outer adipose upregulated across the fast (Fig. 7C), 2) many proteins were downregulated in the outer adipose of late-fasting pups that were found to be at high abundance in all other tissues and time-points (Fig. 7D), and 3) that another set of proteins showed an increased abundance in the outer adipose of late-fasting pups, yet were expressed in low abundance in all other tissues and time-points (Fig. 7E). These trends are revealed by a PCA for our two-way ANOVA (Fig. 2D), which shows a distinct difference in PC1 between the outer adipose of late-fasting pups and all other tissues and time-points, and little difference across PC2 between outer adipose and inner adipose.

There was a small number of proteins that were exclusively expressed in outer adipose during both time-points (Fig. 7C). The majority of these proteins were involved

with the cytoskeleton (4 proteins) and proteostasis (3 proteins), with no increased abundance of energy metabolism or blood proteins. The lack of metabolic proteins found at both time-points in outer adipose tissue is consistent with the interpretation discussed above, hypothesizing that outer adipose is primarily used for thermoregulation and not primarily for metabolism. This is also supported by the cluster of primarily metabolic proteins that decreased abundance in the outer adipose of late-fasting pups and had increased abundance in all other tissues and time-points (Fig. 7D). These two trends further suggest that during the nursing period, the outer adipose has a similar structure and function to the inner adipose, but by the end of the fast it has become more of its own distinct tissue.

Lastly, there were a large number of proteins that had increased abundance in the outer adipose of late-fasting pups and no other tissue or time-point (Fig. 7E). This is particularly apparent in the PCA for the two-way ANOVA including both tissues and time-points (Fig. 2D). Many of these proteins were cytoskeletal (17 proteins), with a handful of proteins involved in proteostasis (9 proteins), metabolism (13 proteins), and oxygen delivery and wound healing – functions of blood (9 proteins). The increase in cytoskeletal proteins logically follows, as we have discussed that the outer adipose becomes a distinct tissue as the fast progresses, potentially as the pups experience cold temperatures as they learn to dive. The upregulated proteostasis proteins are primarily involved with protein biosynthesis and epigenetic regulation (see above). We believe this increase in proteostasis proteins is partly due to our experimental design, in which the late-fasting time-point was composed of pups that had been fasting for 8 weeks. Although some pups are ready to begin their migration to sea at 8 weeks, pups can fast up to 12

weeks if needed (Reiter et al., 1978). Therefore, the outer adipose of the pups in our study is most likely not completely established as the distinct, stable tissue it will become in older juveniles. Also, these pups are still experiencing fasting whether they are about to leave for their migration or not, thus influencing protein regulation as well. The increase of several metabolic proteins provides insight into which metabolic pathways are being utilized to fuel the little metabolic activity that occurs in the outer adipose throughout the post-weaning fast. Lastly, nearly half of the blood proteins that had increased abundance in the outer adipose of late-fasting pups were various isoforms of fibrinogen, which was found in no other tissue or time-point. Fibrinogen is a cytoskeletal protein known to be involved in an organism's inflammatory response through blood-clotting (Amara et al., 2008; Rothfork et al., 2003). Previous studies in terrestrial mammals have shown that fibrinogen levels decrease during periods of fasting and cold-exposure, potentially due to adrenal activity (Henriques et al., 1949). Therefore, the increased abundance of fibrinogen during periods of fasting and diving in NES pups highlights an adaptation v of marine mammals (relative to terrestrial mammals) to diving, potentially to mitigate the impact of temperature and pressure on cytoskeletal function and structure.

2.7 CONCLUSIONS

Proteomics is a common method used in molecular biology and many studies have been conducted on the physiology of NES during the post-weaning fast. However, our study is unique because it is the first to combine these two research areas, examining the post-weaning fast of NES pups using proteomics. Therefore, our results provide new insight into the adaptive capacity of marine mammals throughout development.

These novel insights into the molecular physiology of NES during the post-weaning fast can be used in a variety of ways. First, the results showed that our proteomic workflow for NES can be used as a foundation for future proteomics projects involving pinnipeds, such as an ongoing study exploring the diving physiology of Weddell seal pups (Tomanek, unpublished). Our study also provided a foundation for the creation of protocols to use blood serum rather than tissue samples to analyze NES physiology (data not shown). This is an important progression, as blood serum is a far less invasive to sample from marine mammals than tissue and can therefore be obtained more readily.

Second, our results provide insight into the potential impact that environmental stressors might have on the molecular physiology of NES pups, and how those impacts might influence their overall health and survival. Potential environmental stressors can be produced through both natural and anthropogenic avenues (e.g., disease, weather, pollution, and ecological effects of climate change), which cause stress in a variety of ways, including decreased food and increased toxins, e.g., through the food chain. For example, there is evidence that temperature can affect the cytoskeletal structure of cells (Hokkanen, 1990; Irving and Hart, 1957; Lepock, 2003; Welch and Suhan, 1985; Worthy, 1991b). Warmer surface water temperatures have also been shown to increase the frequency of microbial infections in marine mammals (Harvell et al., 1999). Decreased food (not due to fasting) in marine mammals has been shown to decrease metabolic rate, providing evidence for the general suppression of metabolic pathways (Markussen et al., 1992). Toxins and disease negatively impact immune function and can potentially be fatal to marine mammals (Desforges et al., 2016; Estes, 1998). Toxins and disease also negatively impact normal cellular functions, such as protein folding in the

endoplasmic reticulum (ER) (Marciniak and Ron, 2006; Remotti et al., 2008). These physiological responses to stressors would all be reflected in the proteome, meaning proteomics can be used to investigate the impact of a wide variety of stressors on an organism. It is therefore invaluable to begin addressing marine mammal research questions utilizing molecular tools such as proteomics.

We suggest that future work include a comparative analysis of proteomic responses in NES to fasting across age classes and sexes. Comparing fasts, such as the female lactation fast that lacks a diving component, would allow us to further examine which physiological changes are more closely related to diving or fasting. Furthermore, comparing the proteome of NES to closely related species may give insight to the adaptive capacity of other marine mammals during this critical developmental stage.

REFERENCES

Adams, S. H. and Costa, D. P. (1993). Water conservation and protein metabolism in northern elephant seal pups during the postweaning fast. *J. Comp. Physiol. B* **163**, 367–373.

Al-Fageeh, M. B. and Smales, C. M. (2006). Control and regulation of the cellular responses to cold shock: the responses in yeast and mammalian systems. *Biochem. J.* **397**, 247–259.

Allen, K. N. and Vazquez-Medina, J. P. (2019). Ischemia/reperfusion tolerance in diving mammals: A review. *Front. Physiol.*

Altmann, M. (1958). Social integration of the moose calf. *Anim. Behav.* **6**, 155–159.

Amara, U., Rittirsch, D., Flierl, M., Bruckner, U., Klos, A., Gebhard, F., Lambris, J. D. and Huber-lang, M. (2008). Interaction between the coagulation and complement system. *Adv. Exp. Med. Biol.* **632**, 71–79.

Ambrósio, D. L., Lee, J. H., Panigrahi, A. K., Nguyen, T. N., Cicarelli, R. M. B. and Günzl, A. (2009). Spliceosomal proteomics in Trypanosoma brucei reveal new RNA splicing factors. *Eukaryot. Cell* **8**, 990–1000.

Andrews, N. C. (1999). Disorders of iron metabolism. *N. Engl. J. Med.* **341**, 1986–1995.

Apel, K. and Heribert, H. (2014). Reactive oxygen species: metabolism, oxidative stress, and signal transduction. *Annu. Rev. Plant Biol.* **55**, 373–399.

Bader, G. D., Heilbut, A., Andrews, B., Tyers, M., Hughes, T. and Boone, C. (2003). Functional genomics and proteomics: charting a multidimensional map of the yeast cell. *Trends Cell Biol.* **13**, 344–356.

Ban, N., Beckmann, R., Cate, J. H., Dinman, J. D., Dragon, F., Ellis, S. R., Lafontaine, D. L., Lindahl, L., Liljas, A., Lipton, J. M., et al. (2015). A new system for naming ribosomal proteins. *Curr. Opin. Struct. Biol.* **24**, 165–169.

Bartholomew, G. A. (1970). A model for the evolution of pinniped polygyny. *Evolution (N. Y).* **24**, 546–559.

Benesty, J., Chen, J., Huang, Y. and Cohen, I. (2009). Pearson correlation coefficient. In *Noise reduction in speech processing*, pp. 1–4. Berlin, Heidelberg: Springer.

Beranova-Giorgianni, S. (2003). Proteome analysis by two-dimensional gel electrophoresis and mass spectrometry: Strengths and limitations. *Trends Anal. Chem.* **22**, 273–281.

Berta, A. and Wyss, A. (1994). Pinniped Phylogeny. *Proc. San Diego Soc. Nat. Hist.* **29**, 33–56.

Berta, A., Sumich, J. L. and Kovacs, K. M. (2006). *Marine Mammals: Evolutionary Biology*. 2nd ed. Burlington: Elselvier Inc.

Best, N. J., Bradshaw, C. J., Hindell, M. A. and Nichols, P. D. (2003). Vertical stratification of fatty acids in the blubber of southern elephant seals (Mirounga leonina): Implications for diet analysis. *Comp. Biochem. Physiol. - B Biochem. Mol. Biol.* **134**, 253–263.

Bininda-Emonds, O. R., Gittleman, J. L. and Purvis, A. (1999). Building large trees by combining phylogenetic information: A complete phylogeny of the extant Carnivora (Mammalia). *Biol. Rev.* **74**, 143–175.

Bird, A. (2007). Perceptions of epigenetics. *Nature* **447**, 396–398.

Blanc, V. and Davidson, N. O. (2003). C-to-U RNA editing: Mechanisms leading to genetic diversity. *J. Biol. Chem.* **278**, 1395–1398.

Bourdon, E. and Blache, D. (2004). The importance of proteins in defense against oxidation. *Antioxidants Redox Signal.* **3**, 293–311.

Boutilier, R., Nikinmaa, M. and Tufts, B. (1993). Relationship between blood buffering properties, erythrocyte pH and water content, in gray seals. *Acta Physiol. Scand.* **147**, 241–247.

Bryden, M. (1969). Relative growth of the major body components of the southern elephant seal. Mirounga leonina (L.). *Aust. J. Zool.* **17**, 153–177.

Bryden, M. M. (1973). Growth patterns of individual muscles of the elephant seal, Mirounga leonina (L.). *J. Anat.* **116**, 121–133.

Burns, J. M., Clark, C. A. and Richmond, J. P. (2004). The impact of lactation strategy on physiological development of juvenile marine mammals: implications for the transition to independent foraging. *Int. Congr. Ser.* **1275**, 341–350.

Castellini, M. A. and Somero, G. N. (1981). Buffering capacity of vertebrate muscle: Correlations with potentials for anaerobic function. *J. Comp. Physiol. B* **143**, 191–198.

Castellini, M. A., Costa, D. P. and Huntley, A. (1987). Fatty acid metabolism in fasting elephant seal pups. *J. Comp. Physiol. B Biochem. Syst. Environ. Physiol.* **157**, 445–449.

Chambard, J.-C., Lefloch, R., Pouysségur, J. and Lenormand, P. (2007). ERK implication in cell cycle regulation. *Biochim. Biophys. Acta (BBA)- Mol. Cell Res.* **1773**, 1299–1310.

Champagne, C. D., Houser, D. S. and Crocker, D. E. (2005). Glucose production and substrate cycle activity in a fasting adapted animal, the northern elephant seal. *J. Exp. Biol.* **208**, 859–868.

Chandel, N. S. (2015). *Navigating Metabolism*. Cold Springs Harbor, New York: Cold Spring Harbor Laboratory Press.

Chen, S., Martin, C., Maya-Mendoza, A., Tang, C. W., Lovrić, J., Sims, P. F. and Jackson, D. A. (2009). Reduced expression of lamin A/C results in modified cell signaling and metabolism coupled with changes in expression of structural proteins. *J. Proteome Res.* **8**, 5196–5211.

Clinchy, M., Sheriff, M. J. and Zanette, L. Y. (2013). Predator-induced stress and the ecology of fear. *Funct. Ecol.* **27**, 56–65.

Condit, R. S. and Le Boeuf, B. J. (1984). Feeding habits and feeding grounds of the northern elephant seal. *J. Mammal.* **65**, 281–290.

Condit, R. S. and Ortiz, R. M. (1987). The physiological transition from fasting to feeding in weaned elephant seal pups. *Mar. Mammal Sci.* **3**, 207–219.

Costa, D. P. and Le Boeuf, B. J. (1986). The energetics of lactation in the northern elephant seal, Mirounga angustirostris. *J. Zool.* **209**, 21–33.

Cox, C. R. and Le Boeuf, B. J. (1977). Female incitation of male competition: A mechanism in sexual selection. *Am. Nat.* **111**, 317–335.

Crocker, D. E., Webb, P. M., Costa, D. P. and Le Boeuf, B. J. (1998). Protein catabolism and renal function in lactating northern elephant seals. *Physiol. Zool.* **71**, 485–491.

Crocker, D. E., Khudyakov, J. I. and Champagne, C. D. (2016). Oxidative stress in northern elephant seals: Integration of omics approaches with ecological and experimental studies. *Comp. Biochem. Physiol. Part A Mol. Integr. Physiol.* **200**, 94–103.

Davidson, S. J. (2013). Inflammation and acute phase proteins in haemostasis. In *Acute Phase Proteins* (ed. Janciauskiene, S.), .

Davies, P. F. (1995). Flow-mediated endothelial mechanotransduction. *Physiol. Rev.* **75**, 519–560.

Davis, C. S., Delisle, I., Stirling, I., Siniff, D. B. and Strobeck, C. (2004). A phylogeny of the extant Phocidae inferred from complete mitochondrial DNA coding regions. *Mol. Phylogenet. Evol.* **33**, 363–377.

Davoli, R. and Braglia, S. (2007). Molecular approaches in pig breeding to improve meat quality. *Briefings Funct. Genomics Proteomics* **6**, 313–321.

de la Cuesta, F., Alvarez-Llamas, G., Gil-Dones, F., Martin-Rojas, T., Zubiri, I., Pastor, C., Barderas, M. G. and Vivanco, F. (2009). Tissue proteomics in atherosclerosis: Elucidating the molecular mechanisms of cardiovascular diseases. *Expert Rev. Proteomics* **6**, 395–409.

de Muizon, C. (1982). Phocid phylogeny and dispersal. *Ann. South African Museum* **89**, 175–213.

Deber, C. M., Chen, G., Nadeau, V. G., Glibowicka, M. and Rath, A. (2009). Detergent binding explains anomalous SDS-PAGE migration of membrane proteins. *Proc. Natl. Acad. Sci.* **106**, 1760–1765.

Debier, C., Chalon, C., Le Boeuf, B. J., de Tillesse, T., Larondelle, Y. and Thomé, J. P. (2006). Mobilization of PCBs from blubber to blood in northern elephant seals (Mirounga angustirostris) during the post-weaning fast. *Aquat. Toxicol.* **80**, 149–157.

Desforges, J. P. W., Sonne, C., Levin, M., Siebert, U., De Guise, S. and Dietz, R. (2016). Immunotoxic effects of environmental pollutants in marine mammals. *Environ. Int.* **86**, 126–139.

Dilly, G. F., Young, C. R., Lane, W. S., Pangilinan, J. and Girguis, P. R. (2012). Exploring the limit of metazoan thermal tolerance via comparative proteomics: Thermally induced changes in protein abundance by two hydrothermal vent polychaetes. *Proc. R. Soc. B Biol. Sci.* **279**, 3347–3356.

Dunstan, G., Olley, J. and Ratkowsky, D. (1999). Major environmental and biological factors influencing the fatty acid composition of seafood from Indo-Pacific to Antarctic waters. *Recent Res. Dev. Lipids Res.* **3**, 63–86.

Edwards, P. (2019). Long-term population monitoring, physiological ecology, and behavior of northern elephant seals at Piedras Blancas. *Calif. Polytech. State Univ. San Luis Obispo* **Senior Pro**,.

Emerson, T. E. (1989). Unique features of albumin: A brief review. *Crit. Care Med.* **17**, 690–694.

Esmon, C. T., Xu, J. and Lupu, F. (2012). Innate immunity and coagulation. *J. Thromb. Haemost.* **9**, 182–188.

Estes, J. A. (1998). Killer Whale Predation on Sea Otters Linking Oceanic and Nearshore Ecosystems. *Science (80-.).* **282**, 473–476.

Faserl, K., Sarg, B., Maurer, V. and Lindner, H. H. (2017). Exploiting charge differences for the analysis of challenging post-translational modifications by capillary electrophoresis-mass spectrometry. *J. Chromatogr. A* **1498**, 215–223.

Faulstick, D. A., Lowenstein, J. and Yiengst, M. J. (1962). Clearance kinetics of haptoglobin-hemoglobin complex in the human. *Blood* **20**, 65–71.

Franke, R., Gräfe, M., Schnittler, H., Seiffge, D., Mittermayer, C. and Drenckhahn, D. (1984). Induction of human vascular endothelial stress fibres by fluid shear stress. *Nature* **307**, 648–649.

Futcher, B., Latter, G., Monardo, P., McLaughlin, C. and Garrels, J. (2015). A Sampling of the yeast proteome. *Mol. Cell. Biol.* **19**, 7357–7368.

Fyler, C., Reeder, T., Berta, A., Antonelis, G., Aguilar, A. and Androukaki, E. (2005). Historical biogeography and phylogeny of Monachine seals (Pinnipedia: Phocidae) based on mitochondrial and nuclear DNA data. *J. Biogeogr.* **32**, 1267–1279.

Gabay, C. and Kushner, I. (1999). Acute-phase proteins and other systemic responses to inflammation. *N. Engl. J. Med.* **340**, 448–454.

Gao, Y., Holland, R. D. and Yu, L.-R. (2009). Quantitative proteomics for drug toxicity. *Briefings Funct. Genomics Proteomics* **8**, 158–166.

Gasser, R. F. and Wise, D. M. (1972). The trigeminal nerve in the baboon. *Anat. Rec.* **172**,.

Gettins, P. G. (2002). Serpin structure, mechanism, and function. *Am. Chem. Soc.* **102**, 4751–4804.

Gilman, J. G. (2017). Hemoglobin beta chain structural variation in mice: Evolutionary and functional implications. *Science (80-.).* **178**, 873–874.

Görg, A., Weiss, W. and Dunn, M. J. (2004). Current two-dimensional electrophoresis technology for proteomics. *Proteomics* **4**, 3665–3685.

Gosling, L. M. (1969). Parturition and related behaviour in Coke's Hartebeest, Alcelaphus buselaphus cokei Gunther. *J. Reprod. Fertil.* **S6**, 265–286.

Gruys, E., Toussaint, M., Niewold, T. and Koopmans, S. (2005). Acute phase reaction and acute phase proteins. *J. Zhejiang Univ. Sci. B* **6**, 1045–1056.

Gupta, A. and Kumar, A. (2016). Pros and cons of the proteomics. *Biomed. J.* **37**, 163.

Hamm, H. E. (1998). The many faces of G protein signaling. *J. Biol. Chem.* **273**, 669–672.

Hartl, F. U., Bracher, A. and Hayer-Hartl, M. (2011). Molecular chaperones in protein folding and proteostasis. *Nature* **475**, 324–332.

Harvell, C., Kim, K., Burkholder, J., Colwell, R., Epstein, P., Grimes, D., Hofmann, E., Lipp, E., Osterhaus, A., Overstreet, R., et al. (1999). Emerging Marine Disease - Climate Links and Anthropogenic Factors. *Science (80-.).* **285**, 1505–1510.

Hassrick, J., Crocker, D. E., Teutschel, N., McDonald, B., Robinson, P., Simmons, S. and Costa, D. P. (2010). Condition and mass impact oxygen stores and dive duration in adult female northern elephant seals. *J. Exp. Biol.* **213**, 585–592.

Hauck, E. W., Hauptmann, A., Haag, S. M., Bohnert, A., Weidner, W., Bein, G. and Hackstein, H. (2004). Alpha-1-antitrypsin levels and genetic variation of the alpha-1-antitrypsin gene in Peyronie's disease. *Eur. Urol.* **46**, 623–628.

Haunerland, N. H. and Spener, F. (2004). Fatty acid-binding proteins - Insights from genetic manipulations. *Prog. Lipid Res.* **43**, 328–349.

Hellman, U., Wernstedt, C., Góñez, J. and Heldin, C.-H. (1995). Improvement of an "in-gel" digestion procedure for the micropreparation of internal protein fragments for amino acid sequencing. *Anal. Biochem.* **224**, 451–455.

Henderson, N. C. and Sethi, T. (2009). The regulation of inflammation by galectin-3. *Immunol. Rev.* **230**, 160–171.

Henriques, S., Henriques, O. B. and Selye, H. (1949). Influence of cold on blood fibrinogen concentration. *Exp. Biol. Med.* **71**, 82–84.

Herrmann, K. M. and Weaver, L. M. (1999). The shikimate pathway. *Annu. Rev. Plant Physiol. Plant Mol. Biol.* **50**, 473–503.

Higdon, J. W., Bininda-Emonds, O. R., Beck, R. M. and Ferguson, S. H. (2007). Phylogeny and divergence of the pinnipeds (Carnivora: Mammalia) assessed using a multigene dataset. *BioMed Cent. Evol. Biol.* **7**,.

Ho, Y., Gruhler, A., Heilbut, A., Bader, G. D., Moore, L., Adams, S.-L., Millar, A., Taylor, P., Bennett, K., Boutilier, K., et al. (2002). Systematic identification of protein complexes in Saccharomyces cerevisiae by mass spectrometry. *Nature* **415**, 180–183.

Hoelzel, A. R. (2002). *Marine Mammal Biology: An Evolutionary Approach*. (ed. Hoelzel, A. R.) Oxford: Blackwell Science Ltd.

Hoffmeister, K. M., Falet, H., Toker, A., Barkalow, K. L., Stossel, T. P. and Hartwig, J. H. (2001). Mechanisms of cold-induced platelet actin assembly. *J. Biol. Chem.* **276**, 24751–24759.

Hokkanen, J. (1990). Temperature regulation of marine mammals. *J. Theor. Biol.* **145**, 465–85.

Hooker, S. K., Iverson, S. J., Ostrom, P. and Smith, S. C. (2001). Diet of northern bottlenose whales inferred from fatty-acid and stable-isotope analyses of biopsy samples. *Can. J. Zool.* **79**, 1442–1454.

Hotamisligil, G. S. (2006). Inflammation and metabolic disorders. *Nature* **444**, 860–867.

Houssaye, A. (2009). "Pachyostosis" in aquatic amniotes: a review. *Integr. Zool.* **4**, 325–340.

Hsia, C. C. (1998). Respiratory function of hemoglobin. *N. Engl. J. Med.* **338**, 239–247.

Hultquist, D. E. and Passon, P. G. (1971). Catalysis of methaemoglobin reduction by erythrocyte cytochrome B5 and cytochrome B5 reductase. *Nat. New Biol.* **229**, 252–254.

Irving, L. and Hart, J. (1957). The metabolism and insulation of seals as bare-skinned mammals in cold water. *Can. J. Zool.* **35**, 497–511.

Irving, L., Scholander, P. and Grinnell, S. (1942). The regulation of arterial blood pressure in the seal during diving. *Am. J. Physiol.* **135**, 557–566.

Jacox, M. G., Hazen, E. L., Zaba, K. D., Rudnick, D. L., Edwards, C. A., Moore, A. M. and Bograd, S. J. (2016). Impacts of the 2015–2016 El Niño on the California Current System: Early assessment and comparison to past events. *Geophys. Res. Lett.* **43**, 7072–7080.

Janciauskiene, S., Wrenger, S. and Welte, T. (2013). Immunoregulatory properties of acute phase proteins — Specific focus on α1-antitrypsin. In *Acute Phase Proteins* (ed. Janciauskiene, S.), .

Juhnke, H., Krems, B., Kötter, P. and Entian, K. D. (1996). Mutants that show increased sensitivity to hydrogen peroxide reveal an important role for the pentose phosphate pathway in protection of yeast against oxidative stress. *Mol. Gen. Genet.* **252**, 456–464.

Kanatous, S. B., DiMichele, L. V, Cowan, D. F. and Davis, R. W. (1999). High aerobic capacities in the skeletal muscles of pinnipeds: adaptations to diving hypoxia. *J. Appl. Physiol.* **86**, 1247–1256.

Kaneko, J. J., Harvey, J. W. and Bruss, M. L. (2008). *Clinical biochemistry of domestic animals*. Burlington: Academic Press.

Kawamori, D., Kaneto, H., Nakatani, Y., Matsuoka, T. A., Matsuhisa, M., Hori, M. and Yamasaki, Y. (2006). The forkhead transcription factor Foxo1 bridges the JNK pathway and the transcription factor PDX-1 through its intracellular translocation. *J. Biol. Chem.* **281**, 1091–1098.

King, J. E. (1983). *Seals of the World*. 2nd ed. Queensland: University of Queensland Press.

Koopman, H., Iverson, S. J. and Gaskin, D. (1996). Stratification and age-related differences in blubber fatty acids of the male harbour porpoise (Phocoena phocoena). *J. Comp. Physiol. B* **165**, 628–639.

Kooyman, G. L. (1981). Leoprard seal, Hydrurga leptonyx. In *Handbook of Marine Mammals* (ed. Ridgeway, S.) and Harrison, R.), pp. 261–274. London: Academic Press.

Kruger, N. J. and von Schaewen, A. (2003). The oxidative pentose phosphate pathway: Structure and organisation. *Curr. Opin. Plant Biol.* **6**, 236–246.

Lau, T. Y., Power, K. A., Dijon, S., Gardelle, I. de, McDonnell, S., Duffy, M. J., Pennington, S. R. and Gallagher, W. M. (2010). Prioritization of candidate protein biomarkers from an in vitro model system of breast tumor progression toward clinical verification. *J. Proteome Res.* **9**, 1450–1459.

Le Boeuf, B. J. (1974). Male-male competition and reproductive success in elephant seals. *Am. Zool.* **14**, 163–176.

Le Boeuf, B. J. and Peterson, R. S. (1969). Social status and mating activity in elephant seals. *Science (80-.).* **163**, 91–93.

Le Boeuf, B. J. and Richard, M. (1994). *Elephant seals: population ecology, behavior, and physiology*. Berkeley: University of California Press.

Le Boeuf, B. J., Whiting, R. J. and Gantt, R. F. (1972). Perinatal behavior of northern elephant seal females and their young. *Behaviour* **43**, 121–156.

Le Boeuf, B. J., Costa, D. P., Huntley, A. C. and Feldkamp, S. D. (1987). Continuous, deep diving in female northern elephant seals, Mirounga angustirostris. *Can. J. Zool.* **66**, 446–458.

Le Boeuf, B. J., Crocker, D. E., Costa, D. P., Blackwell, S. B. and Webb, P. M. (2000). Foraging Ecology of Northern Elephant Seals Published by : Wiley on behalf of the Ecological Society of America Stable URL : https://www.jstor.org/stable/2657207 Wiley , Ecological Society of America are collaborating with JSTOR to digitize , preserve and. *Ecol. Soc. Am.* **70**, 353–382.

Lepock, J. R. (2003). Cellular effects of hyperthermia: Relevance to the minimum dose for thermal damage. *Int. J. Hyperth.* **19**, 252–266.

Lester, C. and Costa, D. P. (2006). Water conservation in fasting northern elephant seals (Mirounga angustirostris). *J. Exp. Biol.* **209**, 4283–4294.

Liaw, S.-H., Kuo, I. and Eisenberg, D. (1995). Discovery of the ammonium substrate site on glutamine synthetase, a third cation binding site. *Protein Sci.* **4**, 2358–2365.

Lipps, J. H. and Mitchell, E. (1976). Trophic model for the adaptive radiations and extinctions of pelagic marine mammals. *Paleobiology* **2**, 147–155.

Lovrić, J. (2011). *Introducing proteomics: from concepts to sample separation, mass spectrometry and data analysis*. 1st ed. Oxford, UK: Wiley-Blackwell Publishing, Inc.

Lovrić, J., Dammeier, S., Kieser, A., Mischak, H. and Kolch, W. (1998). Activated Raf induces the hyperphosphorylation of stathmin and the reorganization of the microtubule network. *J. Biol. Chem.* **273**, 22848–22855.

Lowther, A. D. and Goldsworthy, S. D. (2016). When were the weaners weaned? Identifying the onset of Australian sea lion nutritional independence. *J. Mammal.* **97**, 1304–1311.

Lücker, J., Laszczak, M., Smith, D. and Lund, S. T. (2009). Generation of a predicted protein database from EST data and application to iTRAQ analyses in grape (Vitis vinifera cv. Cabernet Sauvignon) berries at ripening initiation. *BioMed Cent. Genomics* **10**, 1–17.

Maimon, O. and Rokach, L. (2005). Clustering methods. In *Data mining and knowledge management*, pp. 321–353. US: Springer.

Mamone, G., Picariello, G., Caira, S., Addeo, F. and Ferranti, P. (2009). Analysis of food proteins and peptides by mass spectrometry-based techniques. *J. Chromatogr. A* **1216**, 7130–7142.

Maniotis, A. J., Chen, C. S. and Ingber, D. E. (1997). Demonstration of mechanical connections between integrins, cytoskeletal filaments, and nucleoplasm that stabilize nuclear structure. *Proc. Natl. Acad. Sci.* **94**, 849–54.

Mann, M., Hendrickson, R. C. and Pandey, A. (2001). Analysis of proteins and proteomes by mass spectrometry. *Annu. Rev. Biochem.* **70**, 437–473.

Marciniak, S. J. and Ron, D. (2006). Endoplasmic Reticulum Stress Signaling in Disease. *Physiol. Rev.* **86**, 1133–1149.

Margaria, R. and Green, A. A. (1933). The first dissociation constant, pK'1, of carbonic acid in hemoglobin solutions and its relation to the existence of a combination of hemoglobin with carbon dioxide. *J. Biol. Chem.* **102**, 611–634.

Marko-Varga, G., Ogiwara, A., Nishimura, T., Kawamura, T., Fujii, K., Kawakami, T., Kyono, Y., Tu, H., Anyoji, H., Kanazawa, M., et al. (2007). Personalized medicine and proteomics: lessons from non-small cell lung cancer. *J. Proteome Res.* **6**, 2925–2935.

Markussen, N. H., Morten, R. and Øritsland, N. A. (1992). Metabolic rate and body composition of harbour seals, Phoca vitulina, during starvation and refeeding. *Can. J. Zool.* **70**, 220–224.

Martinez, B., Gennell, N., Crocker, D. E. and Ortiz, R. M. (2016). Deiodinase type 3 methylation increases in response to thyroid stimulating hormone in a fasting adapted mammal. *Fed. Am. Sci. Exp. Biol. J.* **30**,.

Martins, A. C., Almeida, J. I., Lima, I. S., Kapitão, A. S. and Gozzelino, R. (2017). Iron metabolism and the inflammatory response. *Int. Union Biochem. Mol. Biol. Life* **69**, 442–450.

McCubrey, J. A., Steelman, L. S., Chappell, W. H., Abrams, S. L., Wong, E. W., Chang, F., Lehmann, B., Terrian, D. M., Milella, M., Tafuri, A., et al. (2007). Roles of the Raf/MEK/ERK pathway in cell growth, malignant transformation and drug resistance. *Biochim. Biophys. Acta (BBA)- Mol. Cell Res.* **1773**, 1263–1284.

McIlwain, C., Townsend, D. and Tew, K. D. (2006). Glutathione S-transferase polymorphisms: cancer incidence and therapy. *Oncogene* **25**, 1639–1648.

Mini, R., Bernardinia, G., Salzano, A. M., Renzone, G., Scaloni, A., Figura, N. and Santucci, A. (2006). Comparative proteomics and immunoproteomics of Helicobacter pylori related to different gastric pathologies. *J. Chromatogr. B* **833**, 63–79.

Mitchell, E. and Tedford, R. H. (1973). The Enaliarctinae: a new group of extinct aquatic Carnivora and a consideration of the origin of the Otariidae. *Bull. Am. Museum Nat. Hist.* **151**, 203–284.

Moller, P., Wallin, H. and Knudsen, L. E. (1996). Oxidative stress associated with exercise, psycological stress, and life-style factors. *Chem. Biol. Interact.* **102**, 17–36.

Mookerjee, S. A., Goncalves, R. L., Gerencser, A. A., Nicholls, D. G. and Brandab, M. D. (2015). The contributions of respiration and glycolysis to extracellular acid production. *Biochim. Biophys. Acta - Bioenerg.* **1847**, 171–181.

Mottishaw, P. D., Thornton, S. J. and Hochachka, P. W. (1999). The diving response mechanism and Its surprising evolutionary path in seals and sea lions. *American* **39**, 434–450.

Murdaugh Jr., H., Schmidt-Nielsen, B., Wood, J. and Mitchell, W. (1961). Cessation of renal function during diving in the trained seal (Phoca vitulina). *J. Cell. Physiol.* **58**, 261–265.

Murphy, K. and Weaver, C. (2017). Innate immunity: The first line of defense. In *Janeway's Immunobiology*, p. Garland Science.

Murphy, R., Dutka, T. and Lamb, G. (2008). Hydroxyl radical and glutathione interactions alter calcium sensitivity and maximum force of the contractile apparatus in rat skeletal muscle fibres. *J. Physiol.* **586**, 2203–2216.

Neely, B. A., Ellisor, D. L. and Davis, W. C. (2018). Proteomics as a metrological tool to evaluate genome annotation accuracy following de novo genome assembly:A case study using the Atlantic bottlenose dolphin (Tursiops truncatus). *bioRxiv*.

Neuhaus, H. and Emes, M. (2000). Nonphotosynthetic metabolism in plastids. *Annu. Rev. Plant Biol.* **51**, 111–140.

Noren, S. R., Williams, T., Pabst, D., McLellan, W. and Dearolf, J. (2001). The development of diving in marine endotherms: Preparing the skeletal muscles of dolphins, penguins, and seals for activity during submergence. *J. Comp. Physiol. B* **171**, 127–134.

Noren, D., Crocker, D., Williams, T. and Costa, D. P. (2003). Energy reserve utilization in northern elephant seal (Mirounga angustirostris) pups during the postweaning fast: Size does matter. *J. Comp. Physiol. B Biochem. Syst. Environ. Physiol.* **173**, 443–454.

Oceguera-Yanez, F., Kimura, K., Yasuda, S., Higashida, C., Kitamura, T., Hiraoka, Y., Haraguchi, T. and Narumiya, S. (2005). Ect2 and MgcRacGAP regulate the activation and function of Cdc42 in mitosis. *JThe ournal Cell Biol.* **168**, 221–232.

Ohsawa, I., Nishimaki, K., Yasuda, C., Kamino, K. and Ohta, S. (2003). Deficiency in a mitochondrial aldehyde dehydrogenase increases vulnerability to oxidative stress in PC12 cells. *J. Neurochem.* **84**, 1110–1117.

Ohta, S., Ohsawa, I., Kamino, K., Ando, F. and Shimokata, H. (2004). Mitochondrial ALDH2 deficiency as an oxidative stress. *Ann. N. Y. Acad. Sci.* **1011**, 36–44.

Okano, T., Kondo, T., Fujii, K., Nishimura, T., Takano, T., Ohe, Y., Tsuta, K., Matsuno, Y., Gemma, A., Kato, H., et al. (2007). Proteomic signature corresponding to the response to gefitinib (Iressa, ZD1839), an epidermal growth factor receptor tyrosine kinase inhibitor in lung adenocarcinoma. *Clin. Cancer Res.* **13**, 799–805.

Olsen, J. V, Ong, S.-E. and Mann, M. (2004). Trypsin cleaves exclusively C-terminal to arginine and lysine residues. *Mol. Cell. Proteomics* **3**, 608–614.

Ordway, G. A. and Garry, D. J. (2004). Myoglobin: An essential hemoprotein in striated muscle. *J. Exp. Biol.* **207**, 3441–3446.

Ortiz, R. M. (2001). Osmoregulation in marine mammals. *J. Exp. Biol.* **204**, 1831–1844.

Ortiz, C. L., Costa, D. P. and Le Boeuf, B. J. (1978). Water and energy flux in elephant seal pups fasting under natural conditions. *Physiol. Zool.* **51**, 166–178.

Ortiz, R. M., Adams, S. H., Costa, D. P. and Ortiz, C. L. (1996). Plasma vasopressin levels and water conservation in fasting, postweaned northern elephant seal pups (Mirounga angustirostris). *Mar. Mammal Sci.* **12**, 99–106.

Ortiz, R. M., Wade, C. and Ortiz, C. L. (2000). Prolonged fasting increases the response of the renin – angiotensin – aldosterone system, but not vasopressin levels, in postweaned northern elephant seal pups. *Gen. Comp. Endocrinolgy* **223**, 217–223.

Ortiz, R. M., Wade, C. E. and Ortiz, C. L. (2001). Effects of prolonged fasting on plasma cortisol and TH in postweaned northern elephant seal pups. *Am. J. Physiol. - Regul. Integr. Comp. Physiol.* **280**, R790–R795.

Ortiz, R. M., Crocker, D. E., Houser, D. S. and Webb, P. M. (2006). Angiotensin II and aldosterone increase with fasting in breeding male northern elephant seals (Mirounga angustirostris). *Physiol. Biochem. Zool.* **79**, 1106–1112.

Peck-Burnett, T. (2019). Morphometric trends and sexual dimorphism in weanling northern elephant seals (Mirounga angustirostris) at the Piedras Blancas rookery. *Calif. Polytech. State Univ. San Luis Obispo* **Senior Pro**,.

Peck, H. E., Costa, D. P. and Crocker, D. E. (2016). Body reserves influence allocation to immune responses in capital breeding female northern elephant seals. *Funct. Ecol.* **30**, 389–397.

Percy, M. J., McFerran, N. V and Lappin, T. R. (2005). Disorders of oxidised haemoglobin. *Blood Rev.* **19**, 61–68.

Pernia, S. D., Hill, A. and Ortiz, C. L. (1980). Urea turnover during prolonged fasting in the northern elephant seal. *Comp. Biochem. Physiol. Part B Comp. Biochem.* **65**, 731–734.

Ponganis, P. J. (2011). Diving mammals. *Compr. Physiol.* **1**, 447–465.

Poprac, P., Jomova, K., Simunkova, M., Kollar, V., Rhodes, C. J. and Valko, M. (2017). Targeting free radicals in oxidative stress-related human diseases. *Trends Pharmacol. Sci.* **38**, 592–607.

Powers, E. T., Morimoto, R. I., Dillin, A., Kelly, J. W. and Balch, W. E. (2009). Biological and chemical approaches to diseases of proteostasis deficiency. *Annu. Rev. Biochem.* **78**, 959–991.

Prochnow, C., Bransteitter, R., Klein, M. G., Goodman, M. F. and Chen, X. S. (2007). The APOBEC-2 crystal structure and functional implications for the deaminase AID. *Nature* **445**, 447–51.

Projecto-Garcia, J., Natarajan, C., Moriyama, H., Weber, R. E., Fago, A., Cheviron, Z. A., Dudley, R., McGuire, J. A., Witt, C. C. and Storz, J. F. (2013). Repeated elevational transitions in hemoglobin function during the evolution of Andean hummingbirds. *Proc. Natl. Acad. Sci.* **110**, 20669–20674.

Rai, A. J., Gelfand, C. A., Haywood, B. C., Warunek, D. J., Yi, J., Schuchard, M. D., Mehigh, R. J., Cockrill, S. L., Scott, G. B. I., Tammen, H., et al. (2005). HUPO Plasma Proteome Project specimen collection and handling: Towards the standardization of parameters for plasma proteome samples. *Proteomics* **5**, 3262–3277.

Rajalingam, D., Loftis, C., Xu, J. J. and Kumar, T. K. S. (2009). Trichloroacetic acid-induced protein precipitation involves the reversible association of a stable partially structured intermediate. *Protein Sci.* **18**, 980–993.

Rashid, A. K. and Weber, R. E. (1999). Functional differentiation in trematode hemoglobin isoforms. *Eur. J. Biochem.* **260**, 717–725.

Rea, L. D. and Costa, D. P. (1992). Changes in standard metabolism during long-term fasting in northern elephant seal pups (Mirounga angustirostris). *Physiol. Zool. Zool.* **65**, 97–111.

Reidman, M. (1990). *The pinnipeds: seals, sea lions, and walruses*. University of California Press.

Reiter, J., Stinson, N. L. and Le Boeuf, B. J. (1978). Northern elephant seal development: The transition from weaning to nutritional independence. *Behav. Ecol. Sociobiol.* **3**, 337–367.

Remotti, H., Zinszner, H., Batchvarova, N., Wang, X., Ron, D., Stevens, J., Lightfoot, R. and Kuroda, M. (2008). CHOP is implicated in programmed cell death in response to impaired function of the endoplasmic reticulum. *Genes Dev.* **12**, 982–995.

Riedman, M. and Ortiz, C. L. (1979). Changes in milk composition during lactation in the northern elephant seal. *Physiol. Biochecmical Zool.* **52**, 240–249.

Rix, U. and Superti-Furga, G. (2009). Target profiling of small molecules by chemical proteomics. *Nat. Chem. Biol.* **5**, 616–624.

Robin, J., Boucontet, L., Chillet, P. and Groscolas, R. (1998). Behavioral changes in fasting emperor penguins: evidence for a “refeeding signal” linked to a metabolic shift. *Am. J. Physiol.* **274**, R746–R753.

Roche, M., Rondeau, P., Singh, N. R., Tarnus, E. and Bourdon, E. (2008). The antioxidant properties of serum albumin. *Fed. Eur. Biochem. Soc. Lett.* **582**, 1783–1787.

Rose, R. J., Damoc, E., Denisov, E., Makarov, A. and Heck, A. J. (2012). High-sensitivity orbitrap mass analysis of intact macromolecular assemblies. *Nat. Methods* **9**, 1084–1086.

Rossignol, P., Ho-Tin-Noé, B., Vranckx, R., Bouton, M.-C., Meilhac, O., Lijnen, R. H., Guillin, M.-C., Michel, J.-B. and Anglés-Cano, E. (2004). Protease nexin-1 inhibits plasminogen activation-induced apoptosis of adherent cells. *J. Biol. Chem.* **279**, 10346–10356.

Rothfork, J. M., Dessus-Babus, S., Van Wamel, W. J., Cheung, A. L. and Gresham, H. D. (2003). Fibrinogen depletion attenuates Staphyloccocus aureus infection by preventing density-dependent virulence gene up-regulation. *J. Immunol.* **171**, 5389–5395.

Rüchel, R., Steere, R. L. and Erbe, E. F. (1978). Transmission-electron microscope observations of freeze-etched polyacrylamide gels. *J. Chromatogr. A* **166**, 563–575.

Sato, Y., Probst, H. C., Tatsumi, R., Ikeuchi, Y., Neuberger, M. S. and Rada, C. (2010). Deficiency in APOBEC2 leads to a shift in muscle fiber type, diminished body mass, and myopathy. *J. Biol. Chem.* **285**, 7111–7118.

Sauer, G., Körner, R., Hanisch, A., Ries, A., Nigg, E. A. and Silljé, H. H. (2004). Proteome analysis of the human mitotic spindle. *Mol. Cell. Proteomics* **4**, 35–43.

Schmidt-Nielsen, K., Hainsworth, F. and Murrish, D. (1970). Counter-current heat exchange in the respiratory passages: Effect on water and heat balance. *Respir. Physiol.* **9**, 263–276.

Schmidt, S., Willers, J., Riecker, S., Möller, K., Schuchardt, J. P. and Hahn, A. (2015). Effect of omega-3 polyunsaturated fatty acids on the cytoskeleton: An open-label intervention study. *Lipids Health Dis.* **14**, 1–9.

Schutz, Y. (2011). Protein turnover, ureagenesis and gluconeogenesis. *Int. J. Vitam. Nutr. Res.* **81**, 101–107.

Schwenk, J., Metz, M., Zolles, G., Turecek, R., Fritzius, T., Bildl, W., Tarusawa, E., Kulik, A., Unger, A., Ivankova, K., et al. (2010). Native GABA(B) receptors are heteromultimers with a family of auxiliary subunits. *Nature* **465**, 231–235.

Shaw, M. M. and Riederer, B. M. (2003). Sample preparation for two-dimensional gel electrophoresis. *Proteomics* **3**,.

Shen, W.-J., Sridhar, K., Bernlohr, D. A. and Kraemer, F. B. (1999). Interaction of rat hormone-sensistve lipase with adipocyte lipid-binding protein. *Proc. Natl. Acad. Sci.* **96**, 5528–5532.

Sies, H. (1991). Oxidative stress: From basic research to clinical application. *Am. J. Med.* **91**, S31–S38.

Sigel, A., Sigel, H. and Sigel, R. K. (2013). *Interrelations between essential metal ions and human diseases*. 13th ed.

Simpson, R. (2010). Homogenization of mammalian tissue. *Cold Spring Harb. Protoc.* **7**,.

Smith, A. J., Thompson, B. R., Sanders, M. A. and Bernlohr, D. A. (2007). Interaction of the adipocyte fatty acid-binding protein with the hormone-sensitive lipase: Regulation by fatty acids and phosphorylation. *J. Biol. Chem.* **282**, 32424–32432.

Sobolesky, P. M., Parry, C., Boxall, B., Wells, R., Venn-Watson, S. and Janech, M. G. (2016). Proteomic Analysis of Non-Depleted Serum Proteins from Bottlenose Dolphins Uncovers a High Vanin-1 Phenotype. *Sci. Rep.* **6**, 33879.

Sodek, K. L., Evangelou, A. I., Ignatchenko, A., Agochiya, M., Brown, T. J., Ringuette, M. J., Jurisica, I. and Kislinger, T. (2008). Identification of pathways associated with invasive behavior by ovarian cancer cells using multidimensional protein identification technology (MudPIT). *Mol. Biosyst.* **4**, 762–773.

Somero, G., Lockwood, B. and Tomanek, L. (2017). *Biochemical Adaptation: Response to Environemntal Challeneges from Life's Origins to the Anthropocene*. Sunderland, Massachusetts: Sinauer Associates, Inc. Publishers.

Somo, D. A., Ensminger, D. C., Sharick, J. T., Kanatous, S. B. and Crocker, D. E. (2015). Development of dive capacity in northern elephant seals (Mirounga angustirostris): Reduced body reserves at weaning are associated with elevated body oxygen stores during the postweaning fast. *Physiol. Biochem. Zool.* **88**, 471–482.

Stapulionis, R., Kolli, S. and Deutscher, M. P. (1997). Efficient mammalian protein synthesis requires an intact F-actin system. *J. Biol. Chem.* **272**, 24980–24986.

Station 46028 (LLNR 275) - Cape San Martin - 55NM West NW of Morro Bay, CA (2015). *Natl. Data Buoy Cent.*

Stewart, B. S. and Delong, R. L. (2016). Double migrations of the northern elephant seal, Mirounga angustirostris. *J. Mammal.* **76**, 196–205.

Supuran, C. T. (2008). Diuretics: From classical carbonic anhydrase inhibitors to novel applications of the sulfonamides. *Curr. Pharm. Des.* **14**, 641–648.

Tavoni, S. K., Champagne, C. D., Houser, D. S. and Crocker, D. E. (2013). Lactate flux and gluconeogenesis in fasting, weaned northern elephant seals (Mirounga angustirostris). *J. Comp. Physiol. B* **183**, 537–546.

Thorson, P. and Le Boeuf, B. J. (1994). *Elephant seals: Population biology, behavior, and physiology*. (ed. Le Boeuf, B. J.) and Laws, R. M.) Berkeley: University of California Press.

Tolosano, E. and Altruda, F. (2002). Hemopexin: Structure, function, and regulation. *DNA Cell Biol.* **21**, 297–306.

Tomanek, L. (2011). Environmental proteomics: Changes in the proteome of marine organisms in response to environmental stress, pollutants, infection, symbiosis, and development. *Ann. Rev. Mar. Sci.* **3**, 373–399.

Tomanek, L. (2015). Proteomic responses to environmentally induced oxidative stress. *J. Exp. Biol.* **218**, 1867–1879.

Tomanek, L. and Zuzow, M. J. (2010). The proteomic response of the mussel congeners Mytilus galloprovincialis and M . trossulus to acute heat stress: Implications for thermal tolerance limits and metabolic costs of thermal stress. *J. Exp. Biol.* **213**, 3559–3574.

Tomko, R. J. and Hochstrasser, M. (2013). Molecular architecture and assembly of the eukaryotic proteasom. *Annu. Rev. Biochem.* **82**, 415–445.

Trillmich, F. (1979). Galápagos sea lions and fur seals. *Not. Galápagos* **29**,.

Trites, A. W., Porter, B. P., Deecke, V. B., Coombs, A. P., Marcotte, M. L. and Rosen, D. A. (2006). Insights into the timing of weaning and the attendance patterns of lactating steller sea lions (Eumetopias jubatus) in Alaska during winter, spring, and summer. *Aquat. Mamm.* **32**, 85–97.

Trivers, R. L. (1972). *Parental investment and sexual selection*.

Tryland, M., Krafft, B. A., Lydersen, C., Kovacs, K. M. and Thoresen, S. I. (2006). Serum chemistry values for free-ranging ringed seals (Pusa hispida) in Svalbard. *Vet. Clin. Pathol.* **35**, 405–412.

Uhen, M. D. (2007). Evolution of marine mammals: Back to the sea after 300 million years. *Anat. Rec.* **290**, 514–522.

Vazquez-Medina, J. P., Zenteno-Savín, T., Elsner, R. W. and Ortiz, R. M. (2012). Coping with physiological oxidative stress: A review of antioxidant strategies in seals. *J. Comp. Physiol. B* **182**, 741–750.

Vázquez-Medina, J. P., Crocker, D. E., Forman, H. J. and Ortiz, R. M. (2010). Prolonged fasting does not increase oxidative damage or inflammation in postweaned northern elephant seal pups. *J. Exp. Biol.* **213**, 2524–2530.

Velours, J., Spannagel, C., Soubannier, V., Vaillier, J., Paumard, P., Arselin, G. and Graves, P.-V. (2002). Organisation of the yeast ATP synthase F0: A study based on cysteine mutants, thiol modification and cross-linking reagents. *Biochim. Biophys. Acta - Bioenerg.* **1458**, 443–456.

Welch, W. J. and Suhan, J. P. (1985). Morphological study of the mammalian stress response: Characterization of changes in cytoplasmic organelles, cytoskeleton, and nucleoli, and appearance of intranuclear actin filaments in rat fibroblasts after heat-shock treatment. *J. Cell Biol.* **101**, 1198–1211.

White, F. N., Ikeda, M. and Elsner, R. W. (1973). Adrenergic innervation of large arteries in the seal. *Comp. Gen. Pharmacol.* **4**, 271–276.

Wilhelm Filho, D., Sell, F., Ribeiro, L., Ghislandi, M., Carrasquedo, F., Fraga, C., Wallauer, J., Simões-Lopes, P. and Uhart, M. (2002). Comparison between the antioxidant status of terrestrial and diving mammals. *Comp. Biochem. Physiol. - A Mol. Integr. Physiol.* **133**, 885–892.

Wilson, D. P., Susnjar, M., Kiss, E., Sutherland, C. and Walsh, M. P. (2005). Thromboxane A2-induced contraction of rat caudal arterial smooth muscle involves activation of Ca2+ entry and Ca2+ sensitization: Rho-associated kinase-mediated phosphorylation of MYPT1 at Thr-855, but not Thr-697. *Biochem. J.* **389**, 763–774.

Wold, S. (1987). Principal component analysis. *Chemom. Intell. Lab. Syst.* **2**, 37–52.

Worthy, G. A. J. (1991a). Insulation and thermal balance of fasting harp and grey seal pups. *Comp. Biochem. Physiol. Part A Physiol.* **100A**, 845–851.

Worthy, G. A. J. (1991b). Insulation and thermal balance of fasting harp and grey seal pups. *Comp. Biochem. Physiol. -- Part A Mol. Integr. Physiol.* **100**, 845–851.

Yin, E., Wessler, S. and Stoll, P. J. (1971). Identity of plasma-activated III heparin factor X inhibitor with cofactor. *J. Biol. Chem.* **246**, 3712–3719.

Zapol, W. M., Liggins, G., Schneider, R., Qvist, J., Snider, M., Creasy, R. and Hochachka, P. (1979). Regional blood flow during simulated diving in the conscious Weddell seal. *J. Appl. Physiol.* **47**, 968–973.

Zougman, A., Ziółkowski, P., Mann, M. and Wiśniewski, J. R. (2008). Evidence for Insertional RNA Editing in Humans. *Curr. Biol.* **18**, 1760–1765.

APPENDICES

APPENDIX A: TABLES

Table 1. Fused gel image analysis of *M. angustirostris* pup muscle skeletal muscle, inner adipose, and outer adipose tissue. Identification of proteins by matrix-assisted laser desorption ionization tandem time-of-flight mass spectrometry. Significance refers to changes in abundance between the two time-points (permutation t-test, $P \leq 0.05$).

	Muscle		Inner Adipose		Outer Adipose	
Protein Spots Detected	273 (73.9% ID)		272 (88.9% ID)		315 (92.5% ID)	
Significantly Changed Abundance	44	16.1%	80	29.4%	106	33.7%
Significantly Changed Abundance (Identified)	32	11.7%	73	91.3%	99	93.4%
Metabolism	6	18.8%	17	23.3%	19	19.2%
Cytoskeleton	9	28.1%	25	34.2%	40	40.4%
Proteostasis	11	34.4%	9	12.3%	12	12.1%
Blood (Heme) Proteins	5	15.6%	21	28.8%	28	28.3%

Table 2. Positive and negative loadings for principal components 1 (47.23%) and 2 (16.20%) for the proteins found in *M. angustirostris* pup muscle tissue that significantly changed abundance the most before and after the post-weaning fast.

	Principle Component 1		Principle Component 2	
Component Loading Rank	Protein (Spot ID)	Loading Value	Protein (Spot ID)	Loading Value
Positive Loadings				
1	Chain A, Structures of Actin-Bound (107)	1.1934	Slow Skeletal Muscle Troponin T 3 (212)	1.7553
2	Myoglobin (65)	1.1862	Slow Skeletal Muscle Troponin T 3 (215)	1.5450
3	Glutathione-S-Transferase P (237)	1.1149	α-Crystallin B Chain (267)	1.4559
4	Slow Skeletal Muscle Troponin T 3 (210)	1.0350	Heat Shock Protein β-6 (248)	1.4220
5	Slow Skeletal Muscle Troponin T (27)	1.0224	Glyceraldehyde-3-Phosphate Dehydrogenase (25)	1.3403
6	C→U-Editing Enzyme APOBEC-2 (223)	1.0191	Heat Shock Protein β-1 (230)	1.2668
7	Myosin, Polypeptide 7, Cardiac Muscle, B (76)	0.8365	Peroxiredoxin-6 (228)	1.1576
8	Myoglobin (67)	0.8206	Fructose-Bisphosphate Aldolase A (24)	1.1441
9	Elongation Factor 1 α (56)	0.7599	Fructose-Bisphosphate Aldolase A (23)	1.0050
10			Glutathione-S-Transferase P (207)	0.6389
Negative Loadings				
1	Heat Shock Cognate 71kDa (132)	-1.2384	Serotransferrin (114)	-1.9297
2	Mitochondrial Aconitase (258)	-1.1777	C→U-Editing Enzyme APOBEC-2 (112)	-1.8886
3	Heat Shock Protein β-1 (230)	-1.1644	Triosephosphate Isomerase (233)	-1.7725
4	Peroxiredoxin-6 (228)	-1.1635	Heat Shock Protein (136)	-1.5141
5	Serum Albumin (128)	-1.1413	Myosin, Polypeptide 7, Cardiac Muscle, B (261)	-1.1986
6	Fructose-Bisphosphate Aldolase A (23)	-1.1247	Heat Shock Cognate 71kDa (132)	-1.1484
7	Myosin, Polypeptide 7, Cardiac Muscle, B (261)	-1.1227	Cu-Zn superoxide dismutase (70)	-0.9873
8	α-Crystallin B Chain (267)	-1.0554	Serum Albumin (128)	-0.9140
9	ES1 Protein Homolog, Mitochondrial 1 (255)	-1.0482	ES1 Protein Homolog, Mitochondrial 1 (255)	-0.8840
10	Heat Shock Protein β-6 (248)	-1.0217	Slow Skeletal Muscle Troponin T (27)	-0.5738

Table 3. Positive and negative loadings for principal components 1 (52.96%) and 2 (9.55%) for the proteins found in *M. angustirostris* pup inner adipose tissue that significantly changed abundance the most before and after the post-weaning fast.

	Principle Component 1		Principle Component 2	
Component Loading Rank	Protein (Spot ID)	Loading Value	Protein (Spot ID)	Loading Value
Positive Loadings				
1	Fibulin-5 (120)	1.2681	Keratin, Type II Cuticular Hb5 (127)	2.4069
2	6-phosphogluconate dehydrogenase (268)	1.2659	Glutamate Dehydrogenase 1, Mitochondrial (154)	2.3883
3	Collagen α-2(VI) Chain (55)	1.2642	Serotransferrin (98)	2.3754
4	Pyruvate Kinase (PKM) (17)	1.2567	α-1-Antitrypsin (158)	2.3650
5	Fibulin-5 (115)	1.2437	Serotransferrin (95)	2.0903
6	Collagen α-2(VI) Chain (58)	1.2414	α-2-HS-Glycoprotein Isoform 1 (124)	1.8242
7	Collagen α-1(VI) Chain (59)	1.2407	Serotransferrin (97)	1.8018
8	Collagen α-2(VI) Chain (61)	1.2204	Plasminogen Isoform 1 (269)	1.7062
9	Galectin-3 Isoform 3 (214)	1.2083	Prolargin (271)	1.3981
10	Prolargin (271)	1.2081	Collagen α-1(VI) Chain (56)	1.3566
Negative Loadings				
1	Haptoglobin (208)	-1.3575	Superoxide Dismutase [Cu-Zn], Chloroplastic (247)	-2.1070
2	Haptoglobin (205)	-1.3117	Complement C4-A (23)	-1.9008
3	Calreticulin (150)	-1.2322	Complement C4-A (24)	-1.7594
4	Monoglyceride Lipase (229)	-1.2190	3-Ketoacyl-CoA Thiolase, Mitochondrial (22)	-1.7373
5	Haptoglobin (206)	-1.2028	Actin-Related Protein 3 Isoform 1 (169)	-0.9460
6	Fibrinogen Δ Chain Isoform 1 (84)	-1.1856	Calreticulin (149)	-0.7832
7	Fibrinogen Δ Chain Isoform 1 (79)	-1.1448	Haptoglobin (205)	-0.7624
8	Peroxiredoxin-2 Isoform 1 (242)	-1.0715	Cathepsin D (221)	-0.6519
9	Heterogeneous Nuclear Ribonucleoprotein H1 (166)	-1.0600	Haptoglobin (206)	-0.5367
10	Cathepsin D (221)	-1.0570	Apolipoprotein A-1 (236)	-0.46641

Table 4. Positive and negative loadings for principal components 1 (43.77%) and 2 (7.39%) for the proteins found in *M. angustirostris* pup outer adipose tissue that significantly changed abundance before and after the post-weaning fast.

	Principle Component 1		Principle Component 2	
Component Loading Rank	Protein (Spot ID)	Loading Value	Protein (Spot ID)	Loading Value
Positive Loadings				
1	Collagen α-2(Vl) Chain (43)	1.3803	Serotransferrin (109)	2.4348
2	Collagen α-2(Vl) Chain (42)	1.3661	Complement Factor B (61)	2.0829
3	Collagen α-2(Vl) Chain (44)	1.3620	Fibrinogen β Chain Isoform 1 (135)	1.8572
4	Collagen α-2(V) Chain (30)	1.3272	Transketolase (111)	1.7729
5	Four and a Half LIM Domains 1 (252)	1.3108	Serotransferrin (100)	1.7711
6	Collagen α-2(V) Chain (29)	1.3022	Prolargin (106)	1.6800
7	Collagen α-2(V) Chain (25)	1.2803	NADP Isocitrate Dehydrogenase, Cytoplasmic (199)	1.5711
8	Collagen α-3(VI) Chain (28)	1.2401	Serotransferrin (108)	1.5274
9	Keratin, Type I Cuticular HA1 (194)	1.2149	Selenium- Binding Protein 1 Isoform 1 (159)	1.4979
10	Collagen α -2(V) Chain (26)	1.1746	Triosephosphate Isomerase (272)	1.4235
Negative Loadings				
1	Serum Albumin (88)	-1.2935	Fibrinogen Δ Chain Isoform 1 (170)	-2.4383
2	Calreticulin (137)	-1.2876	Keratin, Type II Cuticular Hb3 (141)	-2.1615
3	Peroxiredoxin-1 (289)	-1.2769	Cytochrome Oxidase Subunit 1, Mitochondrion (215)	-1.7717
4	Cathepsin D (261)	-1.2674	Actin, Cytoplasmic 1 (116)	-1.5672
5	Apolipoprotein A-1 (280)	-1.2376	Keratin, Type II Cuticular Hb3 (164)	-1.4650
6	Fatty Acid-Binding Protein, Adipocyte (307)	-1.2324	Keratin 81 (168)	-1.4168
7	Haptoglobin (228)	-1.2067	Fibrinogen Δ Chain Isoform 1 (66)	-1.3264
8	Triosephosphate Isomerase (272)	-1.1793	BTB/POZ Domain-Containing KCTD12 (229)	-1.2747
9	Calreticulin (128)	-1.1726	Mimecan (226)	-1.2618
10	Haptoglobin (232)	-1.1574	Keratin, Type I, Cytoskeletal 14 (177)	-1.2199

APPENDIX B: FIGURES

A

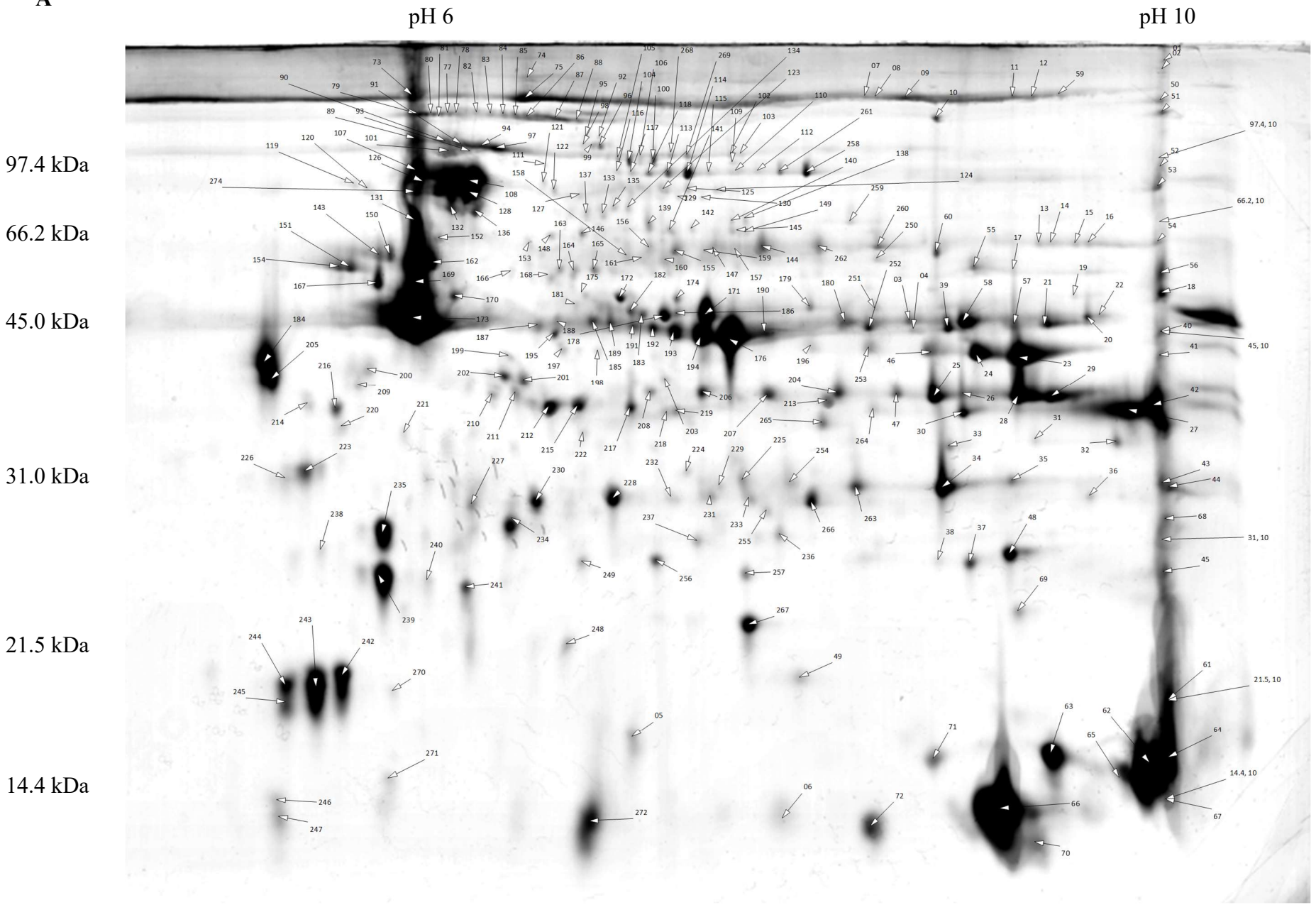

B

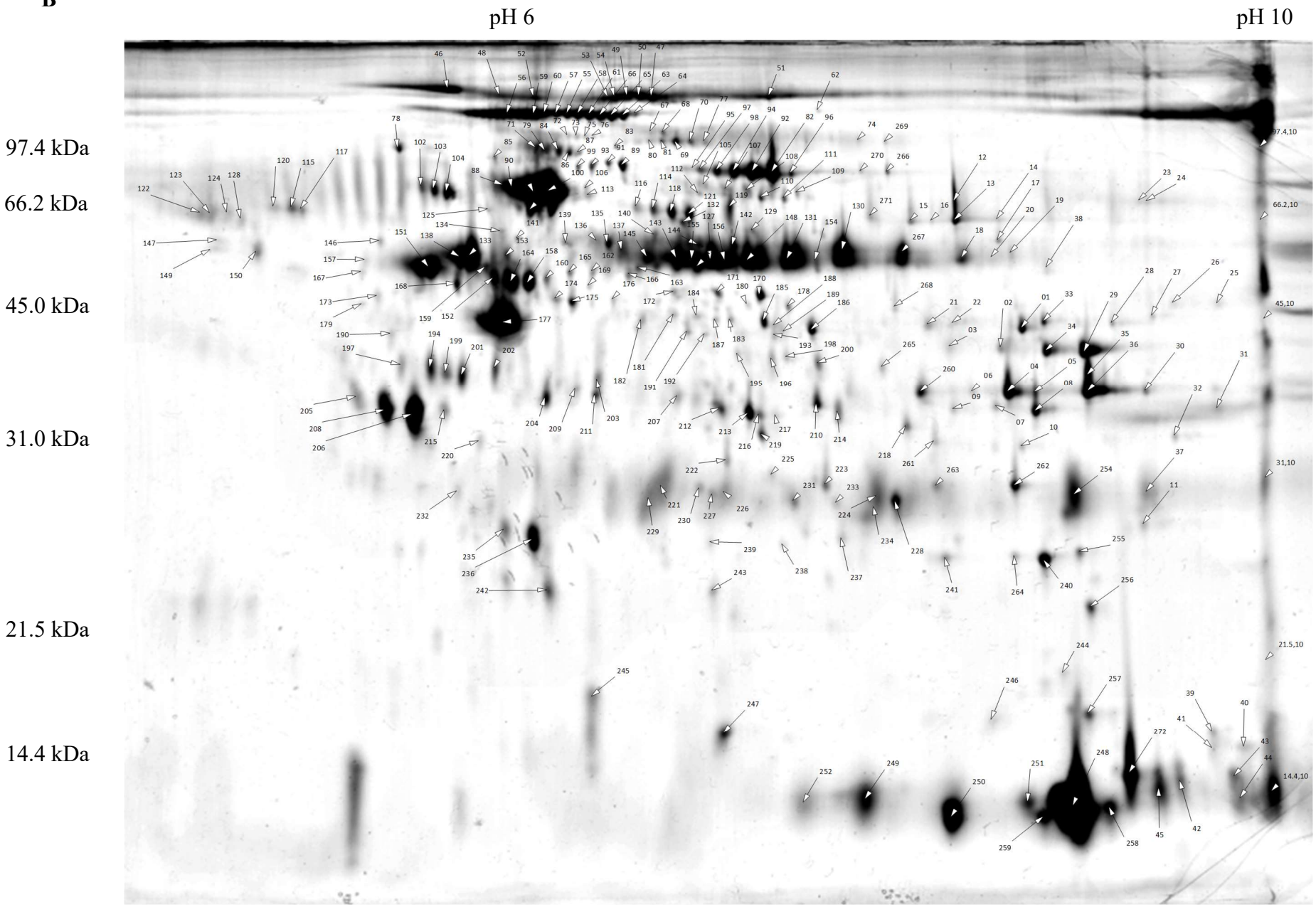
pH 6
pH 10
97.4 kDa
66.2 kDa
45.0 kDa
31.0 kDa
21.5 kDa
14.4 kDa
97.4,10
66.2,10
45,10
31,10
21.5,10
14.4,10

C

pH 6

pH 10

97.4 kDa

66.2 kDa

45.0 kDa

31.0 kDa

21.5 kDa

14.4 kDa

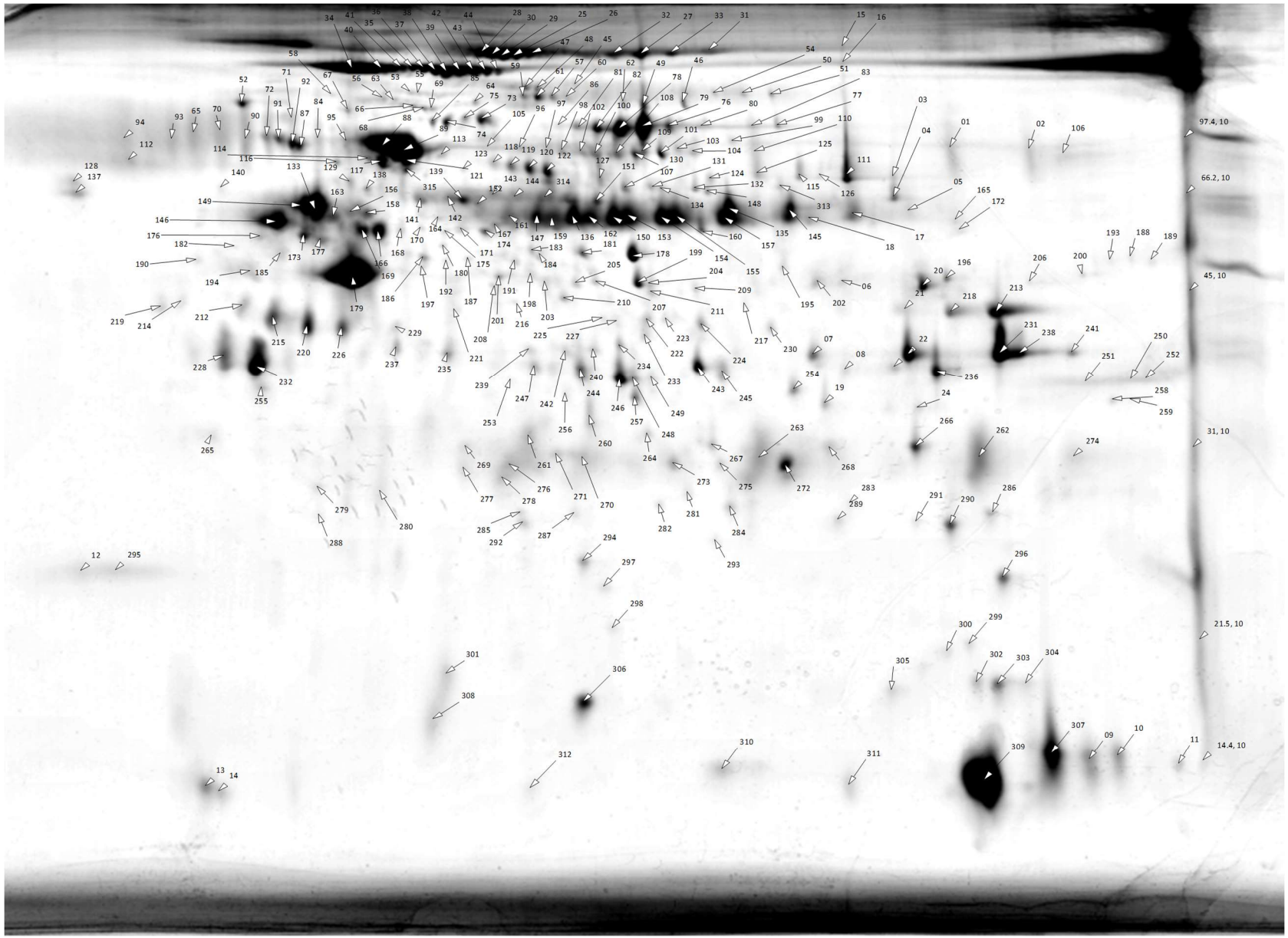

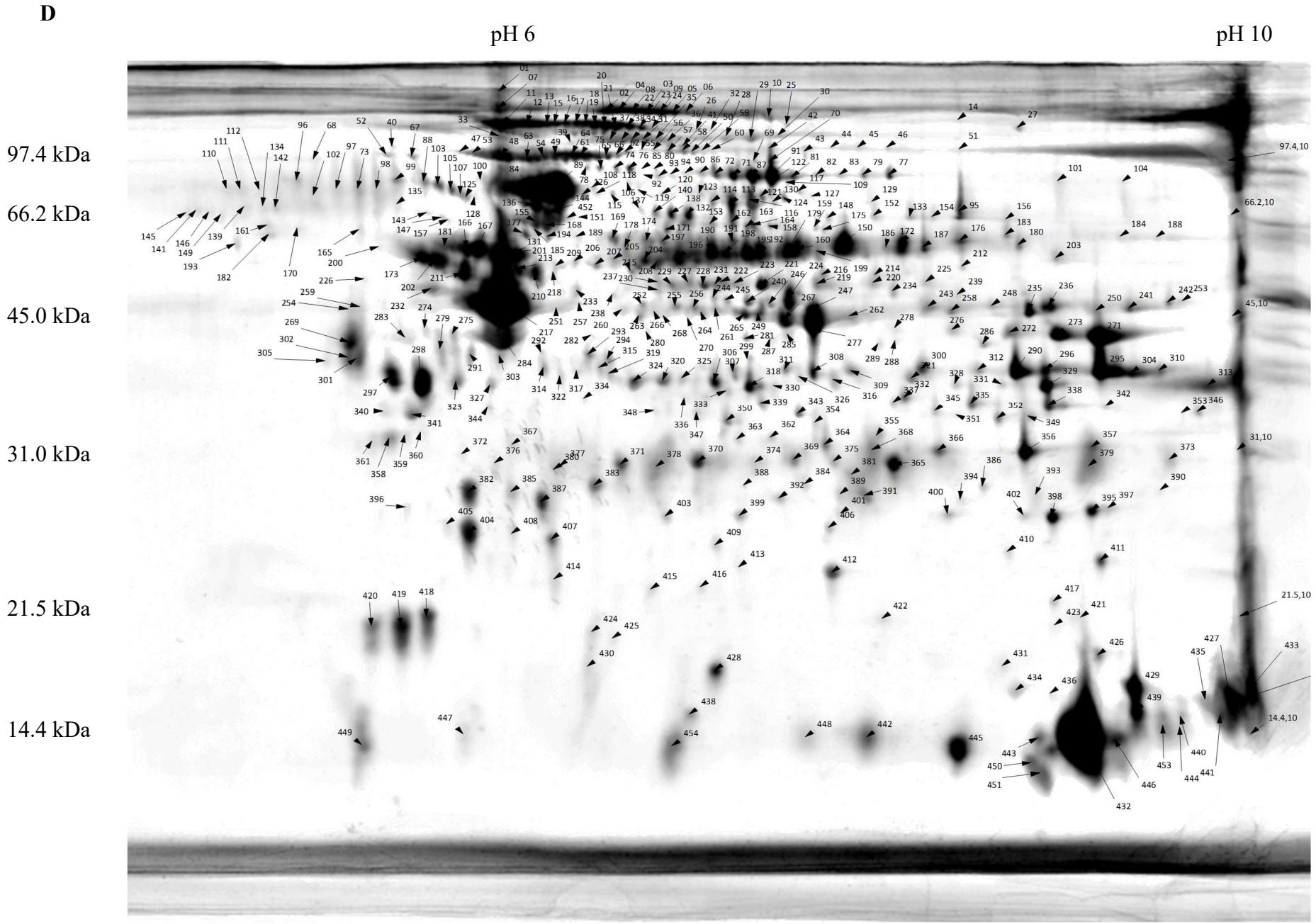

Figure 1. Fused gel image showing all individual protein spots detected in *M. angustirostris* tissue. A) Muscle tissue, B) inner adipose tissue, C) outer adipose tissue, and (D) all tissues combined. The proteome map represents the average normalized pixel volumes for each protein across all gels of each tissue.

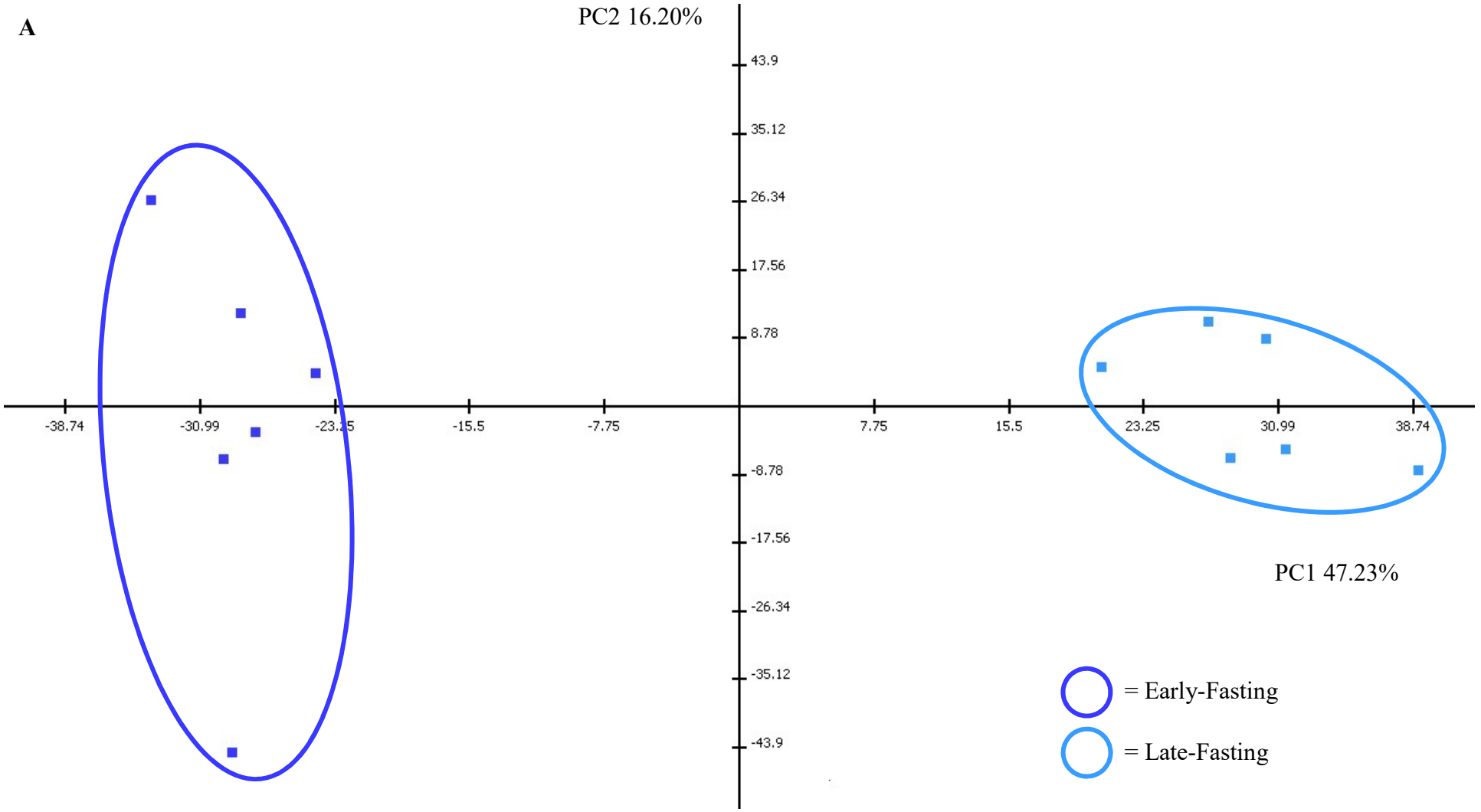
A
PC2 16.20%
43.9
35.12
26.34
17.56
8.78
-8.78
-17.56
-26.34
-35.12
-43.9
-38.74
-30.99
-23.25
-15.5
-7.75
7.75
15.5
23.25
30.99
38.74
PC1 47.23%
= Early-Fasting
= Late-Fasting

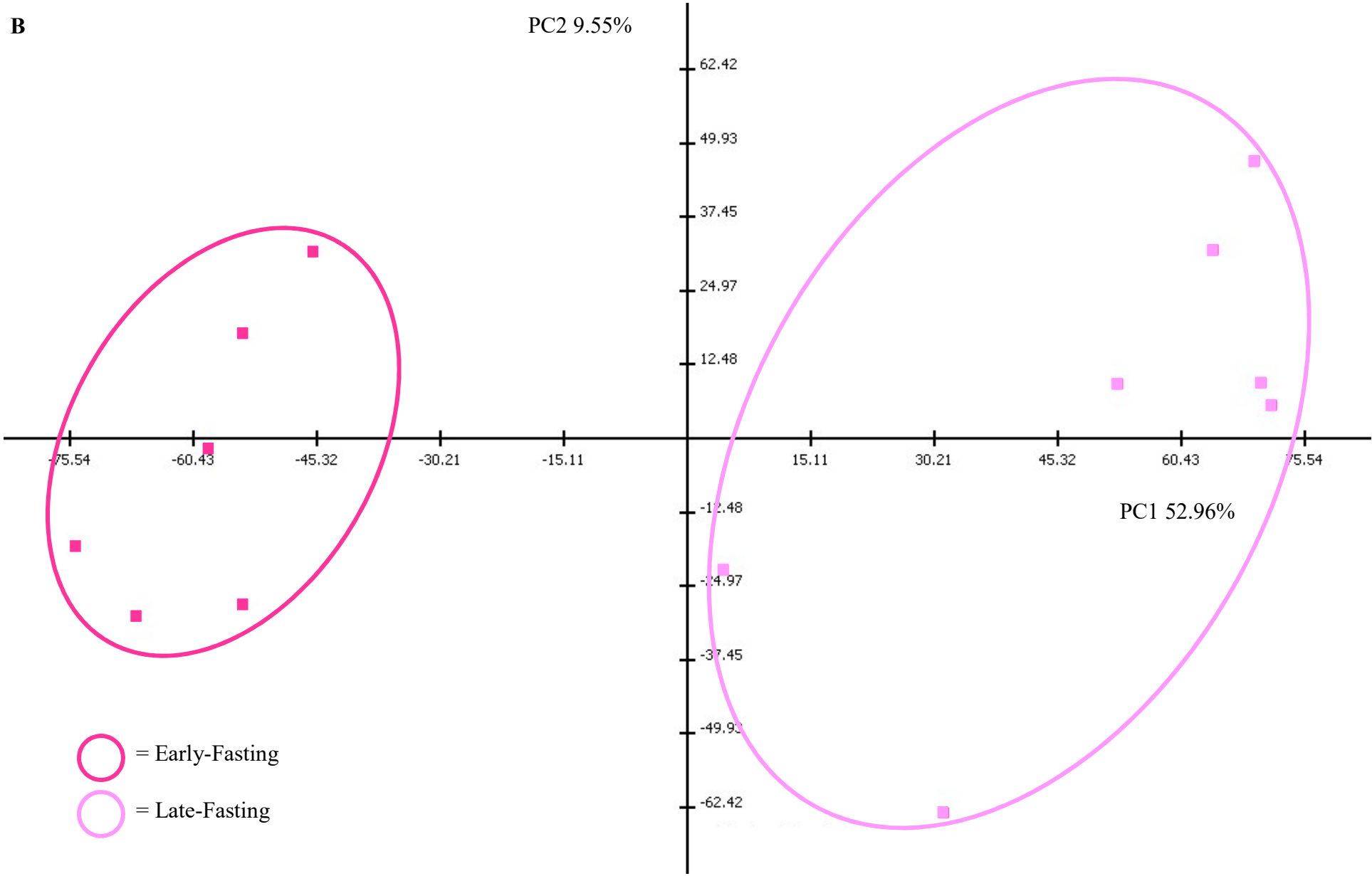
B
PC2 9.55%
62.42
49.93
37.45
24.97
12.48
-12.48
-24.97
-37.45
-49.93
-62.42
-75.54
-60.43
-45.32
-30.21
-15.11
15.11
30.21
45.32
60.43
75.54
PC1 52.96%
= Early-Fasting
= Late-Fasting

C

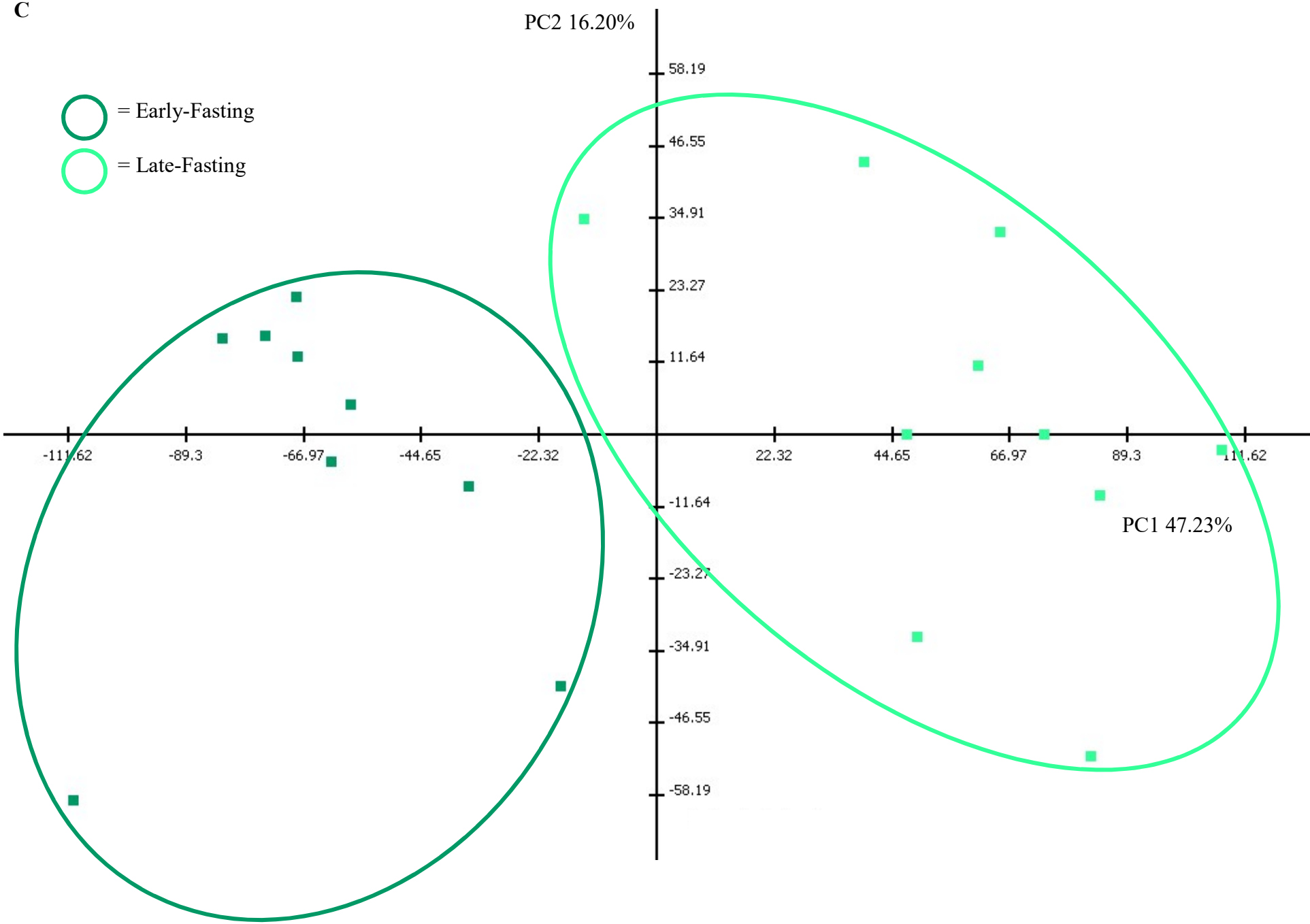
PC2 16.20%
= Early-Fasting
= Late-Fasting
58.19
46.55
34.91
23.27
11.64
-11.64
-23.27
-34.91
-46.55
-58.19
-111.62
-89.3
-66.97
-44.65
-22.32
22.32
44.65
66.97
89.3
111.62
PC1 47.23%

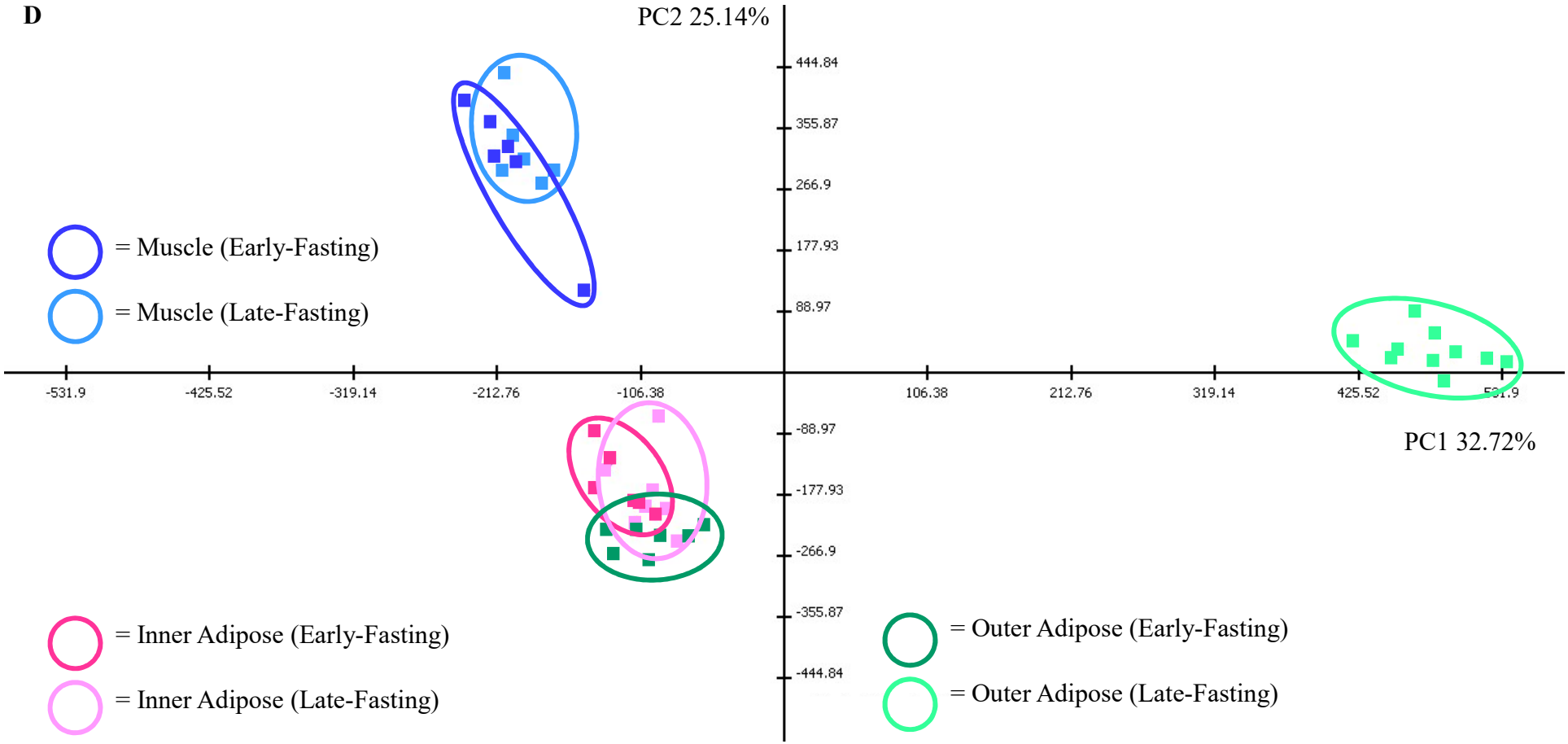

Figure 2. Principal components analysis using expression patterns from (A) 201 identified spots in muscle tissue, (B) 242 identified spots in inner adipose tissue, (C) 291 identified spots in outer adipose tissue, and 258 identified spots in all tissues combined from early- and post-fating groups. Each square represents a sample and the darker color represents late-fasting sample. The amount of variation in protein expression described by each component is identified with percentages on each axis.

A

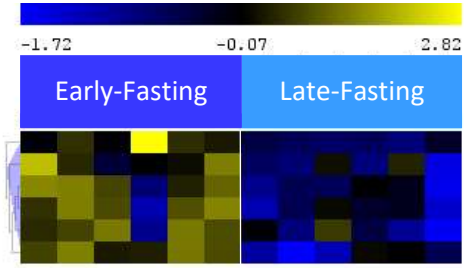

Spot #	Protein Identification
233	Triosephosphate Isomerase
57	Glyceraldehyde-3-Phosphate Dehydrogenase
23	Fructose-bisphosphate Aldolase A
24	Fructose-bisphosphate Aldolase A
25	Glyceraldehyde-3-Phosphate Dehydrogenase
258	Mitochondrial Aconitase

B

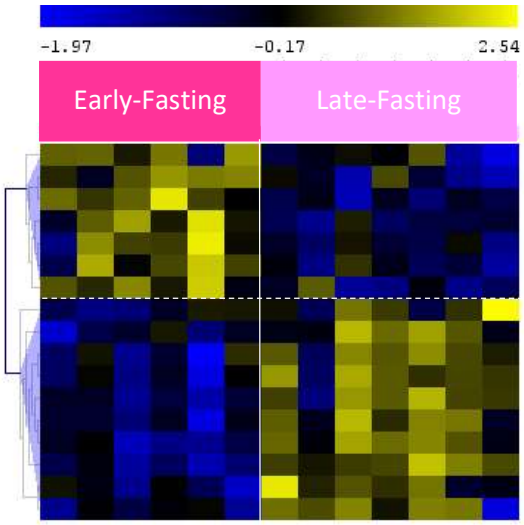

Spot #	Protein Identification
154	Glutamate Dehydrogenase 1, Mitochondrial
211	L-Lactate Dehydrogenase B Chain
229	Monoglyceride Lipase
180	β-Enolase
178	β-Enolase
189	Creatine Kinase M-Type
236	Apolipoprotein A-1
22	3-Ketoacyl-CoA Thiolase, Mitochondrial
08	L-lactate Dehydrogenase A Chain
15	Transketolase
16	Glyceraldehyde-3-Phosphate Dehydrogenase
14	Transketolase
13	Transketolase
17	Pyruvate Kinase PKM
268	6-Phosphogluconate Dehydrogenase
38	ATP Synthase Subunit α, Mitochondrial
272	Fatty Acid-Binding Protein, Adipocyte

C

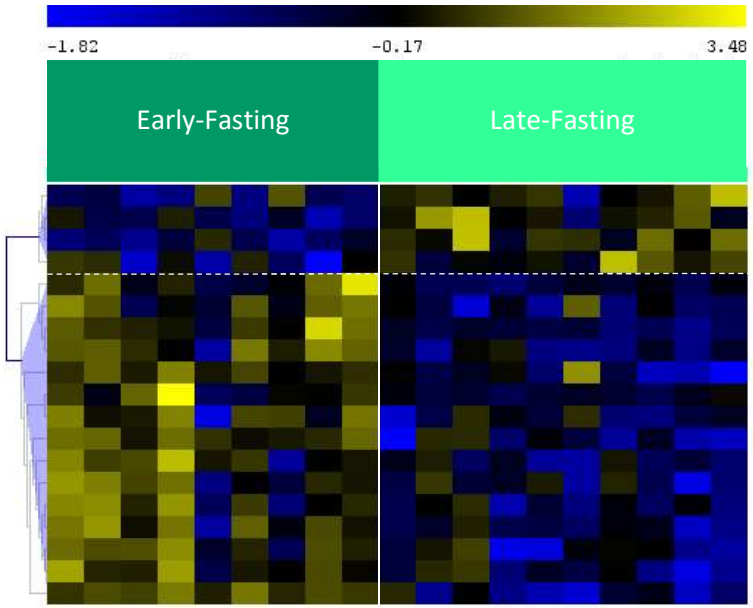

Spot #	Protein Identification
215	Cytochrome Oxidase Subunit 1, Mitochondrial
111	Transketolase
219	Phosphoglycerate Kinase 1
242	Malate Dehydrogenase, Cytoplasmic
11	Fatty Acid-Binding Protein, Adipocyte
167	Aldehyde Dehydrogenase, Mitochondrial
280	Apolipoprotein A-1
290	Flavin Reductase (NADPH)
272	Triosephosphate Isomerase
24	Electron Transfer Flavoprotein Subunit α, Mitochondrial
211	Isocitrate Dehydrogenase (NADP), cytoplasmic
205	Glutamine Synthetase
213	Fructose-Bisphosphate Aldolase A
218	Fructose-Bisphosphate Aldolase A
199	Isocitrate Dehydrogenase (NADP), cytoplasmic
246	Glycerol 3 Phosphate Dehydrogenase (NAD+), Cytoplasmic
257	Monoglyceride Lipase
266	Carbonic Anhydrase 3
307	Fatty Acid-Binding Protein, Adipocyte

Figure 3. Heat map for standardized spot volumes of energy metabolism proteins and their relative changes between the early- and late-fasting time-points in *M. angustirostris* tissue. (A) Skeletal muscle, (B) inner adipose, and (C) outer adipose tissue. Each column represents an individual seal and each row represents a different protein. Yellow represents an increased abundance, blue represents a decreased abundance, and black represents no change from the normalized value for each spot. The number of spots that changed significantly between the two time-points were determined using a permutation t-test ($p < 0.05$).

A

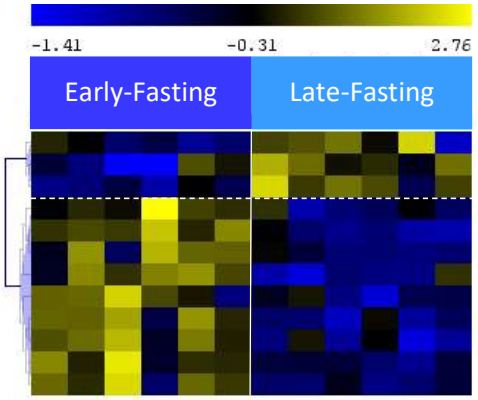

Spot #	Protein Identification
56	Elongation Factor 1 α
223	APOBEC-2
237	Glutathione S-Transferase P
112	APOBEC-2
132	Heat Shock Cognate 71kDa
136	Heat Shock Protein 70kDa
255	ES1 Protein Homolog 1, Mitochondrial
207	Glutathione S-Transferase P
228	Peroxiredoxin-6
230	Heat Shock Protein β-1
248	Heat Shock Protein β-6
267	α-Crystallin B Chain

B

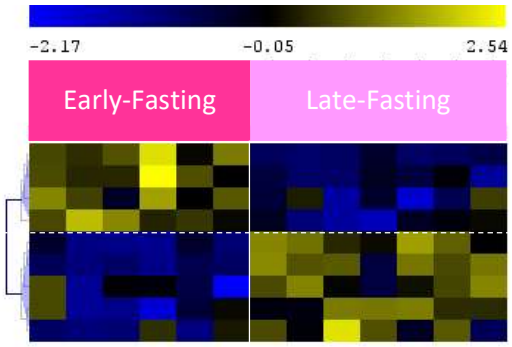

Spot #	Protein Identification
150	Calreticulin
166	Heterogeneous Nuclear Ribonucleoprotein H
221	Cathepsin D
242	Peroxiredoxin-2
247	Superoxide Dismutase [Cu-Zn], Chloroplastic
147	Calreticulin
149	Calreticulin
243	Cell Division Control Protein 42 Homolog
256	Phosphatidylethanolamine-Binding Protein 1

C

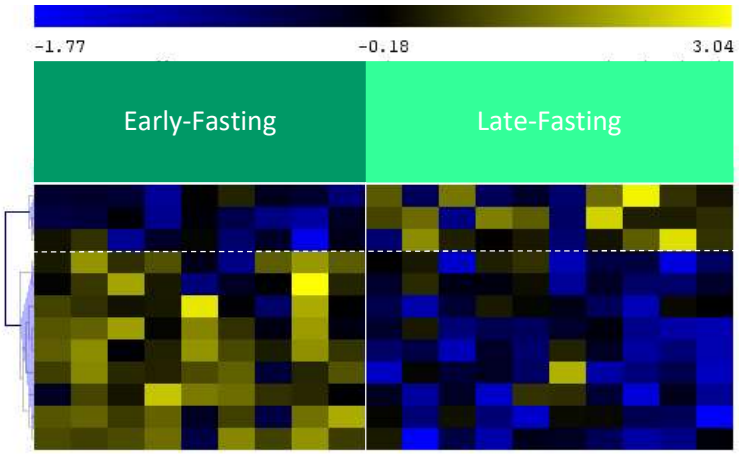

Spot #	Protein Identification
52	Endoplasmin
58	Heat Shock 70kDa Protein 4
101	Prelamin-A/C
229	BTB/POZ Domain-Containing Protein KCTD12
237	Guanine Nucleotide-Binding Protein G(I)/G(S)/G(T) Subunit β
87	78kDa Glucose-Regulated Protein
128	Calreticulin
137	Calreticulin
159	Selenium-Binding Protein 1
283	Proteasome Subunit β Type-1
261	Cathepsin D
289	Peroxiredoxin-1

Figure 4. Heat map for standardized spot volumes of proteostasis proteins and their relative changes between the early- and late-fasting time-points in *M. angustirostris* tissue. (A) Skeletal muscle, (B) inner adipose, and (C) outer adipose tissue. For more details see Fig. 3.

A

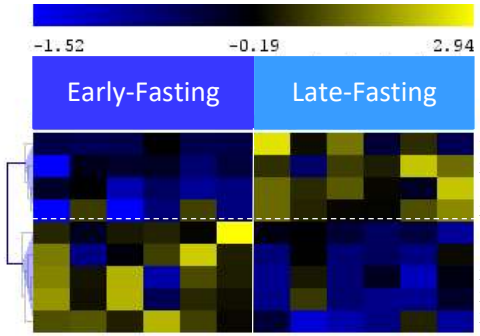

Spot #	Protein Identification
76	Myosin, Heavy Polypeptide 7, Cardiac Muscle β
27	LIM Domain-Binding Protein / Slow Skeletal Muscle Troponin T
107	Chain A, Structures of Actin-Bound Wh2 Domains of Spire
210	Slow Skeletal Muscle Troponin T
152	Chain A, Structures of Actin-Bound Wh2 Domains of Spire
101	α-Actinin-2
212	Slow Skeletal Muscle Troponin T
215	Slow Skeletal Muscle Troponin T
261	Myosin, Heavy Polypeptide 7, Cardiac Muscle β

B

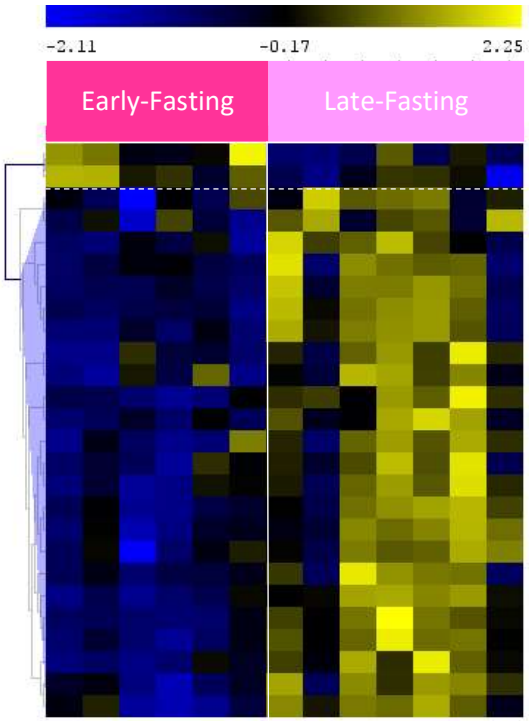

Spot #	Protein Identification
124	α-2-HS-Glycoprotein
127	Keratin, Type II Cuticular Hb5
139	Keratin 81
169	Actin
53	Collagen α-3(VI) Chain
47	Collagen α-2(V) Chain
50	Collagen α-2(V) Chain
49	Collagen α-3(VI) Chain
54	Collagen α-3(VI) Chain
138	Vimentin
177	Actin, Cytoplasmic
197	Keratin, Type II, Cytoskeletal 2 Epidermal
202	Mimecan
57	Collagen α-2(VI) Chain
63	Collagen α-2(VI) Chain
65	Collagen α-2(VI) Chain
58	Collagen α-2(VI) Chain
61	Collagen α-2(VI) Chain
66	Collagen α-2(VI) Chain
56	Collagen α-1(VI) Chain
55	Collagen α-2(VI) Chain
115	Fibulin-5
120	Fibulin-5
214	Galectin-3
59	Collagen α-1(VI) Chain
271	Prolargin

C

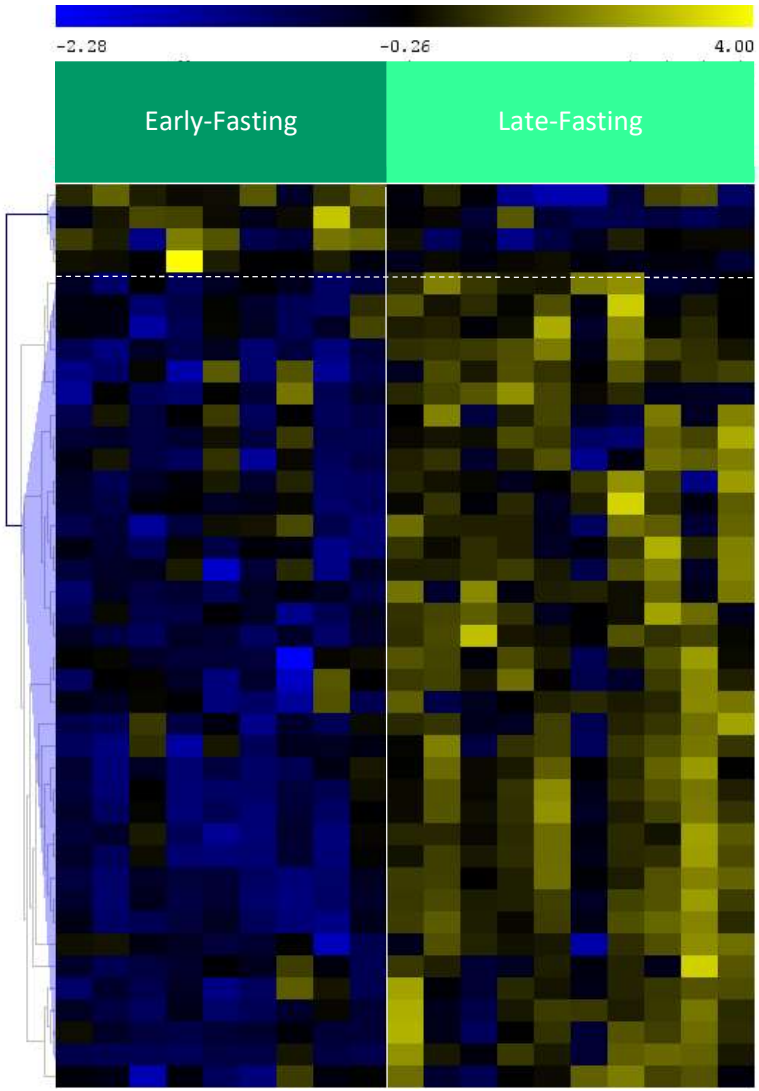

Spot #	Protein Identification
47	Nidogen-2
168	Keratin 81
13	Galectin-1
206	Type II Keratin Subunit
106	Prolargin
31	Collagen α-3(VI) Chain
33	Collagen α-3(VI) Chain
252	Four and a Half LIM Domains Protein 1
179	Actin, Cytoplasmic
298	Transgelin
156	Desmin
116	Actin, Cytoplasmic
226	Mimecan
01	Prolargin
02	Prolargin
83	Prolargin
103	Prolargin
110	Prolargin
70	Lumican
48	Nidogen-2
250	Four and a Half LIM Domains Protein 1
74	Gelsolin
85	Type II Keratin Subunit Protein
164	Keratin, Type II Cuticular Hb3
39	Collagen α-2(VI) Chain
40	Collagen α-1(VI) Chain
26	Collagen α-2(V) Chain
25	Collagen α-2(V) Chain
29	Collagen α-2(V) Chain
28	Collagen α-3(VI) Chain
30	Collagen α-2(V) Chain
42	Collagen α-2(VI) Chain
43	Collagen α-2(VI) Chain
44	Collagen α-2(VI) Chain
104	Prolargin
177	Keratin, Type I Cytoskeletal 14
141	Keratin, Type II Cuticular Hb3
142	Keratin, Type II Cuticular Hb3
143	Collagen α-2(VI) Chain
194	Keratin, Type I Cuticular HA1
314	Dihydropyrimidinase-Related Protein 2

Figure 5. Heat map for standardized spot volumes of cytoskeletal proteins and their relative changes between the early- and late-fasting time-points in *M. angustirostris* tissue. (A) Skeletal muscle, (B) inner adipose, and (C) outer adipose tissue. For more details see Fig. 3.

A

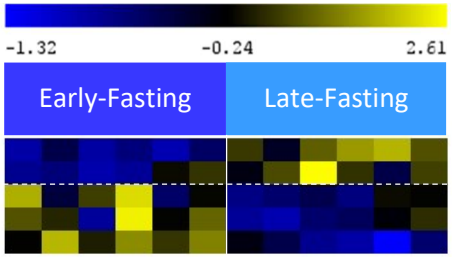

Spot #	Protein Identification
65	Myoglobin
67	Myoglobin
70	Hemoglobin Subunit α
114	Serotransferrin
128	Serum Albumin

B

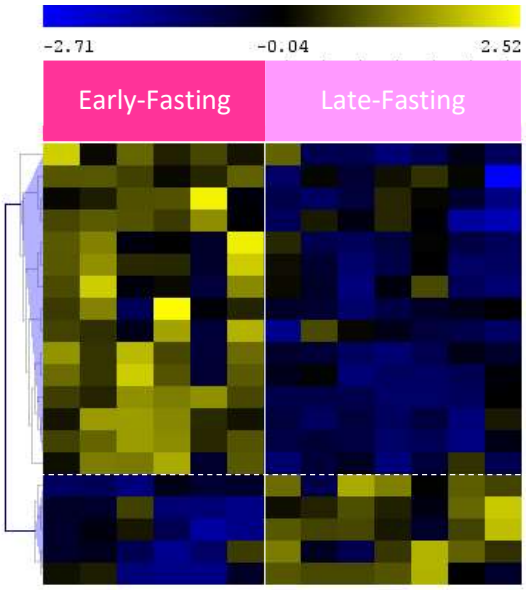

Spot #	Protein Identification
71	Fibrinogen Δ Chain
158	α-1-Antitrypsin
153	Antithrombin-III
164	α-1-Antitrypsin
95	Serotransferrin
97	Serotransferrin
98	Serotransferrin
162	Fibrinogen Δ Chain
175	α-1-Antitrypsin
79	Fibrinogen Δ Chain
84	Fibrinogen Δ Chain
205	Haptoglobin
206	Haptoglobin
208	Haptoglobin
215	Haptoglobin
07	NADH-Cytochrome b5 Reductase 3
23	Complement C4-A
24	Complement C4-A
81	Complement Factor B
269	Plasminogen

C

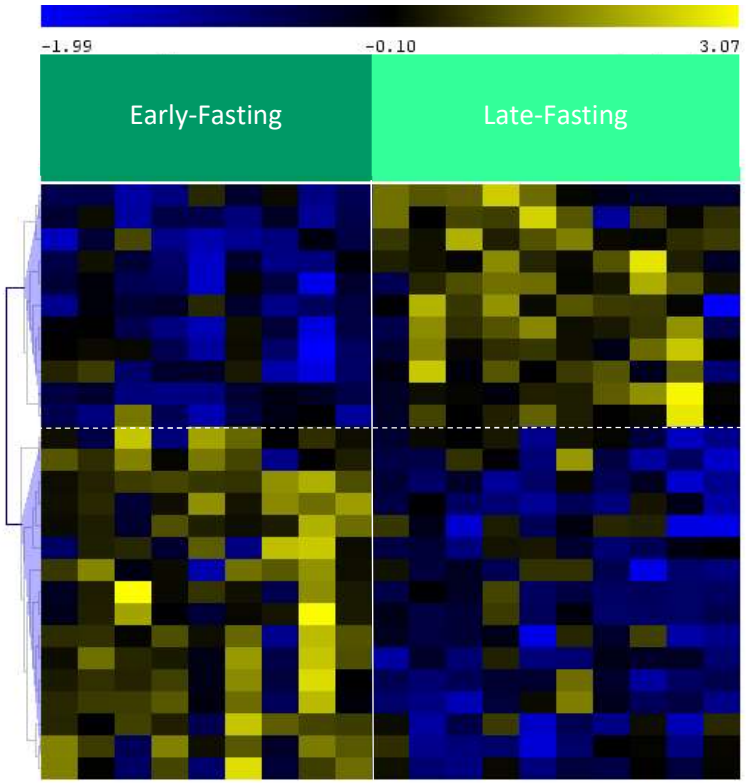

Spot #	Protein Identification
51	Plasminogen
113	Serum Albumin
121	Serum Albumin
97	Fibrinogen α Chain
102	Fibrinogen α Chain
61	Complement Factor B
100	Serotransferrin
108	Serotransferrin
109	Serotransferrin
99	Serum Albumin
127	Complement C3
56	Serum Albumin
135	Fibrinogen β Chain
88	Serum Albumin
95	Serum Albumin
166	α-1-Antitrypsin
170	Fibrinogen Δ Chain
119	Hemopexin
63	Fibrinogen Δ Chain
66	Fibrinogen Δ Chain
81	Serotransferrin
86	Serotransferrin
228	Haptoglobin
232	Haptoglobin
309	Hemoglobin Subunit α
09	Hemoglobin Subunit β
311	Hemoglobin Subunit α

Figure 6. Heat map for standardized spot volumes of blood proteins (iron binding and immunity) and their relative changes between the early- and late-fasting time-points in *M. angustirostris* tissue. (A) Skeletal muscle, (B) inner adipose, and (C) outer adipose tissue. For more details see Fig. 3.

A

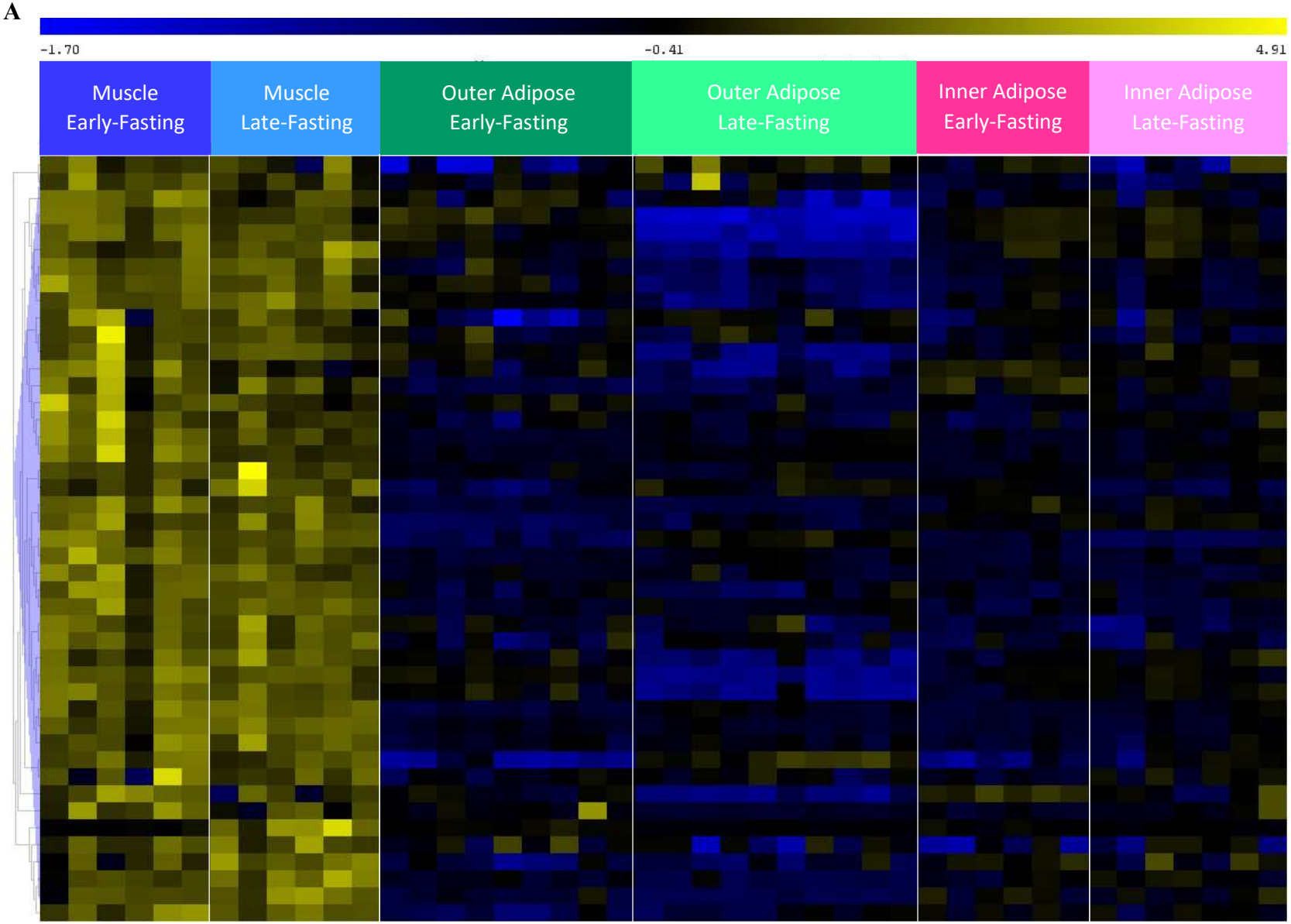

Spot #	Protein Identification
188	actin, alpha cardiac muscle 1
346	51 voltage channel protein 1
77	aconitate hydratase
271	fructose-bisphosphate aldolase A
273	fructose-bisphosphate aldolase A
310	HNR A2/B1 1
241	isocitrate dehydrogenase [NADP]
250	GAPDH
395	peroxiredoxin-1
272	fructose-bisphosphate aldolase A
349	electron transfer flavoprotein α
356	carbonic anhydrase 3
371	heat shock protein beta-1
294	slow skeletal muscle troponin T
259	vimentin-like isoform 1
309	glutathione S-transferase P
324	troponin T, slow skeletal 3
412	alpha-crystallin B chain
248	creatine kinase S-type
383	myosin light chain 6B 1
247	creatine kinase M-type 1
249	creatine kinase M-type
240	GAPDH
262	creatine kinase M-type
269	Tropomyosin alpha-1 chain
285	acetyl-CoA acetyltransferase
311	myozenin-1 2
244	glutamine synthetase 1
245	isocitrate dehydrogenase [NADP]
243	phosphogycerate kinase 1
236	3 ketoacyl-CoA thiolase
258	3-ketoacyl-CoA thiolase
418	myosin light chain 2
419	myosin regulatory light chain 2
420	myosin regulatory light chain 2
406	superoxide dismutase [Mn]
422	cofilin-2
433	myoglobin
437	fatty acid-binding protein
435	myoglobin
217	actin, cytoplasmic 1
317	troponin T, slow skeletal 3
313	LIM domain-binding 3
427	desmin
454	fatty acid-binding protein

* heterogeneous nuclear ribonucleoproteins A2/B1 1 = HNR A2/B1 1
* glyceraldehyde 3 phosphate dehydrogenase = GAPDH
* 51 voltage-dependent anion-selective channel protein 1 isoform 1 = 51 voltage channel protein 1

B

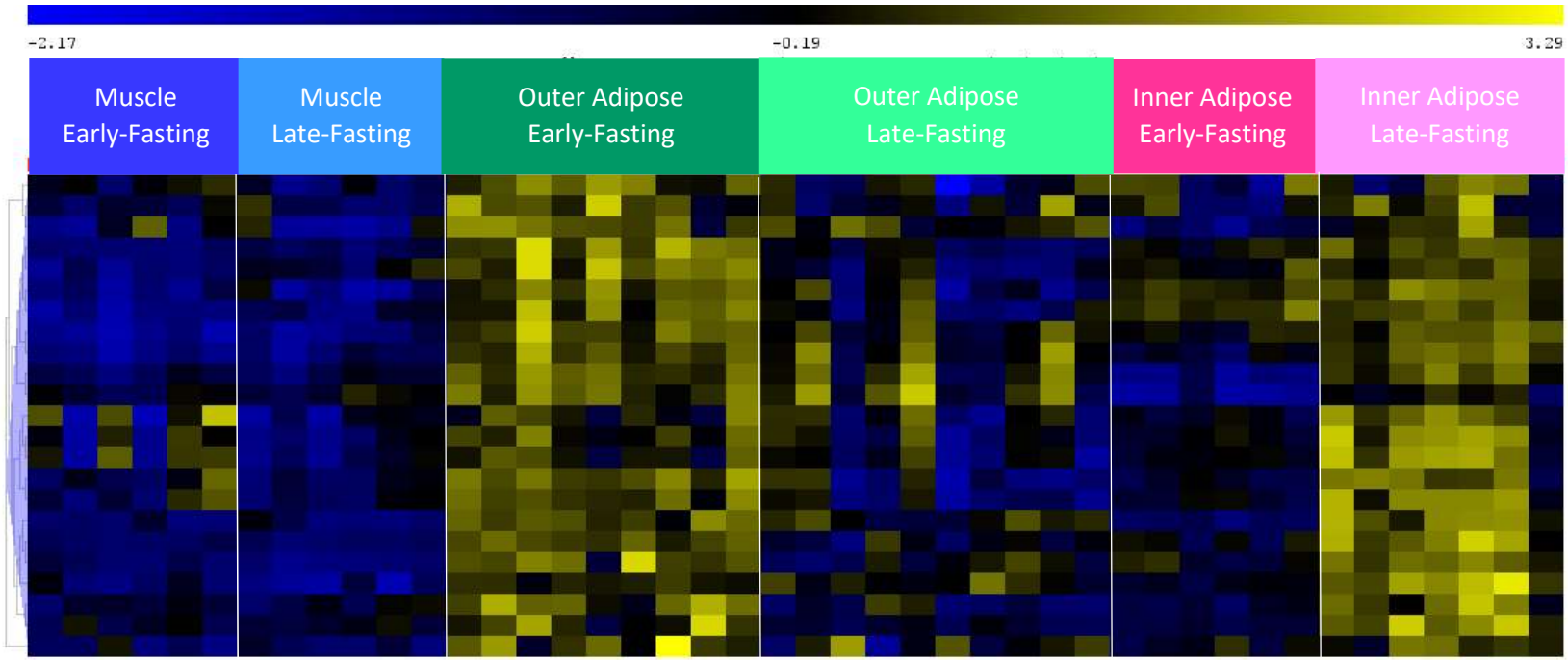

Spot #	Protein Identification
58	complement factor B
43	C-1-tetrahydrofolate synthase
127	prolargin-like, partial
12	collagen alpha-1(VI) chain
13	collagen alpha-2(VI) chain
11	collagen alpha-1(VI) chain
15	collagen alpha-2(VI) chain
20	collagen alpha-2(VI) chain
21	collagen alpha-2(VI) chain
22	collagen alpha-2(VI) chain
23	collagen-alpha-2(VI) chain
4	collagen alpha-3(VI) chain
3	collagen alpha 2(V) chain
8	collagen alpha 2(V) chain
5	collagen alpha-2(V) chain
9	collagen alpha-2(V) chain
76	gelsolin-like
41	nidogen-2
152	prolargin-like
171	myosin-binding protein H
292	BTB/POZ KCTD12
314	guanine nucleotide-binding protein 2
345	guanine nucleotide-binding protein 2

C

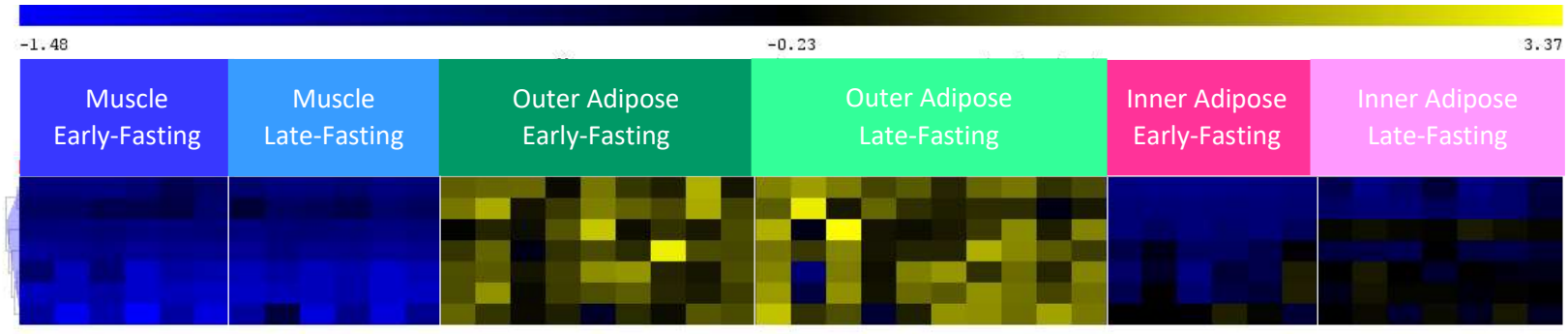

Spot #	Protein Identification
161	calreticulin
182	calreticulin
98	lumican
102	fibromodulin
73	lumican
97	lumican
215	HNR H8

* heterogenous nuclear ribonucleoprotein H isoform X8 = HNR H8

D

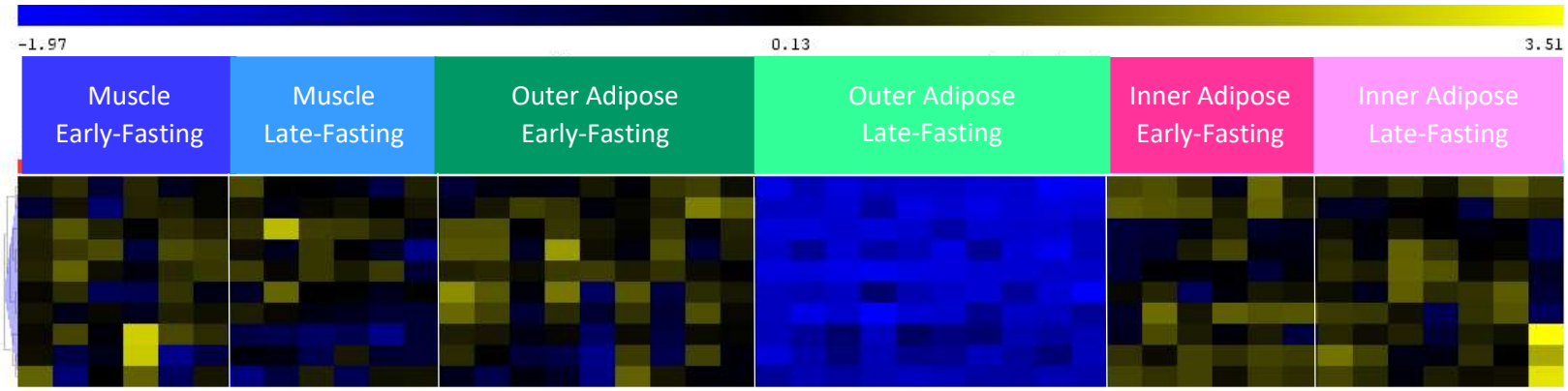

Spot #	Protein Identification
84	serum albumin
89	serum albumin
235	phosphoglycerate kinase 1
290	GAPDH
295	glyceraldehyde-3-phosphate dehydroge
306	malate dehydrogenase 1
369	triosephosphate isomerase
375	triosephosphate isomerase
364	carbonic anhydrase 2
432	hemoglobin subunitα

* glyceraldehyde 3 phosphate, dehydrogenase = GAPDH

E

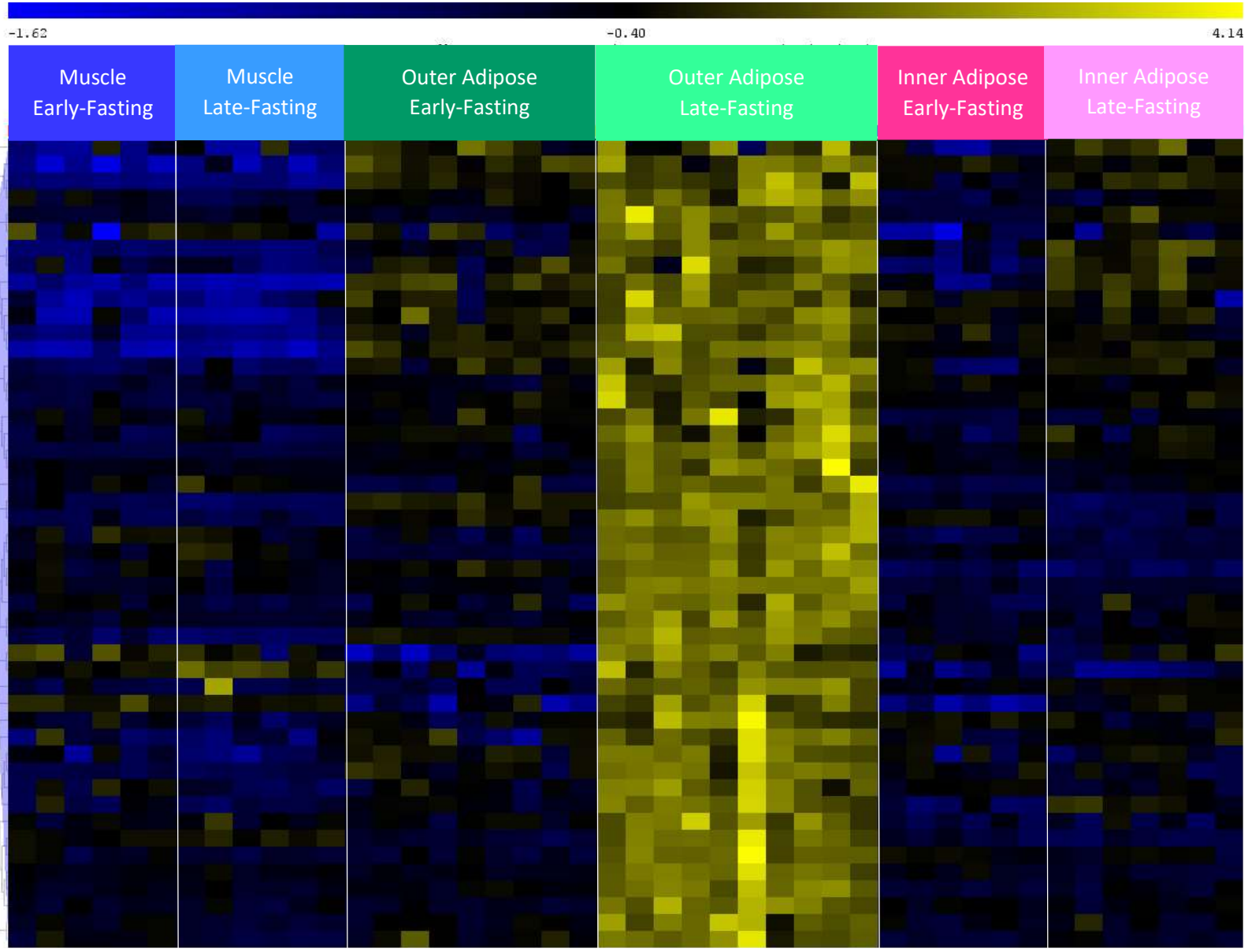

Spot #	Protein Identification
44	elongation factor 2
215	heterogenous nuclear ribonucleoprotein H8
156	transketolase
348	muscle glycogen phosphorylase
170	fibulin-5-like OR alpha-2-HS-glycoprotein 1
296	glyceraldehyde-3-phosphate dehydrogenase
36	nidogen-2
39	nidogen-1
129	prolargin-like, partial
164	phosphoglucomutase-1
162	complement C3-like
187	keratin, type I cytoskeletal 16 3
197	hemopexin-like
46	plasminogen-like 1
207	fibrinogen gamma chain 1
283	keratin, type II, cytoskeletal 2
47	heat shock 70kDa protein 4 1
62	neutral alpha-glucosidase AB 1
31	myosin-binding protein C, slow-type 1
212	MSDH 1
232	keratin, type I cytoskeletal 17
303	mimecan
323	haptoglobin
61	fibrinogen gamma chain 1
65	serum albumin
211	ATP synthase subunit β
284	mimecan
342	voltage-dependent anion-selective channel 1
288	haptoglobin
350	purine nucleoside phosphorylase
184	myotilin
392	glutathione S-transferase P
238	annexin A7 isoform X1
234	6-phosphogluconate dehydrogenase 1
402	flavin reductase (NADPH)
389	GTP-binding nuclear protein Ran 1
114	fibrinogen alpha chain
130	carbonic anhydrase 3
144	serum albumin
391	cytochrome b-c1 complex subunit Rieske
237	adenosylhomocysteinase
228	enoyl-CoA hydratase, mitochondrial
231	elongation factor 1-gamma
227	alpha-centractin
230	malate dehydrogenase 1
347	phosphatidylinositol transfer α
151	keratin, type II cuticular Hb3
452	heat shock 70kDa 1

* methylmalonate-semialdehyde dehydrogenase [acylating], mitochondrial isoform X1 = MSDH 1

Figure 7. Heat map for standardized spot volumes of proteins and their relative abundances between the early- and late-fasting time-points in skeletal muscle, inner adipose, and outer adipose tissue in *M. angustirostris* tissue. Each column represents an individual seal and each row represents a different protein. Yellow represents an increased abundance, blue represents a decreased abundance, and black represents no difference from the normalized value for each spot. General trends shown are A) an increased abundance of proteins in muscle tissue, B) an increased abundance of proteins in the outer adipose of early-fasting pups and the inner adipose of late-fasting pups, C) an increased abundance in outer adipose, D) a decreased abundance in late-fasting outer adipose, and E) an increased abundance in late-fasting outer adipose.

APPENDIX C: SUPPLEMENTARY INFORMATION

Table S1. List of acronyms. Written in alphabetical order.

2D	Two-Dimensional
AFABP	Adipocyte Fatty Acid-Binding Protein
ALDH	Aldehyde Dehydrogenase
ANOVA	Analysis of Variance
APOBEC	Apolipoprotein B mRNA Editing Enzyme, Catalytic Polypeptide-like
APP	Acute Phase Protein
ADP	Adenosine Diphosphate
ATP	Adenosine Triphosphate
BTB/POZ	Broad Complex/Tram-Track/Bric-a-Brac/Poxvirus and Zinc Finger
C3	Complement Factor 3
CAC	Citric Acid Cycle
DI3	Deiodinase Type 3
DNA	Deoxyribonucleic Acids
DTT	Dithiothreitol
DTE	Dithioerythritol
ER	Endoplasmic Reticulum
EST	Expressed Sequence Tag
ETC	Electron Transport Chain
FADH2	Flavin Adenine Dinucleotide (Hydroquinone Form)
GST	Glutathione-S-Transferase
GTP	Guanosine Triphosphate
HCCA	α-cyano-4-hydroxycinnamic acid
HSL	Hormone-Sensitive Lipase
HSP	Heat Shock Protein
KCTD	Potassium Channel Tetramerization Domain
MALDI-TOF-TOF	Matrix-Assisted Laser Desorption Ionization Tandem Time-of-Flight
MAP	Mitogen-Activated Protein
MOWSE	Molecular Weight Search
MS	Mass Spectrometry
MUFA	Monounsaturated Fatty Acids
mya	Million Years Ago
NADPH	Nicotinamide Adenine Dinucleotide Phosphate Hydrogen
NCBI	National Center for Biotechnology Information
NES	Northern Elephant Seal
PCA	Principle Component Analysis
PKM	Pyruvate Kinase Muscle Isozyme
PMF	Peptide Mass Fingerprint
PPP	Pentose Phosphate Pathway
PRX	Peroxiredoxin
PUFA	Polyunsaturated Fatty Acid
RNA	Ribonucleic Acid

ROS	Reactive Oxygen Species
SOD	Superoxide Dismutase
T3	Triiodothyronine
TFA	Trifluoroacetic Acid
UPS	Ubiquitin-Proteasome System

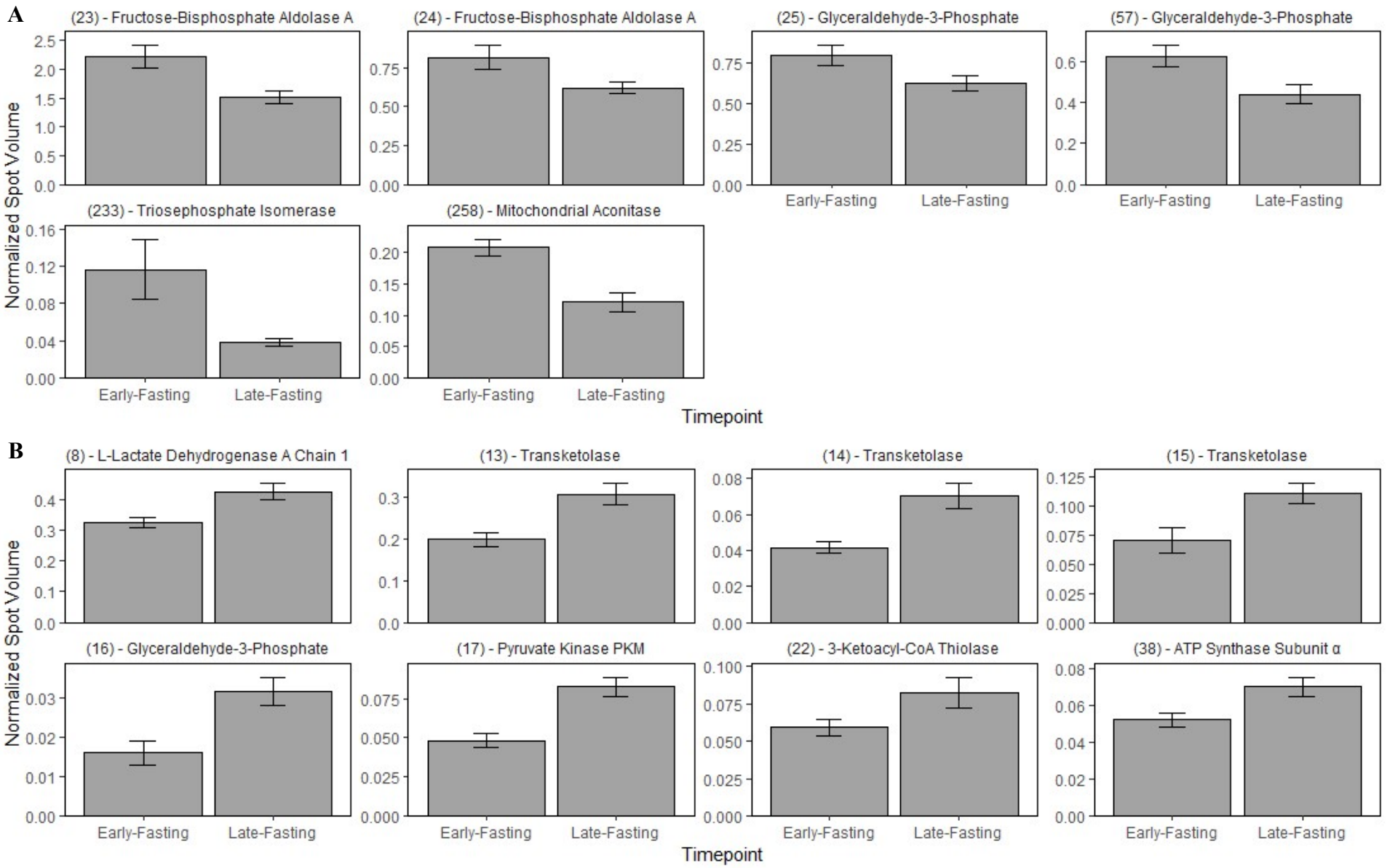
A
(23) - Fructose-Bisphosphate Aldolase A
(24) - Fructose-Bisphosphate Aldolase A
(25) - Glyceraldehyde-3-Phosphate
(57) - Glyceraldehyde-3-Phosphate
(233) - Triosephosphate Isomerase
(258) - Mitochondrial Aconitase
Normalized Spot Volume
Early-Fasting
Late-Fasting
Timepoint
B
(8) - L-Lactate Dehydrogenase A Chain 1
(13) - Transketolase
(14) - Transketolase
(15) - Transketolase
(16) - Glyceraldehyde-3-Phosphate
(17) - Pyruvate Kinase PKM
(22) - 3-Ketoacyl-CoA Thiolase
(38) - ATP Synthase Subunit α
Normalized Spot Volume
Early-Fasting
Late-Fasting
Timepoint

B cont.

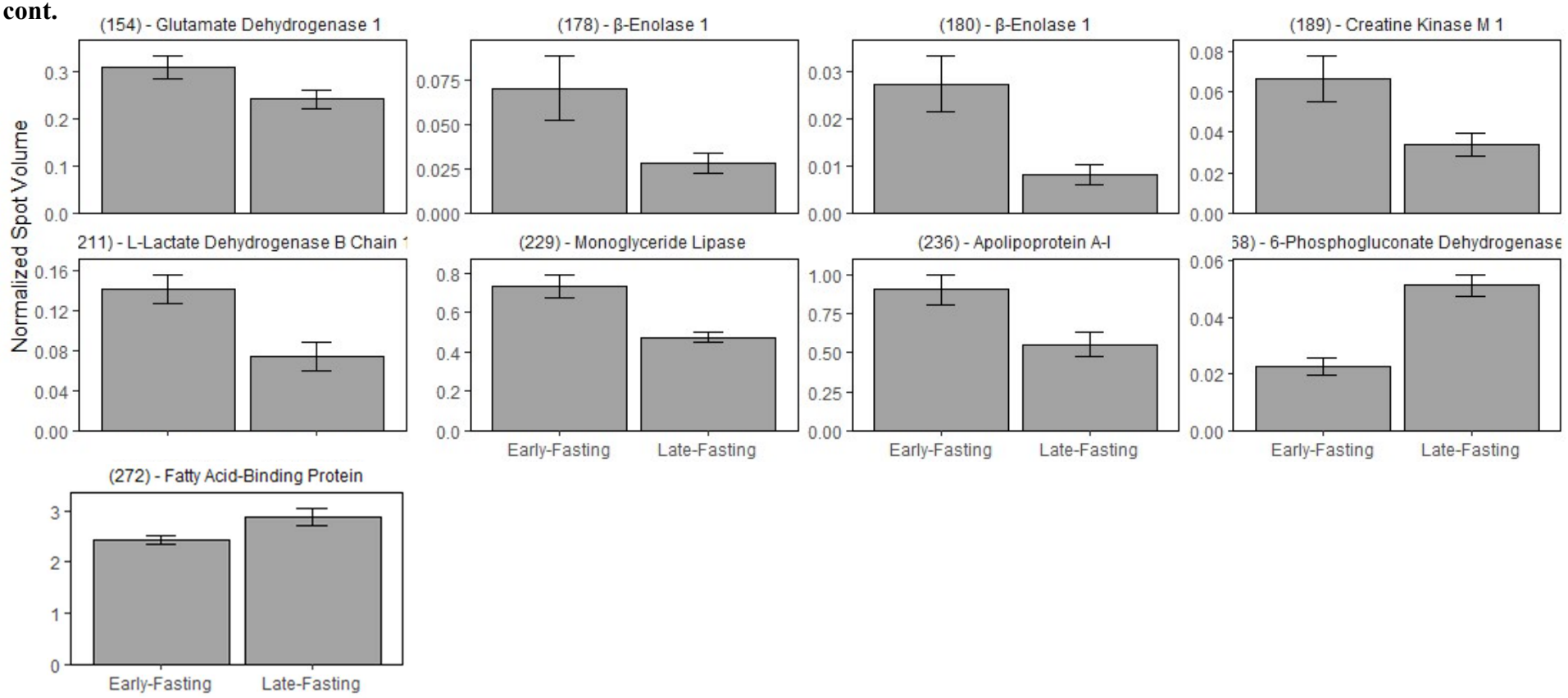
(154) - Glutamate Dehydrogenase 1
(178) - β-Enolase 1
(180) - β-Enolase 1
(189) - Creatine Kinase M 1
211) - L-Lactate Dehydrogenase B Chain 1
(229) - Monoglyceride Lipase
(236) - Apolipoprotein A-I
58) - 6-Phosphogluconate Dehydrogenase
(272) - Fatty Acid-Binding Protein
Normalized Spot Volume
Early-Fasting
Late-Fasting
Timepoint

C

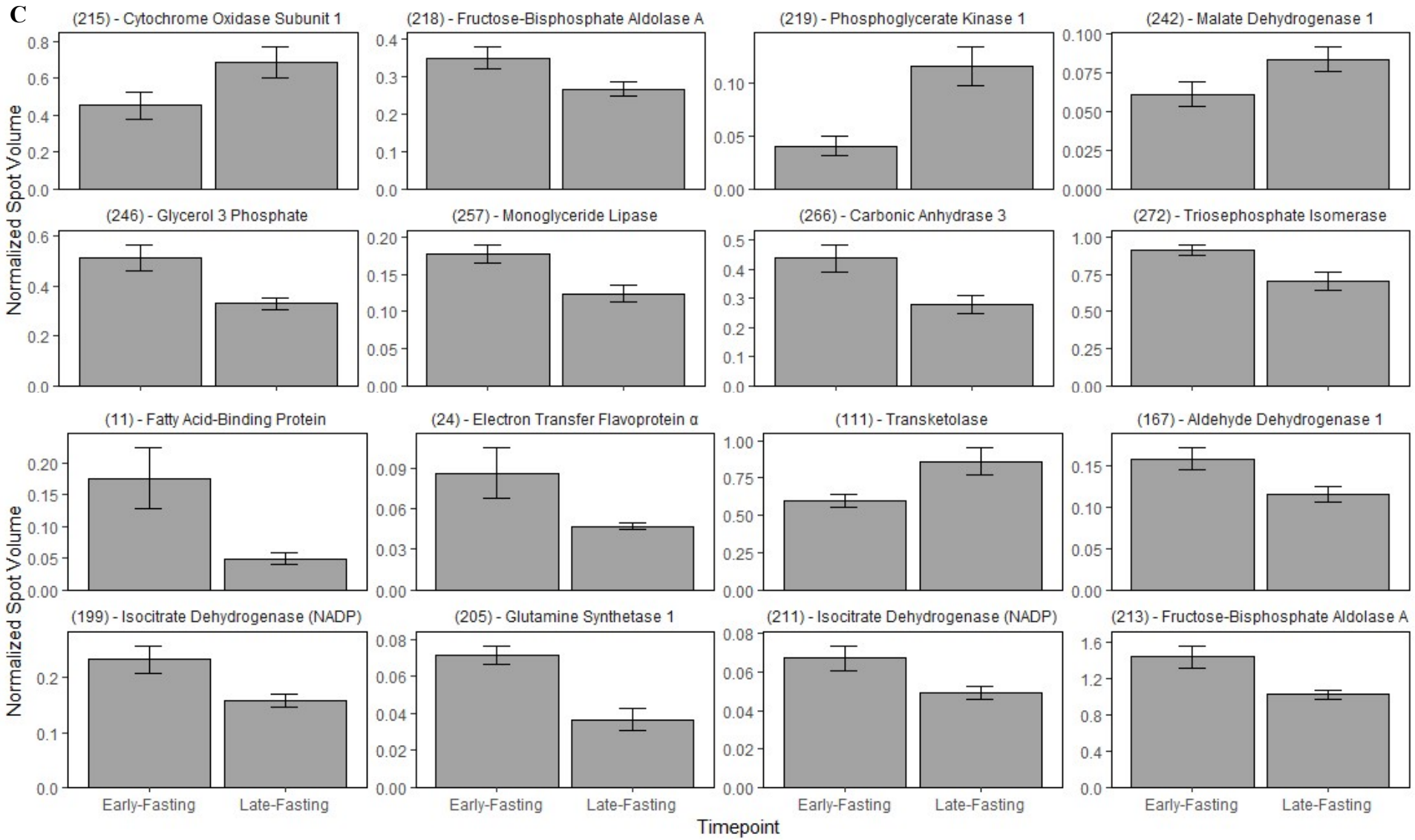
(215) - Cytochrome Oxidase Subunit 1
(218) - Fructose-Bisphosphate Aldolase A
(219) - Phosphoglycerate Kinase 1
(242) - Malate Dehydrogenase 1
(246) - Glycerol 3 Phosphate
(257) - Monoglyceride Lipase
(266) - Carbonic Anhydrase 3
(272) - Triosephosphate Isomerase
(11) - Fatty Acid-Binding Protein
(24) - Electron Transfer Flavoprotein α
(111) - Transketolase
(167) - Aldehyde Dehydrogenase 1
(199) - Isocitrate Dehydrogenase (NADP)
(205) - Glutamine Synthetase 1
(211) - Isocitrate Dehydrogenase (NADP)
(213) - Fructose-Bisphosphate Aldolase A
Normalized Spot Volume
Early-Fasting
Late-Fasting
Timepoint

C cont.

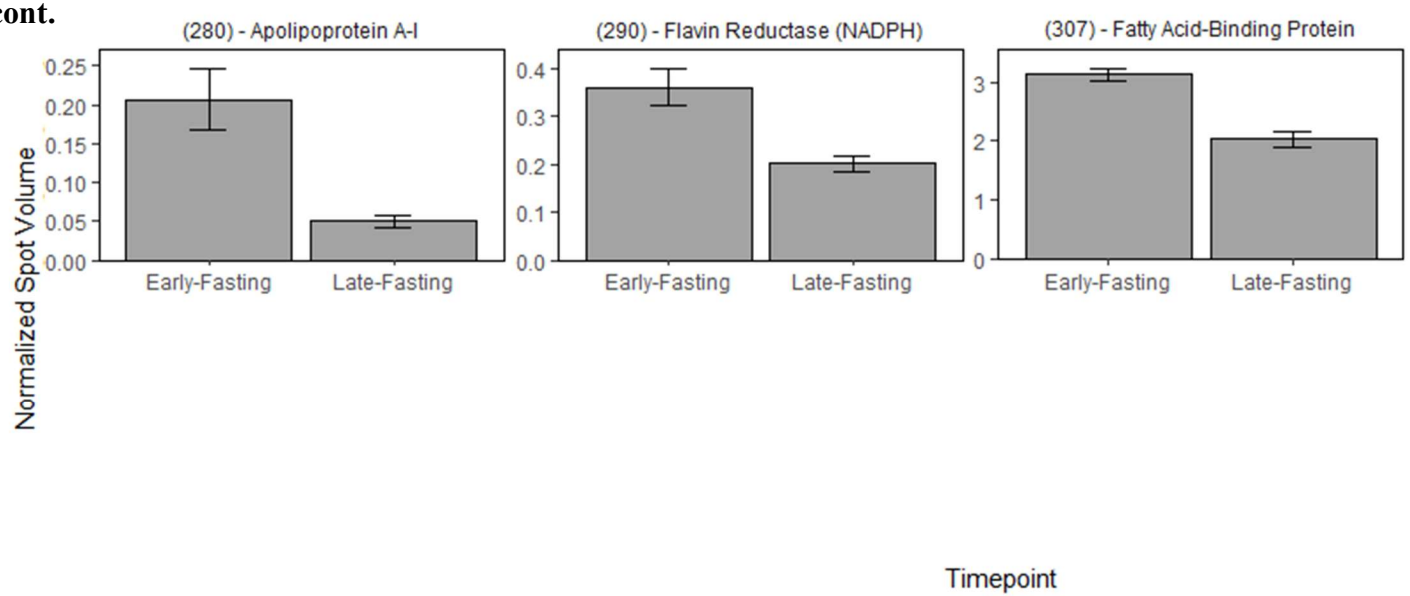

Figure S1. The abundance of energy metabolism proteins in *M. angustirostris* tissue before and after the post-weaning fast. (A) Muscle tissue, (B) inner adipose, and (C) outer adipose tissue. We obtained protein abundances by normalizing the spot volume against the volume of all proteins for each tissue separately, and abundances are displayed as the mean abundance ± 1 s.e.m.. Significance determined using a permutation t-test; $p < 0.05$.

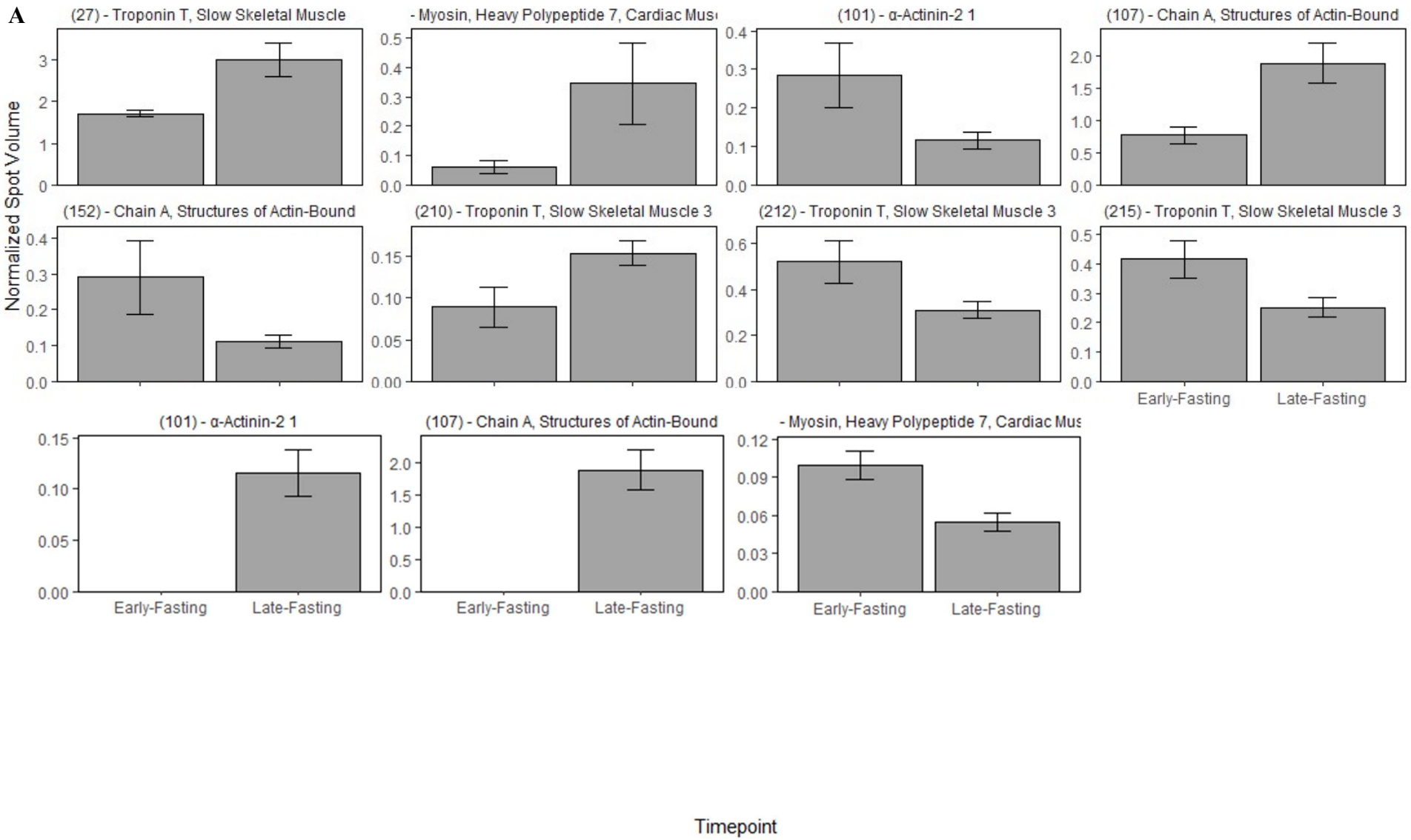
A
(27) - Troponin T, Slow Skeletal Muscle
- Myosin, Heavy Polypeptide 7, Cardiac Mus
(101) - α-Actinin-2 1
(107) - Chain A, Structures of Actin-Bound
(152) - Chain A, Structures of Actin-Bound
(210) - Troponin T, Slow Skeletal Muscle 3
(212) - Troponin T, Slow Skeletal Muscle 3
(215) - Troponin T, Slow Skeletal Muscle 3
(101) - α-Actinin-2 1
(107) - Chain A, Structures of Actin-Bound
- Myosin, Heavy Polypeptide 7, Cardiac Mus
Normalized Spot Volume
Early-Fasting
Late-Fasting
Timepoint

B

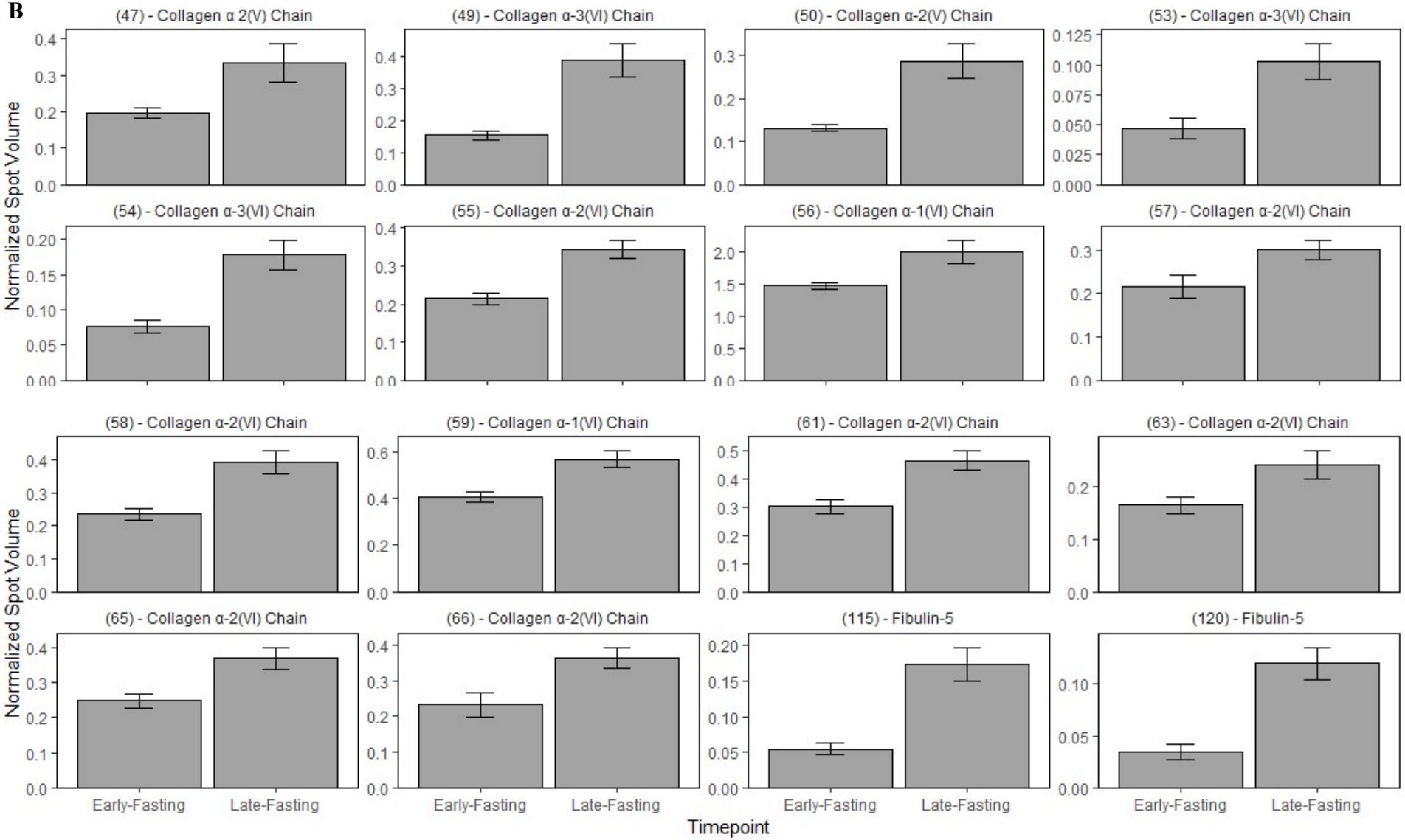
(47) - Collagen α 2(V) Chain
(49) - Collagen α-3(VI) Chain
(50) - Collagen α-2(V) Chain
(53) - Collagen α-3(VI) Chain
(54) - Collagen α-3(VI) Chain
(55) - Collagen α-2(VI) Chain
(56) - Collagen α-1(VI) Chain
(57) - Collagen α-2(VI) Chain
(58) - Collagen α-2(VI) Chain
(59) - Collagen α-1(VI) Chain
(61) - Collagen α-2(VI) Chain
(63) - Collagen α-2(VI) Chain
(65) - Collagen α-2(VI) Chain
(66) - Collagen α-2(VI) Chain
(115) - Fibulin-5
(120) - Fibulin-5
Normalized Spot Volume
Early-Fasting
Late-Fasting
Timepoint

B cont.

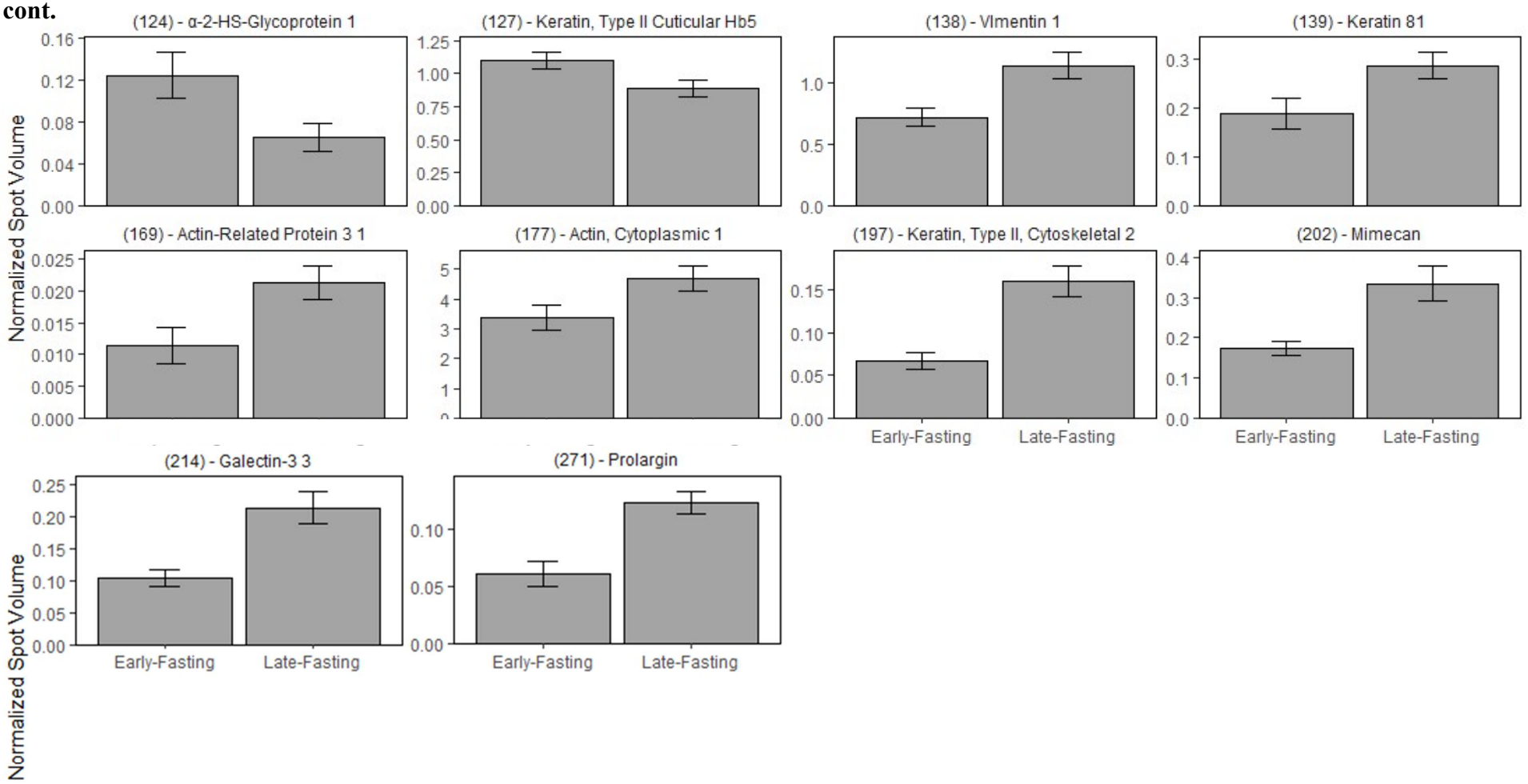
(124) - α-2-HS-Glycoprotein 1
(127) - Keratin, Type II Cuticular Hb5
(138) - Vimentin 1
(139) - Keratin 81
(169) - Actin-Related Protein 3 1
(177) - Actin, Cytoplasmic 1
(197) - Keratin, Type II, Cytoskeletal 2
(202) - Mimecan
(214) - Galectin-3 3
(271) - Prolargin
Normalized Spot Volume
Early-Fasting
Late-Fasting
Timepoint

C

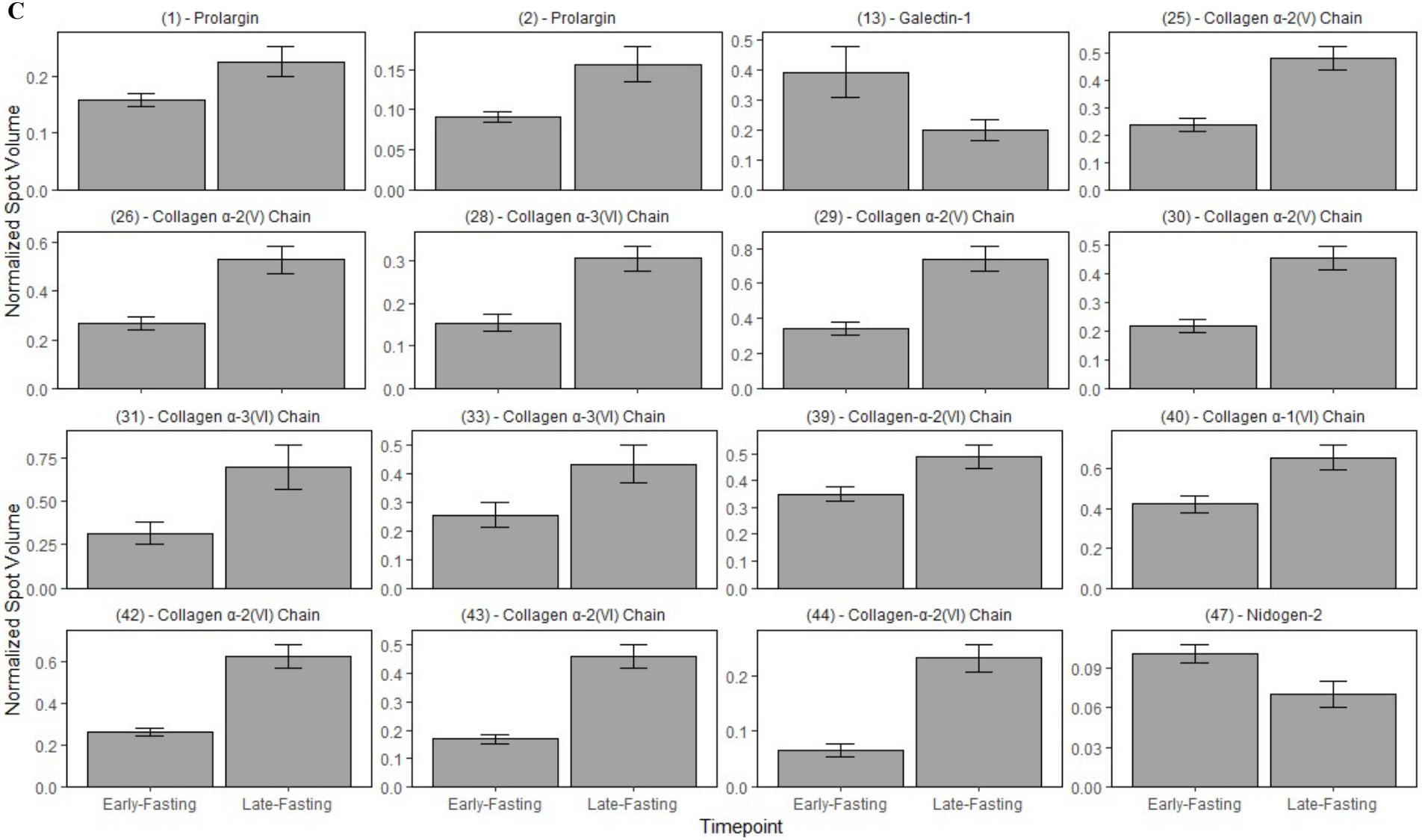
(1) - Prolargin
(2) - Prolargin
(13) - Galectin-1
(25) - Collagen α-2(V) Chain
(26) - Collagen α-2(V) Chain
(28) - Collagen α-3(VI) Chain
(29) - Collagen α-2(V) Chain
(30) - Collagen α-2(V) Chain
(31) - Collagen α-3(VI) Chain
(33) - Collagen α-3(VI) Chain
(39) - Collagen-α-2(VI) Chain
(40) - Collagen α-1(VI) Chain
(42) - Collagen α-2(VI) Chain
(43) - Collagen α-2(VI) Chain
(44) - Collagen-α-2(VI) Chain
(47) - Nidogen-2
Normalized Spot Volume
Early-Fasting
Late-Fasting
Timepoint

C cont.

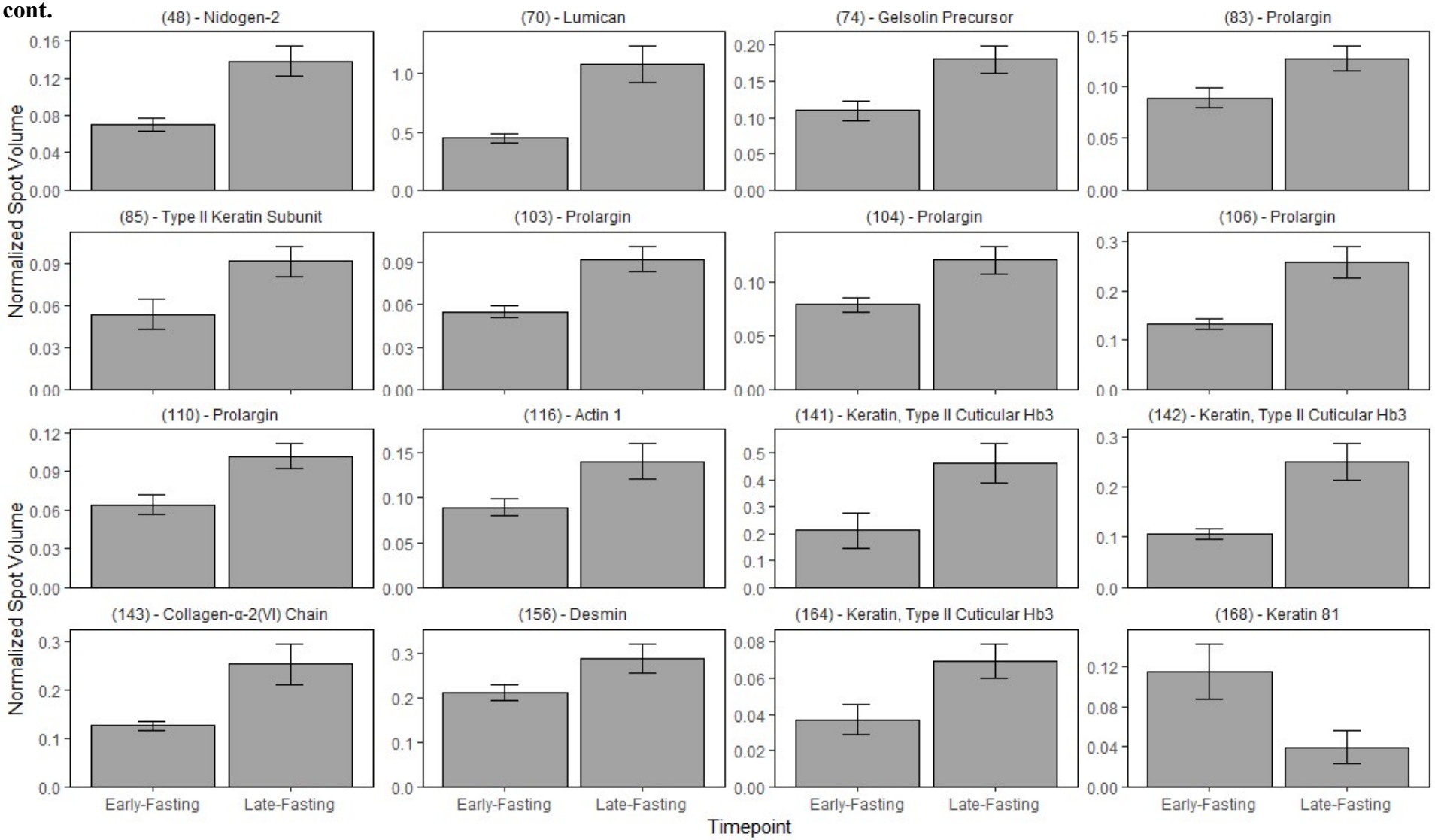
(48) - Nidogen-2
(70) - Lumican
(74) - Gelsolin Precursor
(83) - Prolargin
(85) - Type II Keratin Subunit
(103) - Prolargin
(104) - Prolargin
(106) - Prolargin
(110) - Prolargin
(116) - Actin 1
(141) - Keratin, Type II Cuticular Hb3
(142) - Keratin, Type II Cuticular Hb3
(143) - Collagen-α-2(VI) Chain
(156) - Desmin
(164) - Keratin, Type II Cuticular Hb3
(168) - Keratin 81
Normalized Spot Volume
Early-Fasting
Late-Fasting
Timepoint

C cont.

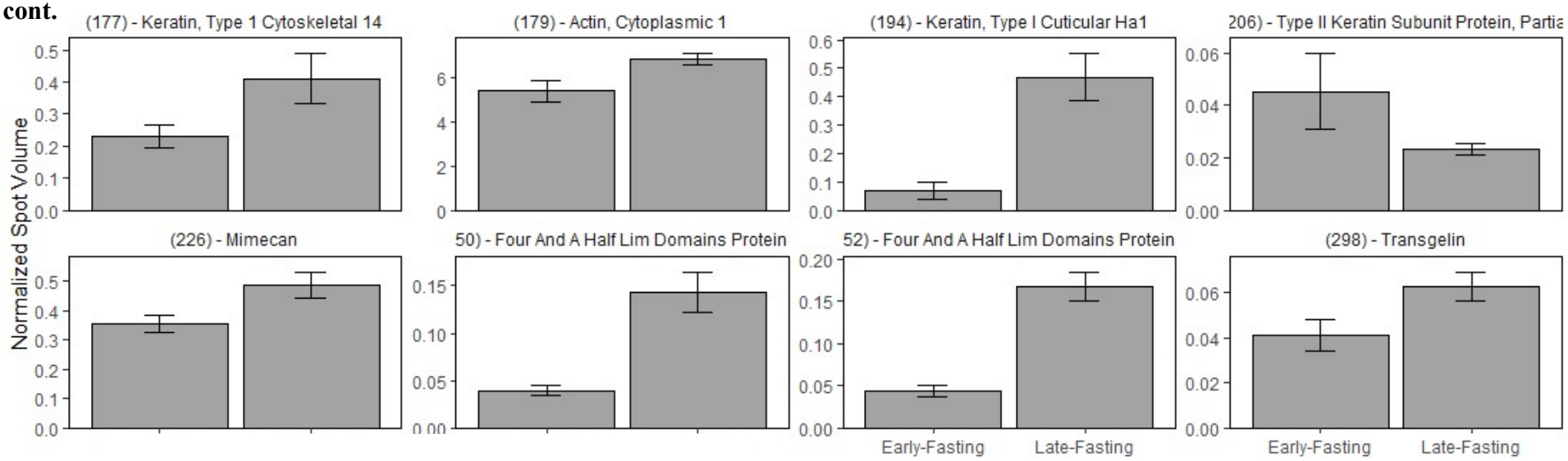

Figure S2. The abundance of cytoskeletal proteins in *M. angustirostris* tissue before and after the post-weaning fast. (A) Muscle tissue, (B) inner adipose, and (C) outer adipose tissue. For more details see Fig. S1.

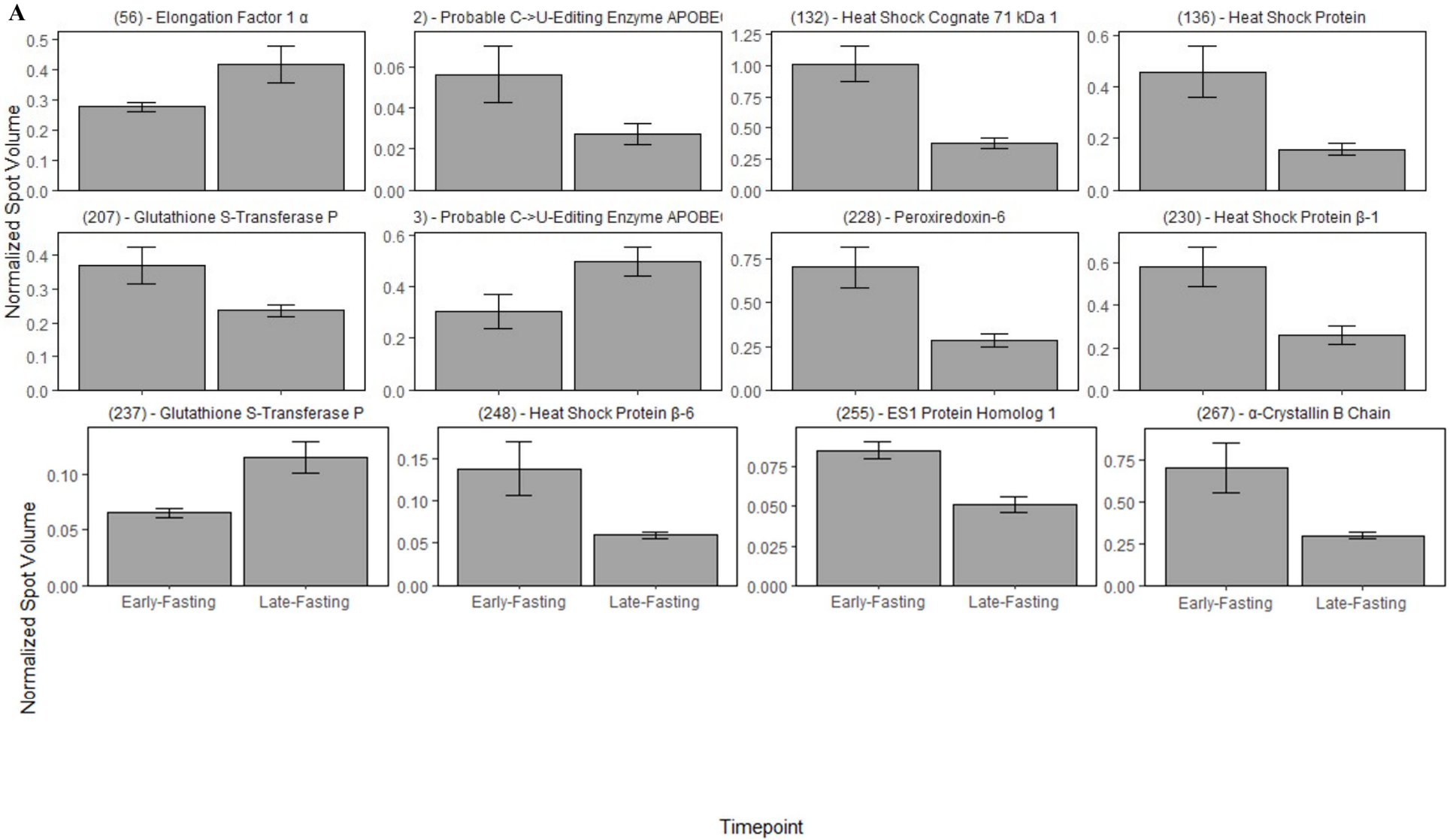
A
(56) - Elongation Factor 1 α
2) - Probable C->U-Editing Enzyme APOBE
(132) - Heat Shock Cognate 71 kDa 1
(136) - Heat Shock Protein
(207) - Glutathione S-Transferase P
3) - Probable C->U-Editing Enzyme APOBE
(228) - Peroxiredoxin-6
(230) - Heat Shock Protein β-1
(237) - Glutathione S-Transferase P
(248) - Heat Shock Protein β-6
(255) - ES1 Protein Homolog 1
(267) - α-Crystallin B Chain
Normalized Spot Volume
Normalized Spot Volume
Early-Fasting
Late-Fasting
Timepoint

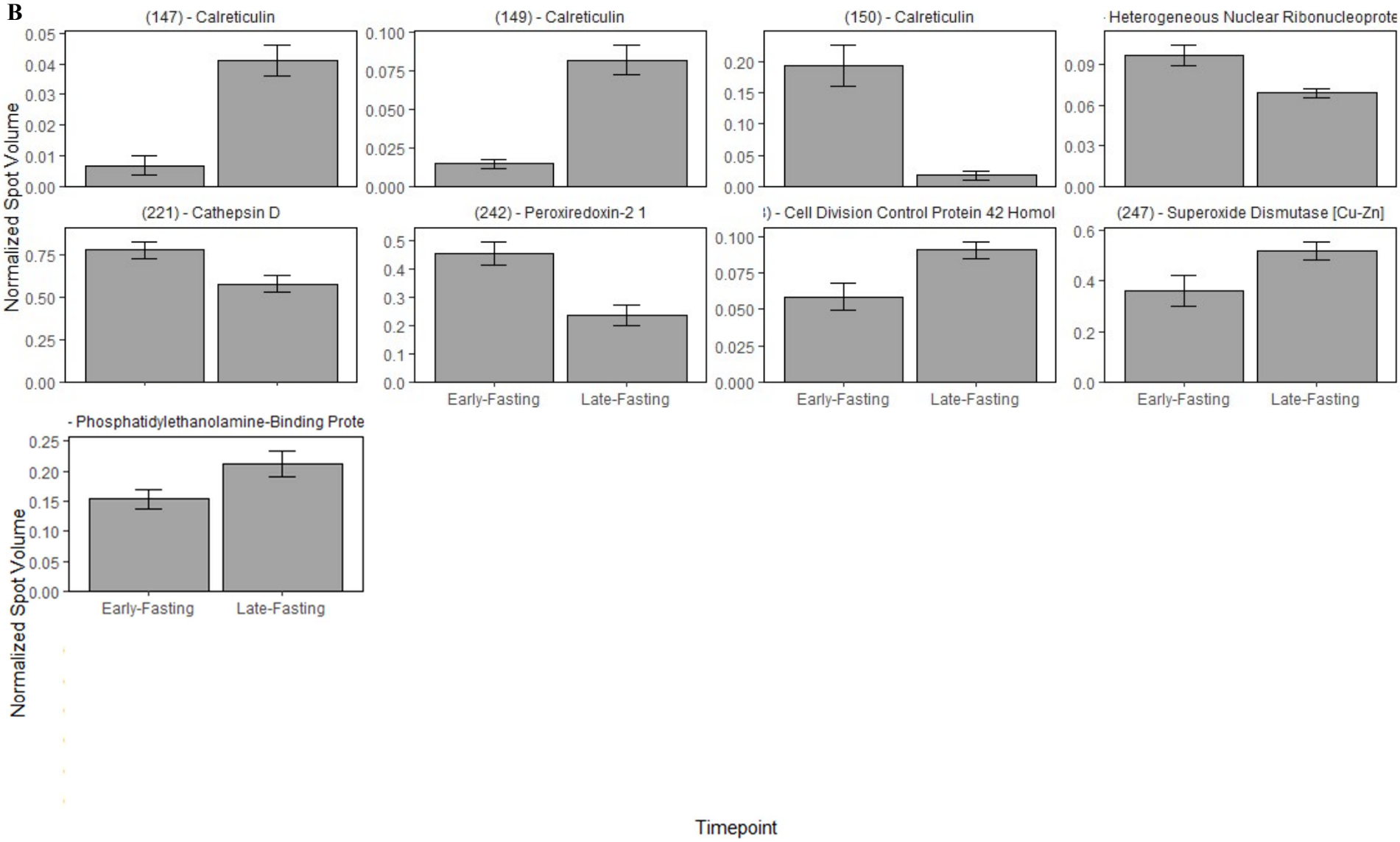
B
(147) - Calreticulin
(149) - Calreticulin
(150) - Calreticulin
Heterogeneous Nuclear Ribonucleoprote
(221) - Cathepsin D
(242) - Peroxiredoxin-2 1
) - Cell Division Control Protein 42 Homol
(247) - Superoxide Dismutase [Cu-Zn]
- Phosphatidylethanolamine-Binding Prote
Normalized Spot Volume
Early-Fasting
Late-Fasting
Timepoint

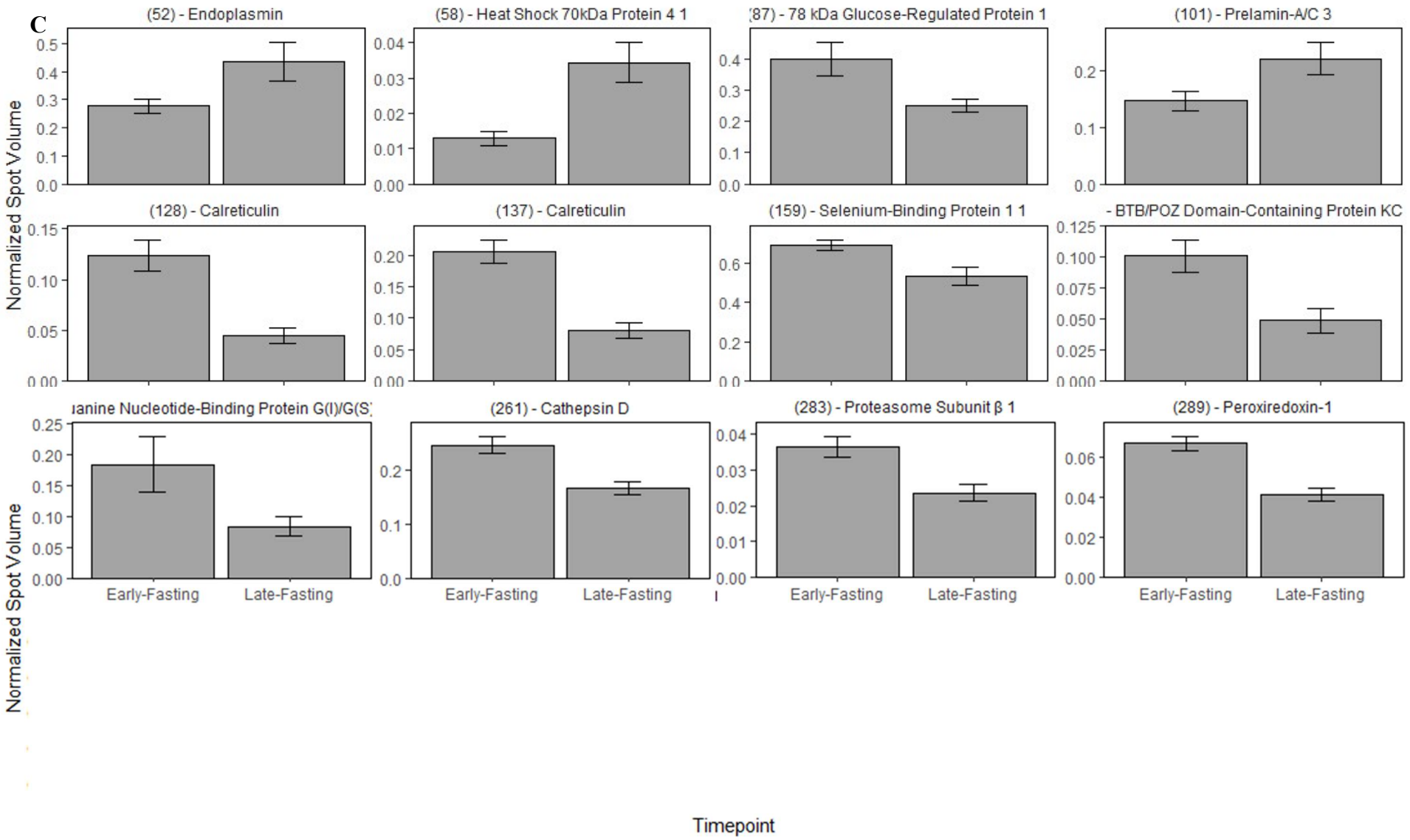

Figure S3. The abundance of proteostasis proteins in *M. angustirostris* tissue before and after the post-weaning fast. (A) Muscle tissue, (B) inner adipose, and (C) outer adipose tissue. For more details see Fig. S1.

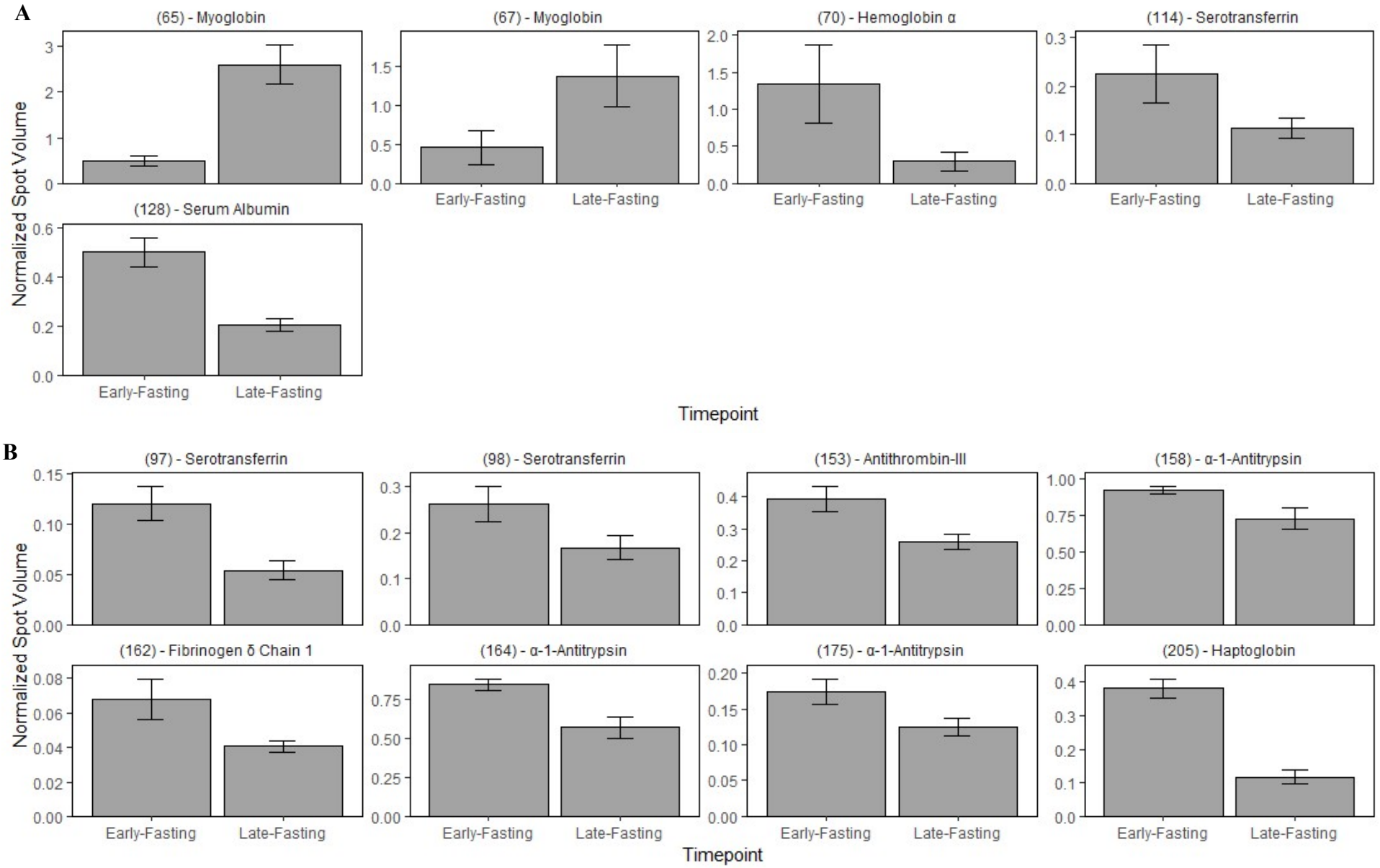
A
(65) - Myoglobin
(67) - Myoglobin
(70) - Hemoglobin α
(114) - Serotransferrin
(128) - Serum Albumin
Normalized Spot Volume
Early-Fasting
Late-Fasting
Timepoint
B
(97) - Serotransferrin
(98) - Serotransferrin
(153) - Antithrombin-III
(158) - α-1-Antitrypsin
(162) - Fibrinogen δ Chain 1
(164) - α-1-Antitrypsin
(175) - α-1-Antitrypsin
(205) - Haptoglobin
Normalized Spot Volume
Early-Fasting
Late-Fasting
Timepoint

B cont.

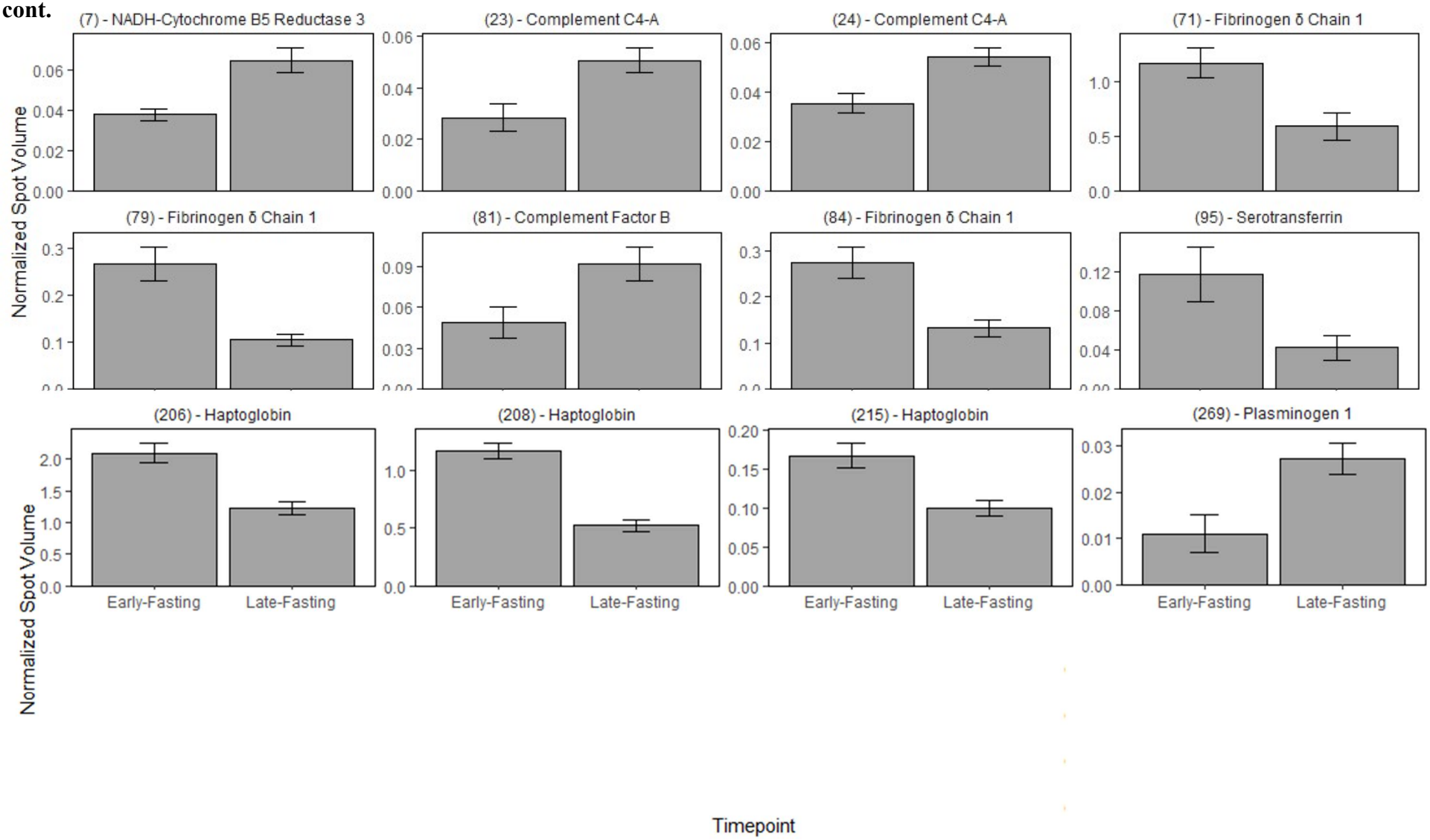
(7) - NADH-Cytochrome B5 Reductase 3
(23) - Complement C4-A
(24) - Complement C4-A
(71) - Fibrinogen δ Chain 1
(79) - Fibrinogen δ Chain 1
(81) - Complement Factor B
(84) - Fibrinogen δ Chain 1
(95) - Serotransferrin
(206) - Haptoglobin
(208) - Haptoglobin
(215) - Haptoglobin
(269) - Plasminogen 1
Normalized Spot Volume
Normalized Spot Volume
Early-Fasting
Late-Fasting
Timepoint

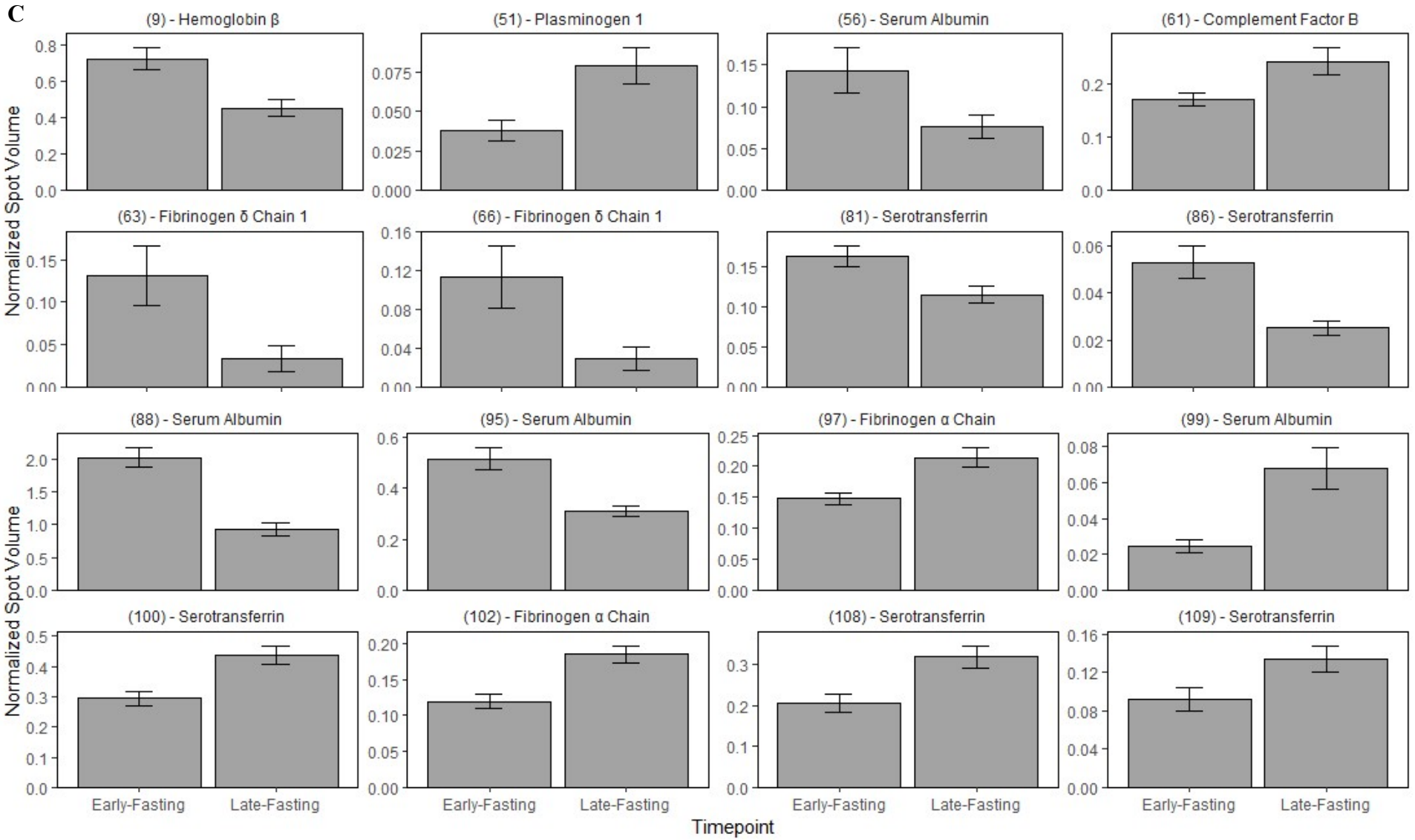
C
(9) - Hemoglobin β
(51) - Plasminogen 1
(56) - Serum Albumin
(61) - Complement Factor B
(63) - Fibrinogen δ Chain 1
(66) - Fibrinogen δ Chain 1
(81) - Serotransferrin
(86) - Serotransferrin
(88) - Serum Albumin
(95) - Serum Albumin
(97) - Fibrinogen α Chain
(99) - Serum Albumin
(100) - Serotransferrin
(102) - Fibrinogen α Chain
(108) - Serotransferrin
(109) - Serotransferrin
Normalized Spot Volume
Early-Fasting
Late-Fasting
Timepoint

C cont.

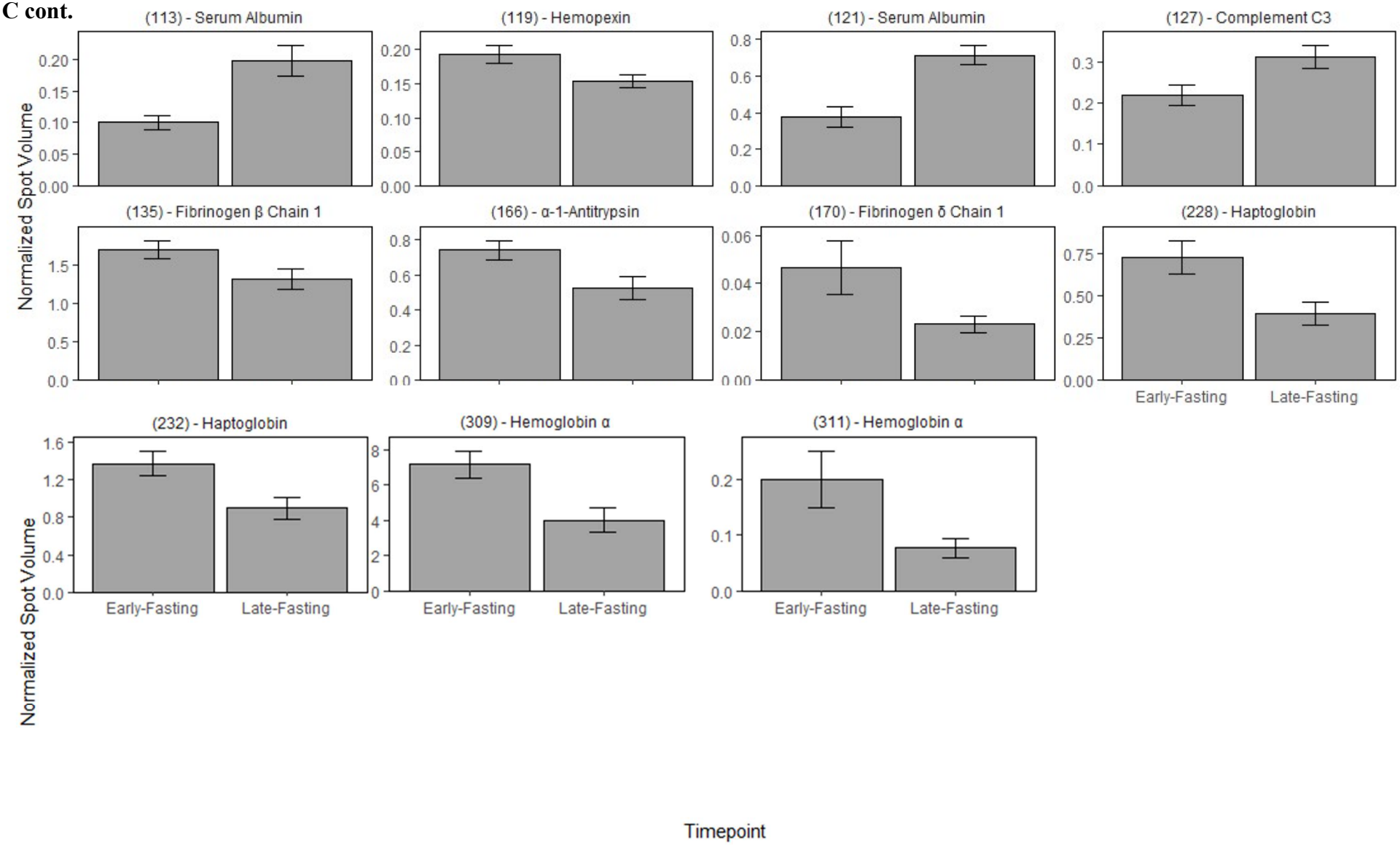

Figure S4. The abundance of blood proteins (iron binding and immunity) in *M. angustirostris* tissue before and after the post-weaning fast. (A) Muscle tissue, (B) inner adipose, and (C) outer adipose tissue. For more details see Fig. S1.

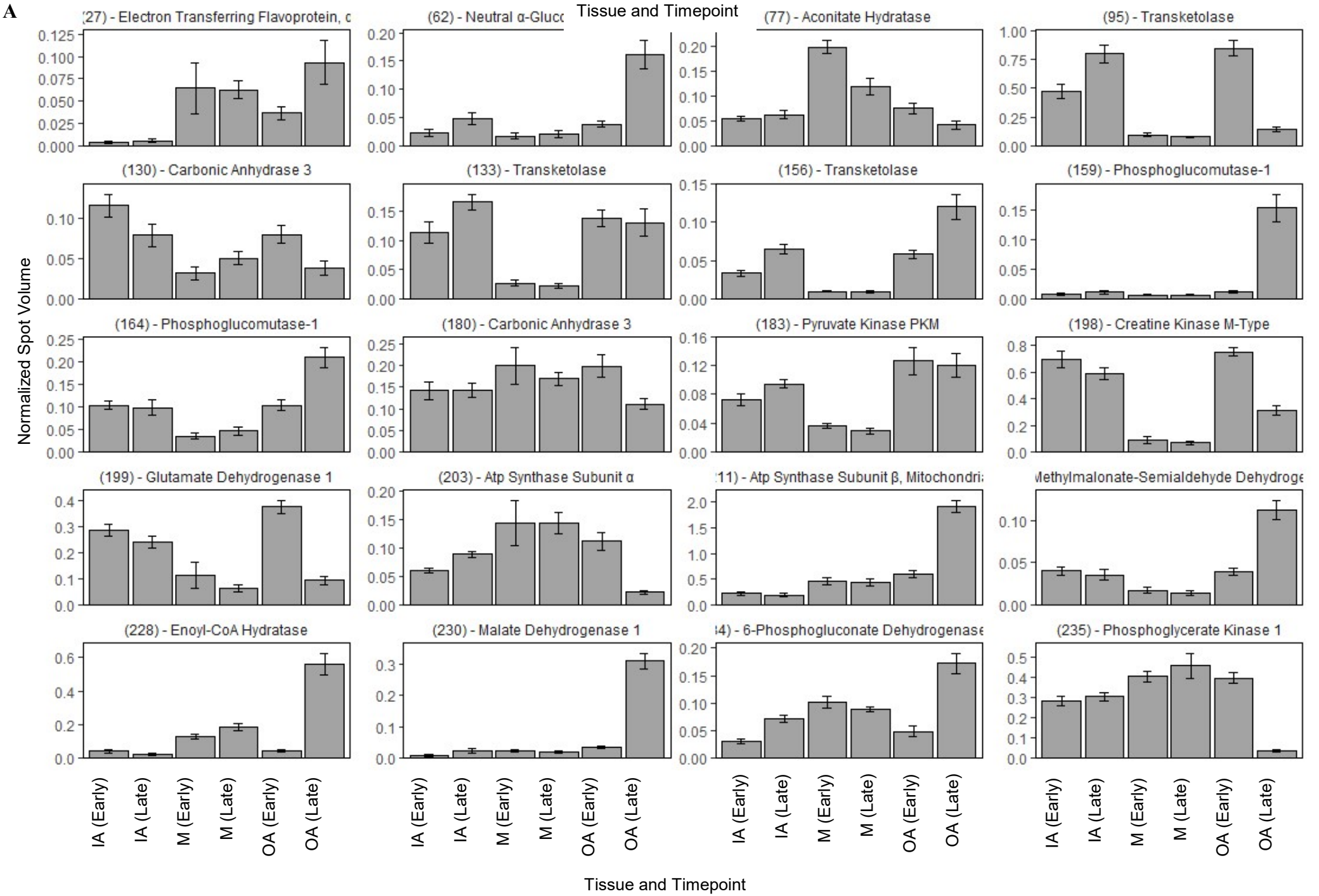
A
Tissue and Timepoint
(27) - Electron Transferring Flavoprotein, c
(62) - Neutral α-Gluc
(77) - Aconitate Hydratase
(95) - Transketolase
(130) - Carbonic Anhydrase 3
(133) - Transketolase
(156) - Transketolase
(159) - Phosphoglucomutase-1
(164) - Phosphoglucomutase-1
(180) - Carbonic Anhydrase 3
(183) - Pyruvate Kinase PKM
(198) - Creatine Kinase M-Type
(199) - Glutamate Dehydrogenase 1
(203) - Atp Synthase Subunit α
11) - Atp Synthase Subunit β, Mitochondri
Methylmalonate-Semialdehyde Dehydroge
(228) - Enoyl-CoA Hydratase
(230) - Malate Dehydrogenase 1
4) - 6-Phosphogluconate Dehydrogenase
(235) - Phosphoglycerate Kinase 1
Normalized Spot Volume
IA (Early)
IA (Late)
M (Early)
M (Late)
OA (Early)
OA (Late)
Tissue and Timepoint

A cont.

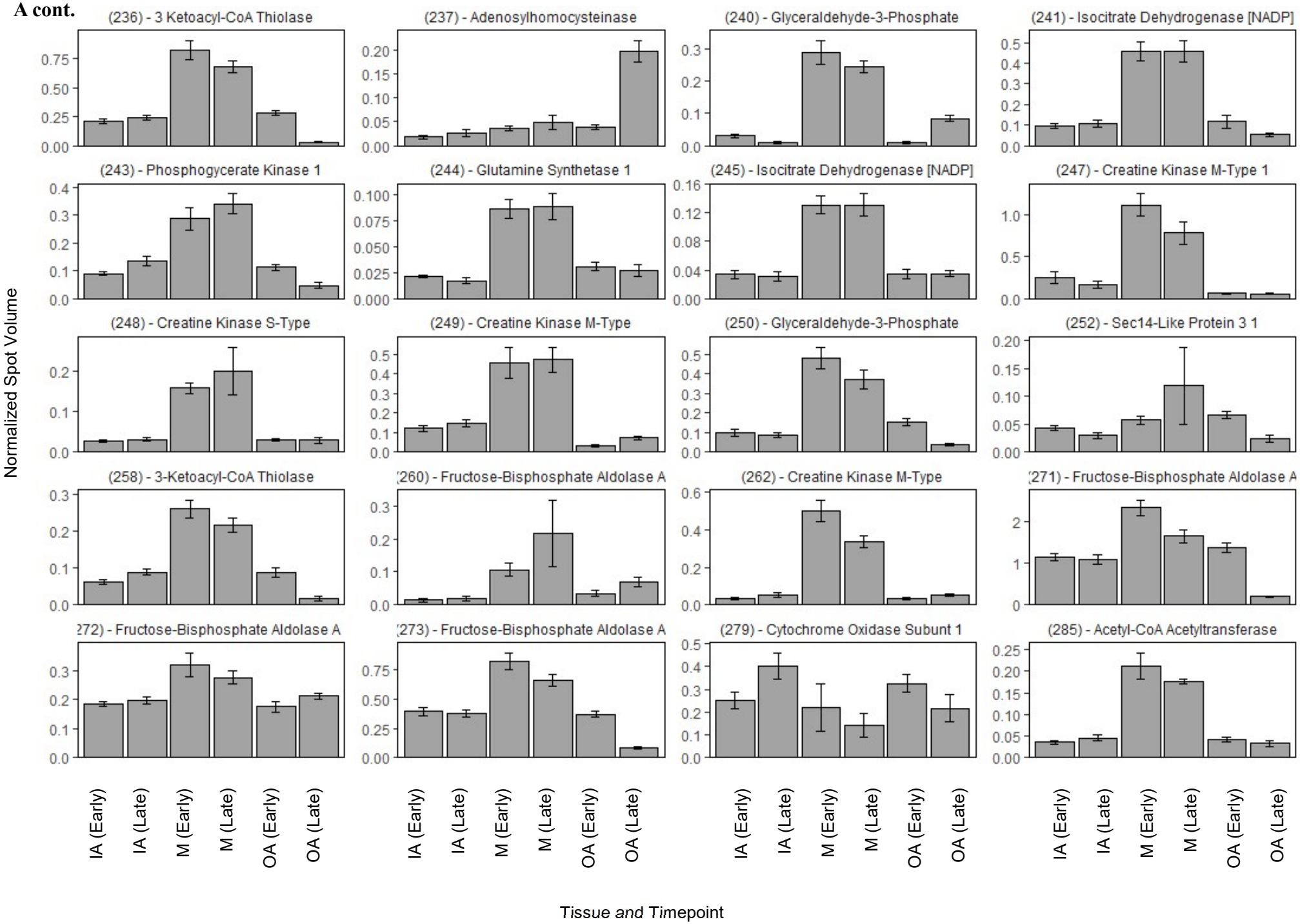
(236) - 3 Ketoacyl-CoA Thiolase
(237) - Adenosylhomocysteinase
(240) - Glyceraldehyde-3-Phosphate
(241) - Isocitrate Dehydrogenase [NADP]
(243) - Phosphogycerate Kinase 1
(244) - Glutamine Synthetase 1
(245) - Isocitrate Dehydrogenase [NADP]
(247) - Creatine Kinase M-Type 1
(248) - Creatine Kinase S-Type
(249) - Creatine Kinase M-Type
(250) - Glyceraldehyde-3-Phosphate
(252) - Sec14-Like Protein 3 1
(258) - 3-Ketoacyl-CoA Thiolase
(260) - Fructose-Bisphosphate Aldolase A
(262) - Creatine Kinase M-Type
(271) - Fructose-Bisphosphate Aldolase A
272) - Fructose-Bisphosphate Aldolase A
(273) - Fructose-Bisphosphate Aldolase A
(279) - Cytochrome Oxidase Subunt 1
(285) - Acetyl-CoA Acetyltransferase
Normalized Spot Volume
IA (Early)
IA (Late)
M (Early)
M (Late)
OA (Early)
OA (Late)
Tissue and Timepoint

A cont.

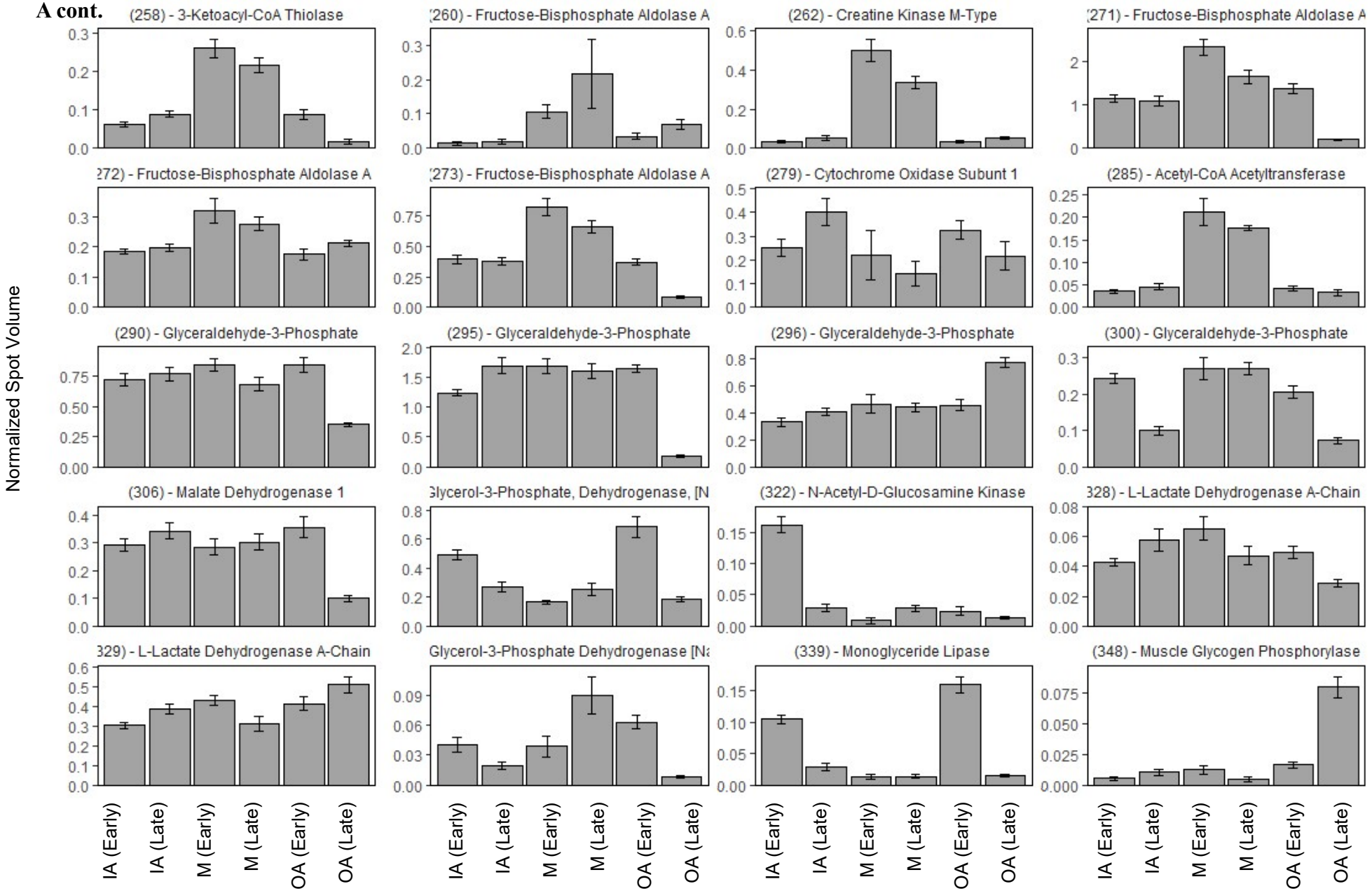

Normalized Spot Volume

Tissue and Timepoint

A cont.

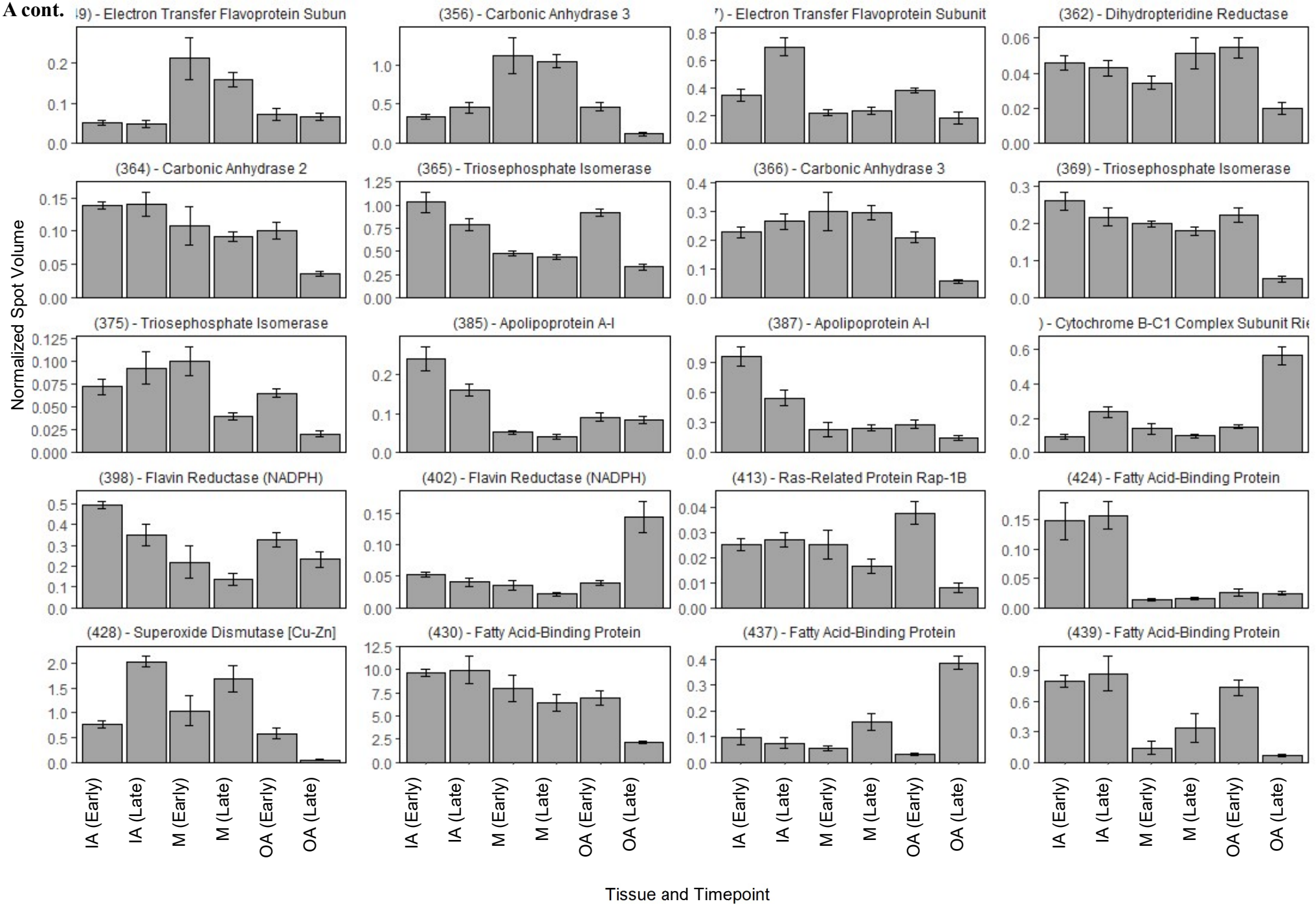
(9) - Electron Transfer Flavoprotein Subun
(356) - Carbonic Anhydrase 3
') - Electron Transfer Flavoprotein Subunit
(362) - Dihydropteridine Reductase
(364) - Carbonic Anhydrase 2
(365) - Triosephosphate Isomerase
(366) - Carbonic Anhydrase 3
(369) - Triosephosphate Isomerase
(375) - Triosephosphate Isomerase
(385) - Apolipoprotein A-I
(387) - Apolipoprotein A-I
) - Cytochrome B-C1 Complex Subunit Rie
(398) - Flavin Reductase (NADPH)
(402) - Flavin Reductase (NADPH)
(413) - Ras-Related Protein Rap-1B
(424) - Fatty Acid-Binding Protein
(428) - Superoxide Dismutase [Cu-Zn]
(430) - Fatty Acid-Binding Protein
(437) - Fatty Acid-Binding Protein
(439) - Fatty Acid-Binding Protein
Normalized Spot Volume
IA (Early)
IA (Late)
M (Early)
M (Late)
OA (Early)
OA (Late)
Tissue and Timepoint

A cont.

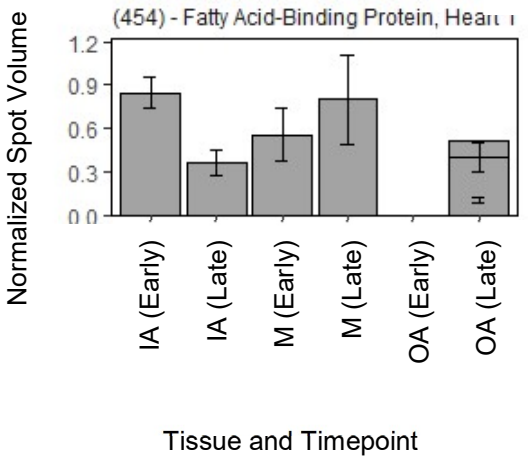
(454) - Fatty Acid-Binding Protein, Heart
Normalized Spot Volume
1.2
0.9
0.6
0.3
0.0
IA (Early)
IA (Late)
M (Early)
M (Late)
OA (Early)
OA (Late)
Tissue and Timepoint

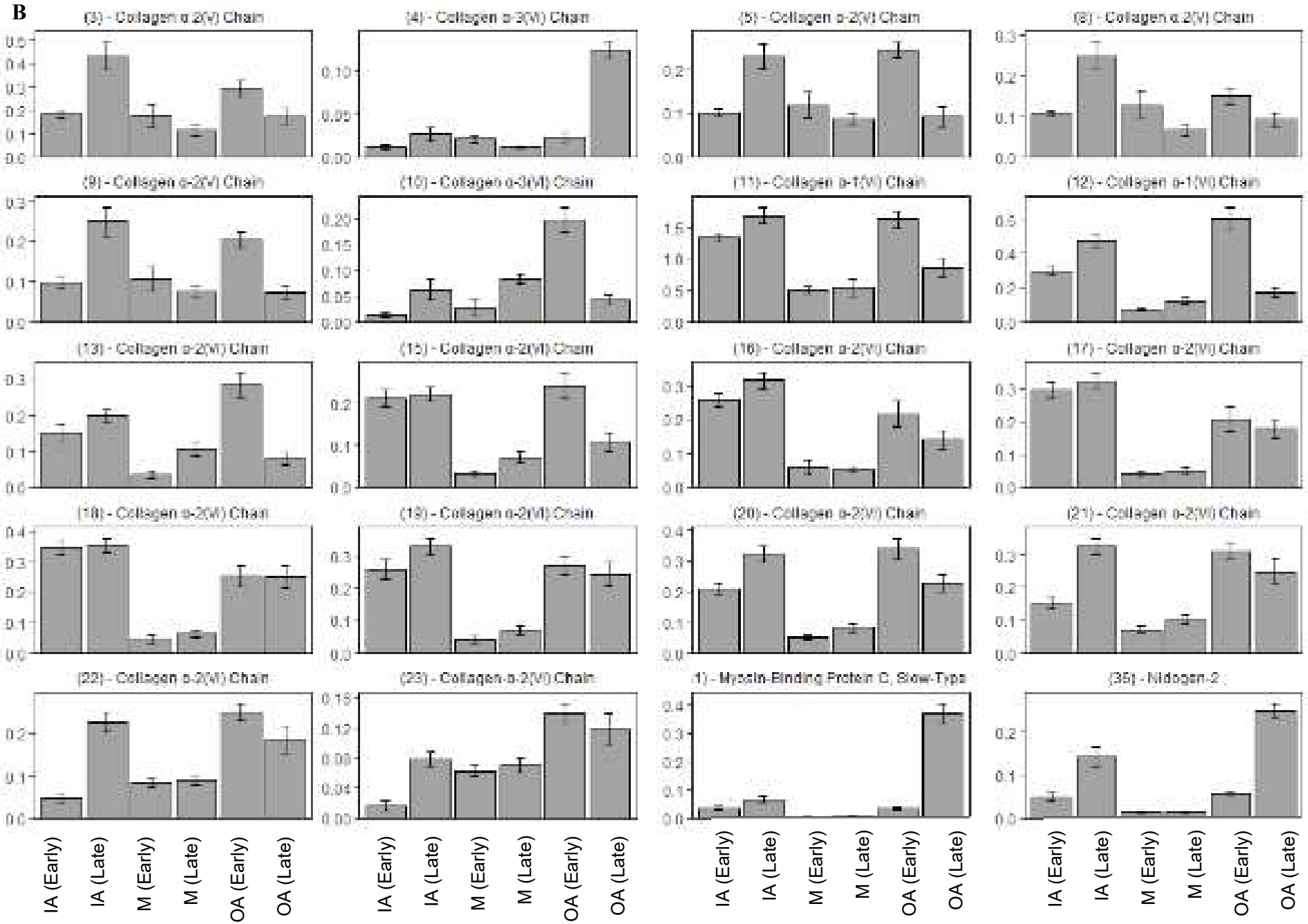
B
(3) - Collagen α-2(V) Chain
(4) - Collagen α-3(VI) Chain
(5) - Collagen α-2(V) Chain
(6) - Collagen α-2(VI) Chain
(9) - Collagen α-2(V) Chain
(10) - Collagen α-3(VI) Chain
(11) - Collagen α-1(VI) Chain
(12) - Collagen α-1(VI) Chain
(13) - Collagen α-2(VI) Chain
(15) - Collagen α-2(VI) Chain
(16) - Collagen α-2(VI) Chain
(17) - Collagen α-2(VI) Chain
(18) - Collagen α-2(VI) Chain
(19) - Collagen α-2(VI) Chain
(20) - Collagen α-2(VI) Chain
(21) - Collagen α-2(VI) Chain
(22) - Collagen α-2(VI) Chain
(23) - Collagen α-2(VI) Chain
(1) - Myosin-Binding Protein C, Slow-Type
(35) - Nidogen-2
IA (Early)
IA (Late)
M (Early)
M (Late)
OA (Early)
OA (Late)
Normalized Spot Volume
Tissue and Timepoint

B cont.

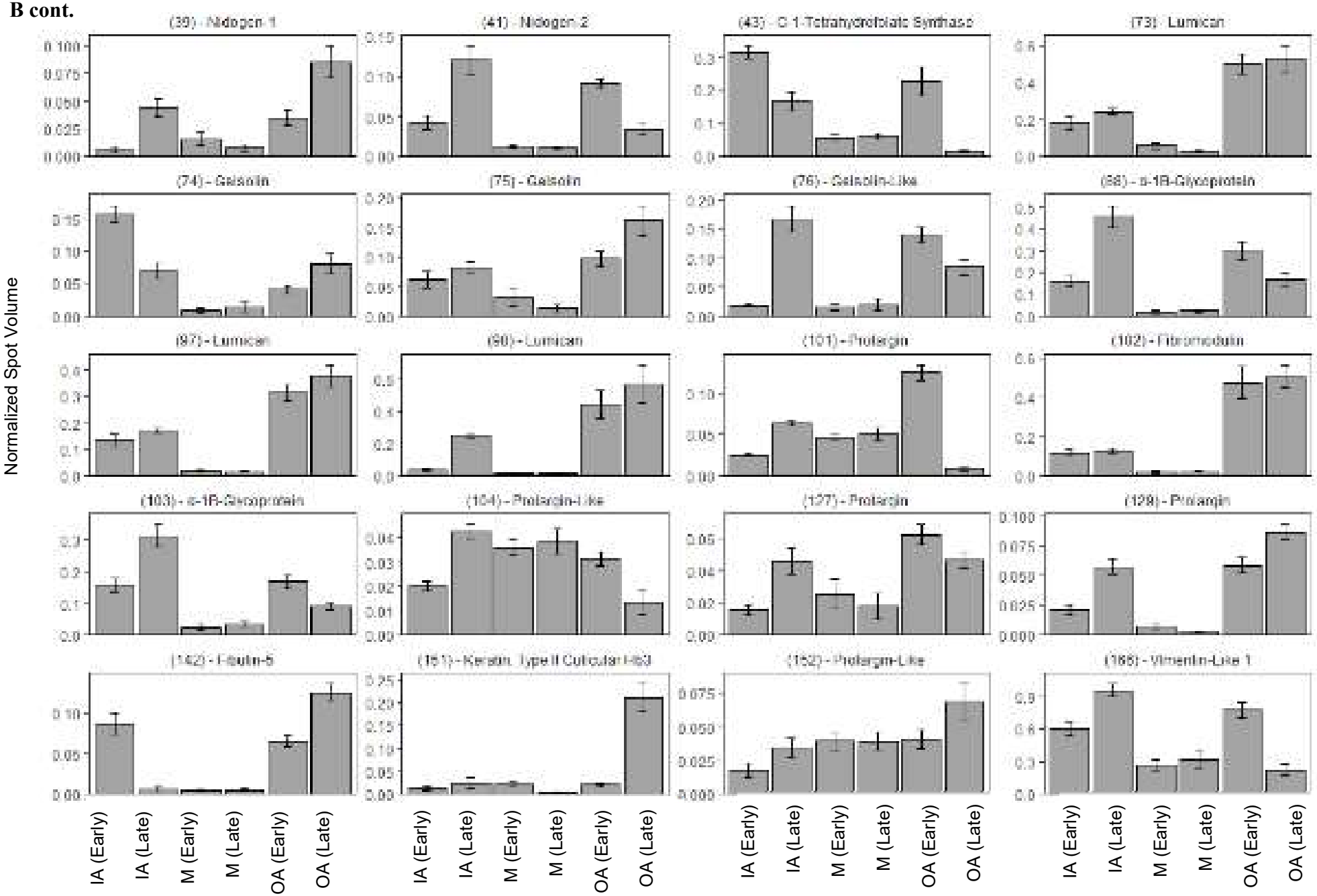
(39) - Nidogen 1
(41) - Nidogen 2
(43) - C 1-Tetrahydrofolate Synthase
(73) - Lumican
(74) - Gelsolin
(75) - Gelsolin
(76) - Gelsolin-Like
(88) - α-1B-Glycoprotein
(97) - Lumican
(98) - Lumican
(101) - Prolargin
(102) - Fibromodulin
(103) - α-1B-Glycoprotein
(104) - Prolargin-Like
(127) - Prolargin
(128) - Prolargin
(142) - Fibulin-5
(151) - Keratin, Type II Cuticular Hb3
(152) - Prolargin-Like
(166) - Vimentin-Like 1
Normalized Spot Volume
IA (Early)
IA (Late)
M (Early)
M (Late)
OA (Early)
OA (Late)
Tissue and Timepoint

B cont.

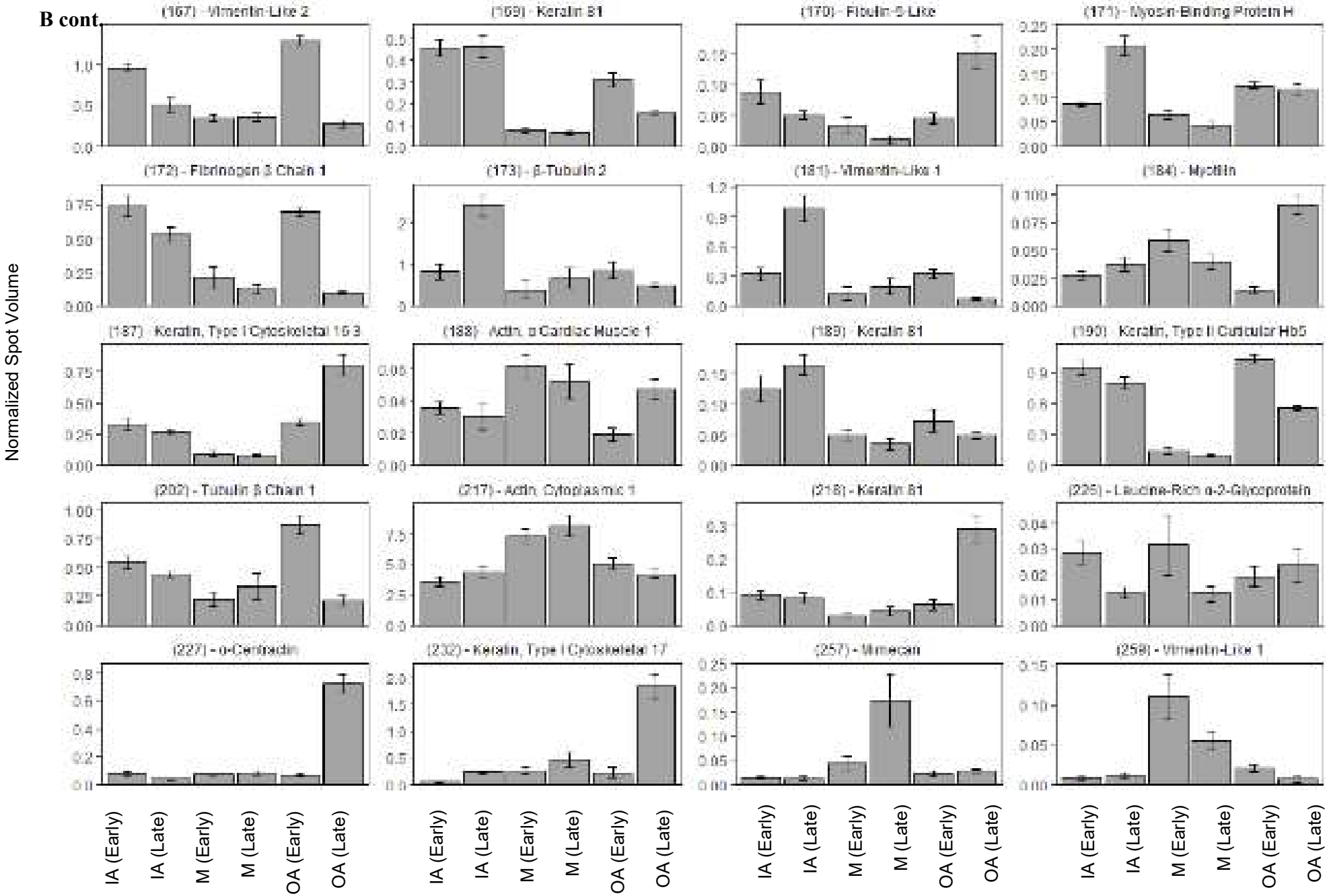
(167) - Vimentin-Like 2
(169) - Keratin 81
(170) - Fibulin-5 Like
(171) - Myosin-Binding Protein H
(172) - Fibrinogen β Chain 1
(173) - β-Tubulin 2
(181) - Vimentin-Like 1
(184) - Myotilin
(187) - Keratin, Type I Cytoskeletal 10 3
(188) - Actin, α Cardiac Muscle 1
(189) - Keratin 81
(190) - Keratin, Type II Cuticular Hb5
(202) - Tubulin β Chain 1
(217) - Actin, Cytoplasmic 1
(218) - Keratin 81
(225) - Leucine-Rich α-2-Glycoprotein
(227) - α-Centractin
(232) - Keratin, Type I Cytoskeletal 17
(257) - Vimecan
(259) - Vimentin-Like 1
Normalized Spot Volume
IA (Early)
IA (Late)
M (Early)
M (Late)
OA (Early)
OA (Late)
Tissue and Timepoint

B cont.

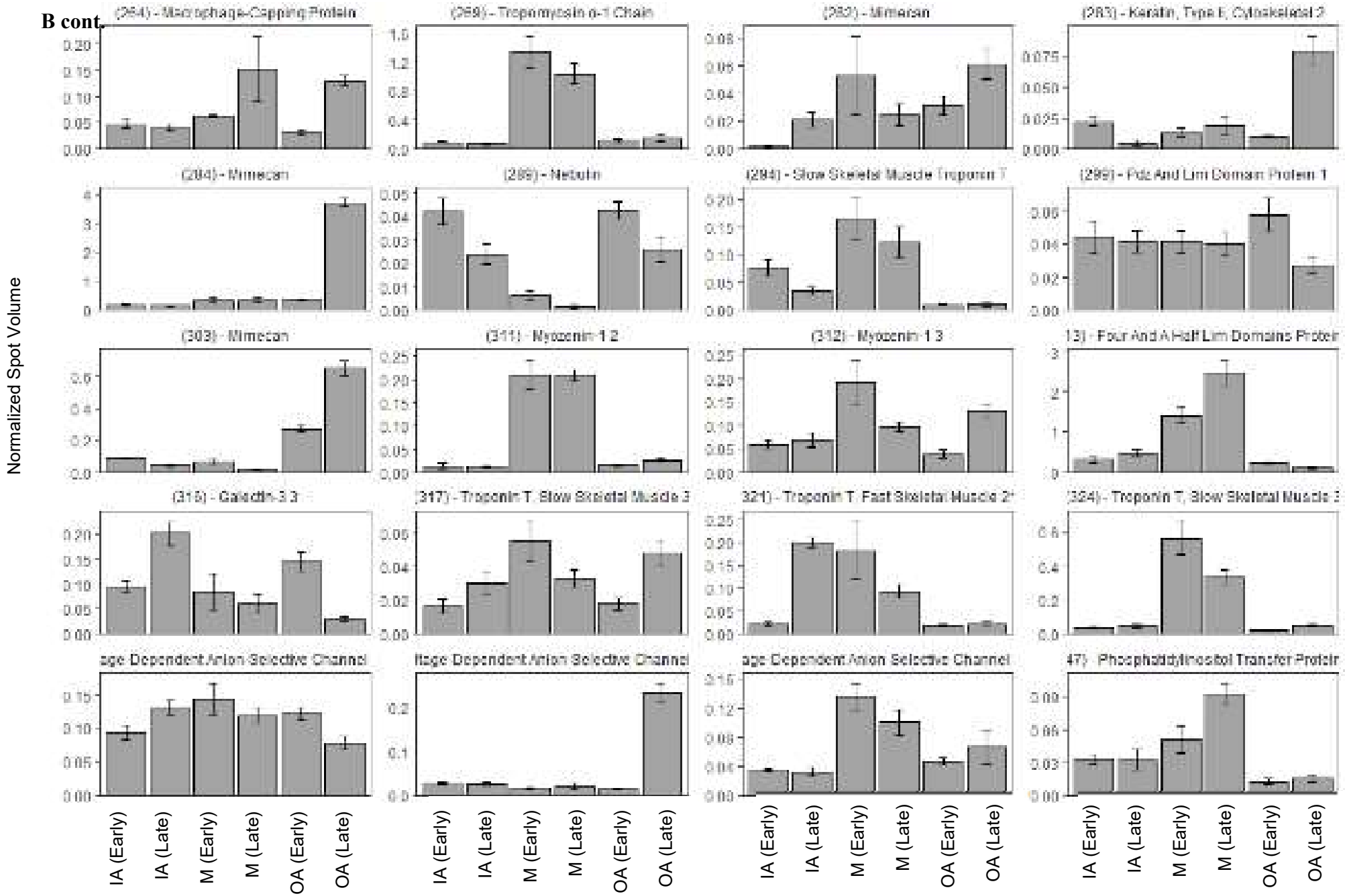
(264) - Macrophage-Capping Protein
(269) - Tropomyosin α-1 Chain
(282) - Mimecan
(283) - Keratin, Type II, Cytoskeletal 2
(284) - Mimecan
(289) - Nebulin
(294) - Slow Skeletal Muscle Troponin T
(299) - Pdz And Lim Domain Protein 1
(303) - Mimecan
(311) - Myozenin 1 2
(312) - Myozenin 1 3
13) - Four And A Half Lim Domains Protein
(315) - Galectin-3 3
317) - Troponin T, Slow Skeletal Muscle 3
321) - Troponin T, Fast Skeletal Muscle 2
324) - Troponin T, Slow Skeletal Muscle 3
age Dependent Anion Selective Channel
tage Dependent Anion Selective Channel
age Dependent Anion Selective Channel
47) - Phosphatidylinositol Transfer Protein
Normalized Spot Volume
IA (Early)
IA (Late)
M (Early)
M (Late)
OA (Early)
OA (Late)
Tissue and Timepoint

B cont.

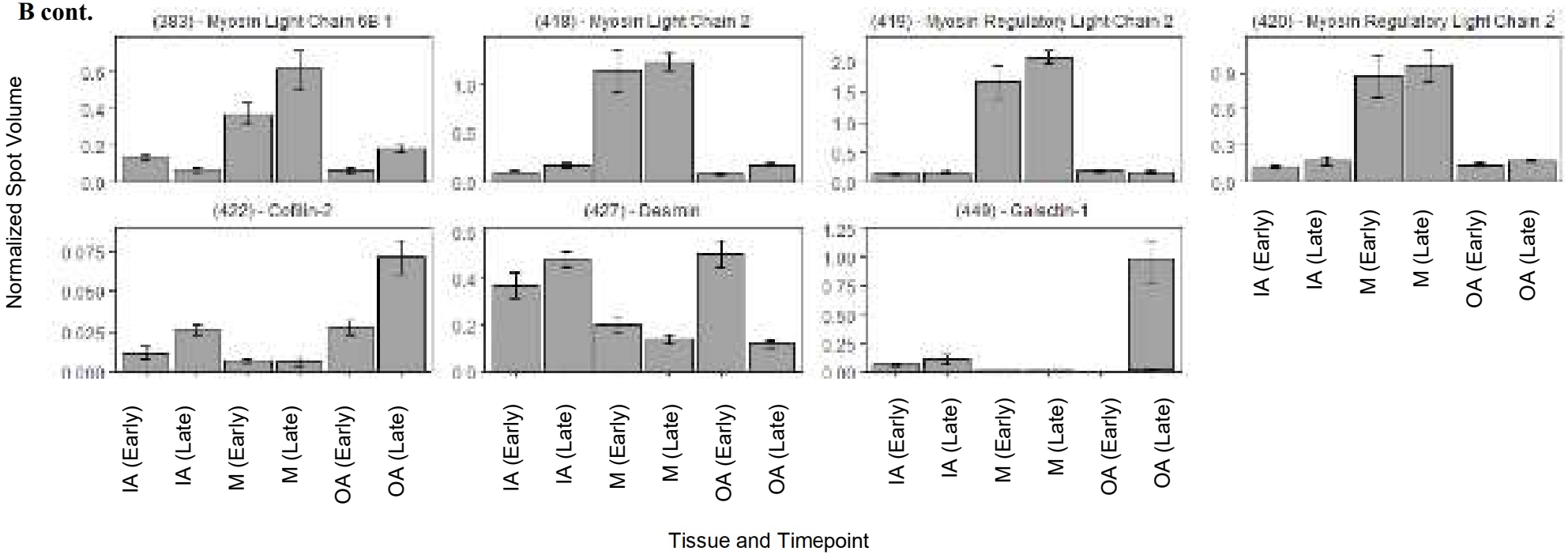
(393) - Myosin Light Chain 6B 1
(418) - Myosin Light Chain 2
(419) - Myosin Regulatory Light Chain 2
(420) - Myosin Regulatory Light Chain 2
(422) - Cofilin-2
(427) - Desmin
(449) - Galectin-1
Normalized Spot Volume
IA (Early)
IA (Late)
M (Early)
M (Late)
OA (Early)
OA (Late)
Tissue and Timepoint

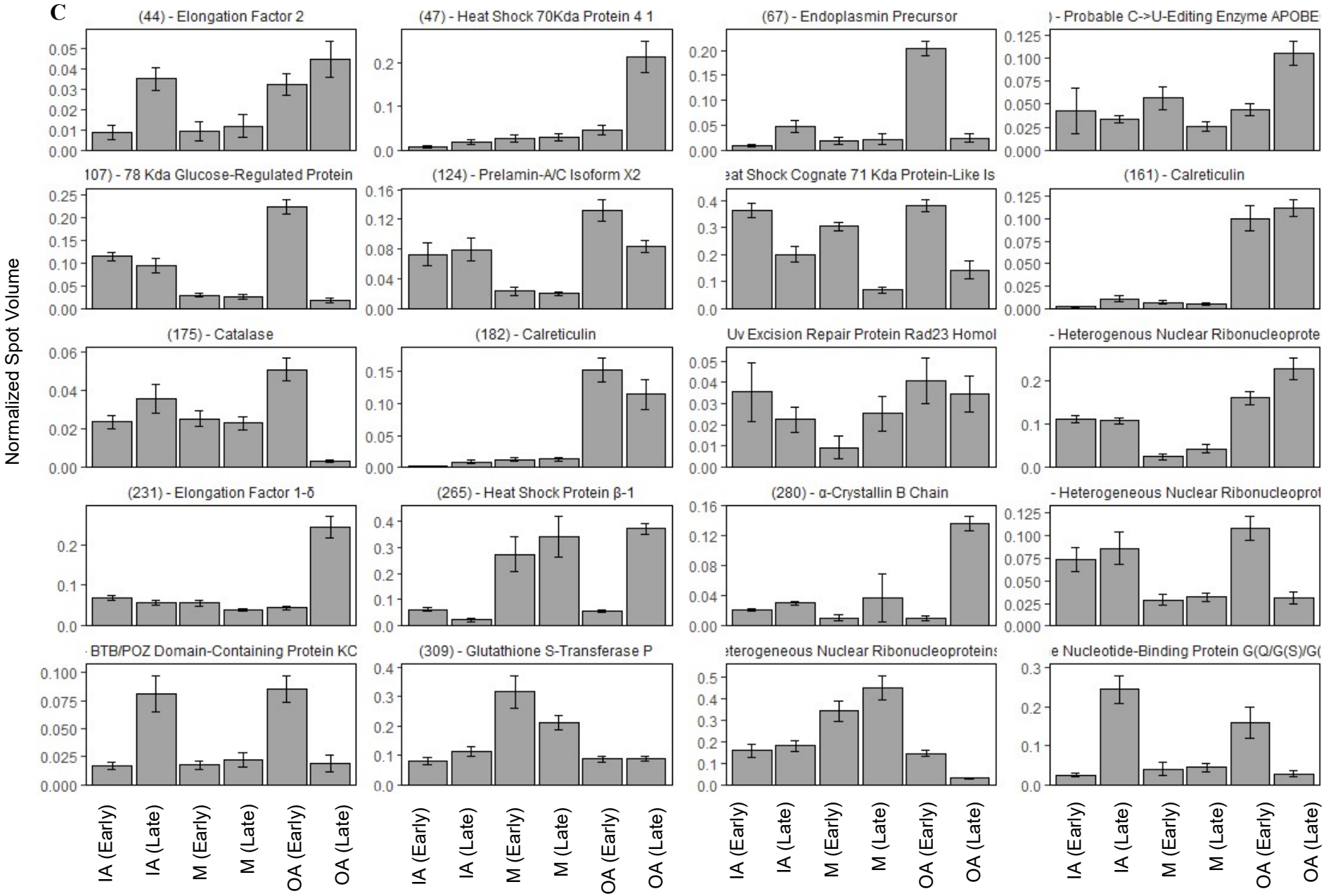
C
(44) - Elongation Factor 2
(47) - Heat Shock 70Kda Protein 4 1
(67) - Endoplasmin Precursor
) - Probable C->U-Editing Enzyme APOBE
107) - 78 Kda Glucose-Regulated Protein
(124) - Prelamin-A/C Isoform X2
eat Shock Cognate 71 Kda Protein-Like Is
(161) - Calreticulin
(175) - Catalase
(182) - Calreticulin
Uv Excision Repair Protein Rad23 Homol
- Heterogenous Nuclear Ribonucleoprote
(231) - Elongation Factor 1-δ
(265) - Heat Shock Protein β-1
(280) - α-Crystallin B Chain
- Heterogeneous Nuclear Ribonucleoprot
BTB/POZ Domain-Containing Protein KC
(309) - Glutathione S-Transferase P
eterogeneous Nuclear Ribonucleoproteins
e Nucleotide-Binding Protein G(Q/G(S)/G(
IA (Early)
IA (Late)
M (Early)
M (Late)
OA (Early)
OA (Late)
Normalized Spot Volume
Tissue and Timepoint

C cont.

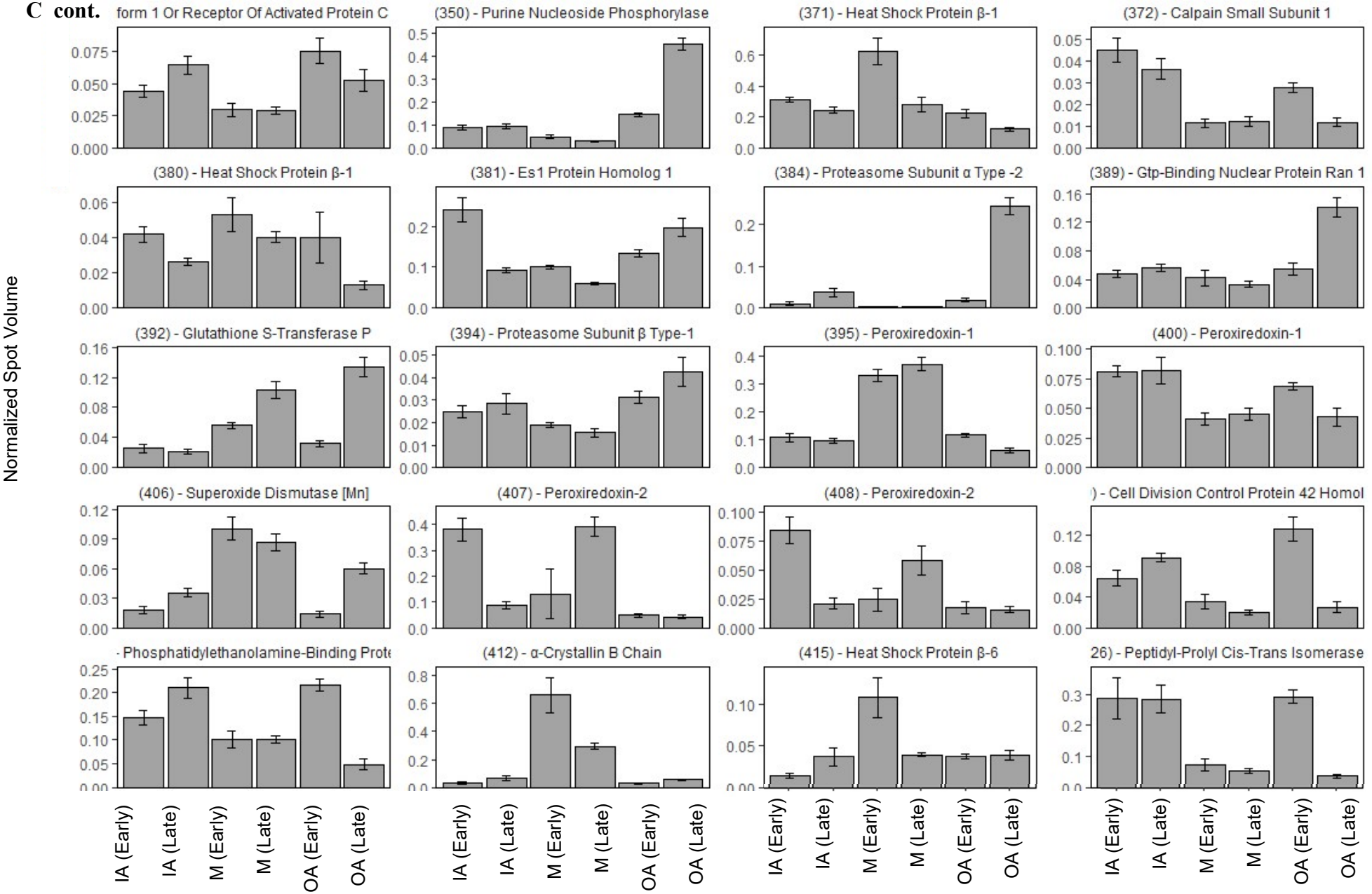
form 1 Or Receptor Of Activated Protein C
(350) - Purine Nucleoside Phosphorylase
(371) - Heat Shock Protein β-1
(372) - Calpain Small Subunit 1
(380) - Heat Shock Protein β-1
(381) - Es1 Protein Homolog 1
(384) - Proteasome Subunit α Type -2
(389) - Gtp-Binding Nuclear Protein Ran 1
(392) - Glutathione S-Transferase P
(394) - Proteasome Subunit β Type-1
(395) - Peroxiredoxin-1
(400) - Peroxiredoxin-1
(406) - Superoxide Dismutase [Mn]
(407) - Peroxiredoxin-2
(408) - Peroxiredoxin-2
) - Cell Division Control Protein 42 Homol
- Phosphatidylethanolamine-Binding Prote
(412) - α-Crystallin B Chain
(415) - Heat Shock Protein β-6
26) - Peptidyl-Prolyl Cis-Trans Isomerase
IA (Early)
IA (Late)
M (Early)
M (Late)
OA (Early)
OA (Late)
Normalized Spot Volume
Tissue and Timepoint

C cont.

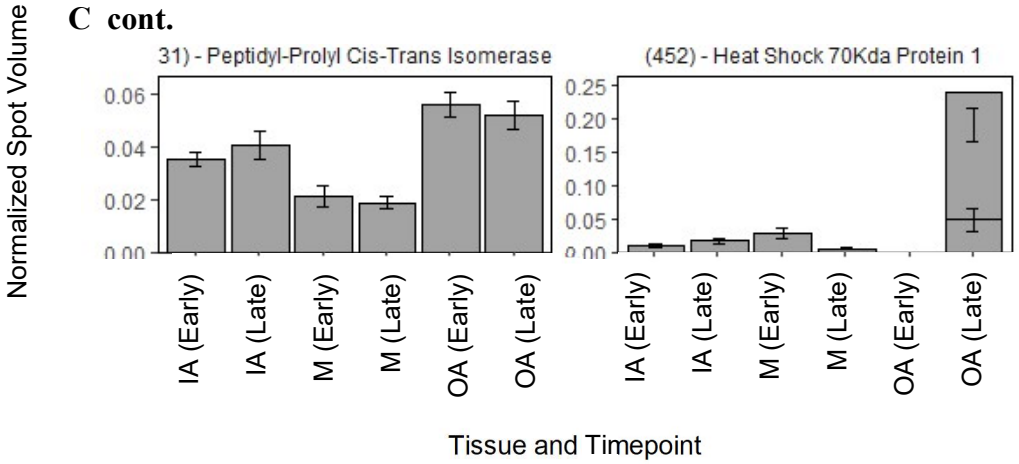
31) - Peptidyl-Prolyl Cis-Trans Isomerase
(452) - Heat Shock 70Kda Protein 1
Normalized Spot Volume
0.06
0.04
0.02
0.00
0.25
0.20
0.15
0.10
0.05
0.00
IA (Early)
IA (Late)
M (Early)
M (Late)
OA (Early)
OA (Late)
Tissue and Timepoint

D.

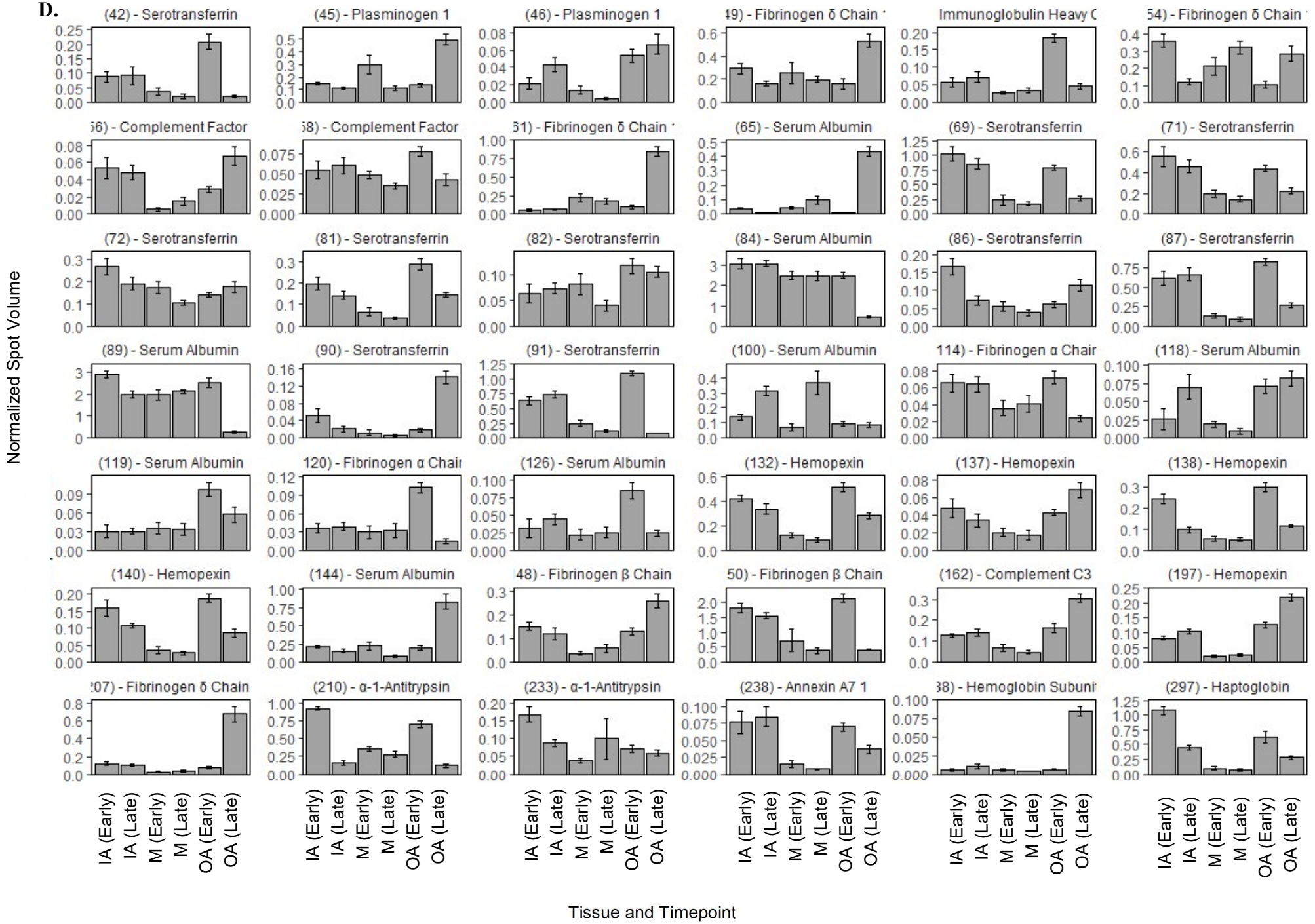
(42) - Serotransferrin
(45) - Plasminogen 1
(46) - Plasminogen 1
49) - Fibrinogen δ Chain
Immunoglobulin Heavy C
54) - Fibrinogen δ Chain
56) - Complement Factor
58) - Complement Factor
61) - Fibrinogen δ Chain
(65) - Serum Albumin
(69) - Serotransferrin
(71) - Serotransferrin
(72) - Serotransferrin
(81) - Serotransferrin
(82) - Serotransferrin
(84) - Serum Albumin
(86) - Serotransferrin
(87) - Serotransferrin
(89) - Serum Albumin
(90) - Serotransferrin
(91) - Serotransferrin
(100) - Serum Albumin
114) - Fibrinogen α Chair
(118) - Serum Albumin
(119) - Serum Albumin
120) - Fibrinogen α Chair
(126) - Serum Albumin
(132) - Hemopexin
(137) - Hemopexin
(138) - Hemopexin
(140) - Hemopexin
(144) - Serum Albumin
148) - Fibrinogen β Chain
150) - Fibrinogen β Chain
(162) - Complement C3
(197) - Hemopexin
207) - Fibrinogen δ Chain
(210) - α-1-Antitrypsin
(233) - α-1-Antitrypsin
(238) - Annexin A7 1
238) - Hemoglobin Subuni
(297) - Haptoglobin
IA (Early)
IA (Late)
M (Early)
M (Late)
OA (Early)
OA (Late)
Normalized Spot Volume
Tissue and Timepoint

D cont.

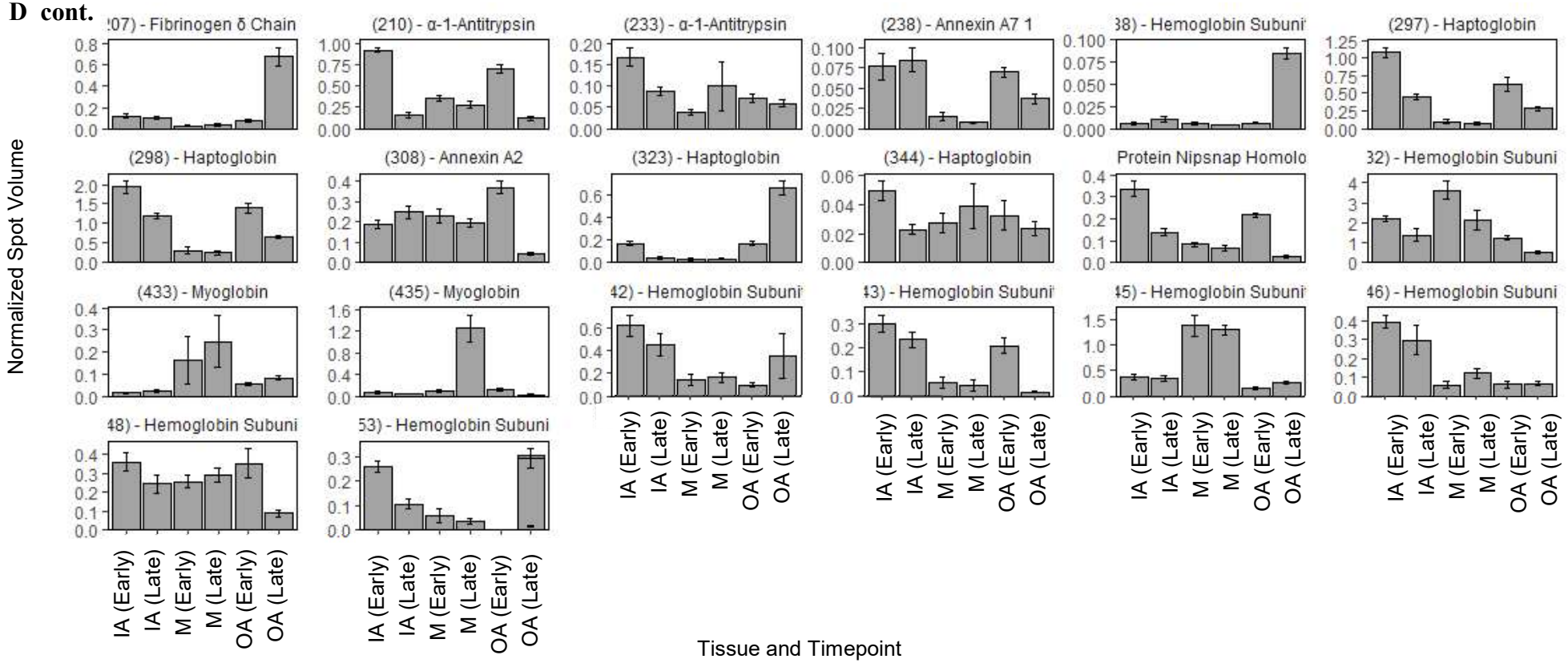

Figure S5. The abundance of proteins in *M. angustirostris* skeletal muscle, inner adipose, and outer adipose tissue before and after the post-weaning fast. We obtained protein abundances by normalizing the spot volume against the volume of all proteins for all tissues, and abundances are displayed as the mean abundance ± 1 s.e.m.. Significance determined using a permutation two-way ANOVA; $p < 0.05$. (A) Energy metabolism, (B) cytoskeletal, (C) proteostasis, and (D) blood (iron binding and immunity) proteins.